UiO : Department of Geosciences
University of Oslo

Transport of metals from mine waste - evaluation of ongoing and future mine deposits at Titania AS

Hedvig Eikeng Sterri

September 2017

Transport of metals from mine waste - evaluation of ongoing and future mine deposits at Titania AS

Hedvig Eikeng Sterri

Master's Thesis

Geochemistry and Mineralogy

Department of Geosciences

The Faculty of Mathematics and Natural Sciences

UNIVERSITY OF OSLO

September 2017

Supervisor: Helge Hellevang

Title: Transport of metals from mine waste- evaluation of ongoing and future mine deposits at Titania AS

Author: Hedvig Eikeng Sterri

This thesis is published digitally through DUO and BIBSYS at the following addresses:

http://www.duo.uio.no

http://www.bibsys.no/en/

Print: Reprosentralen, University of Oslo

Abstract

Mineral processing is crucial to the modern life, as we know it, with its technology, industry and increased individual consumption. Due to this, the global demand for metals has increased correspondingly. However, the targeted metal from the ore constitutes only a small part of the total rock volume, indicating a high ratio between target metal to waste rock and tailings. Where and how to store these vast amounts varies globally due to government guidelines, and locally as storage is site specific. The most common storage option worldwide is an on-land storage site, but marine storage is also used. A mining company with experience with both solutions is Titania AS located in the southwest of Norway. The host rock is norite and the product is ilmenite concentrate ($FeTiO_2$), with the by-products magnetite and sulphides. The present solution is on-land storage, but it is estimated to reach its capacity within 2025. Prior to the on-land site, the marine storage was used with deposition into the nearby Jøssingfjord and Dyngadypet. When evaluating where to store the tailings after 2025, the goal must be an economically possible yet environmentally safe solution. The aim of this thesis was to evaluate and potentially quantify transport of metals from the mine waste at Titania AS, where nickel is regarded as the element of concern. To investigate the spread of metals from the on-land setting, water samples was gathered in the proximities of the on-land storage site, and dust filters placed in a near-by village were analysed. The marine setting was investigated by collecting box cores with “clean” fjord sediments overlain by Titania tailings, placed in a mesocosm to simulate a fjord environment. Here, electrode measurements and metal fluxes were obtained.
Results and calculations revealed a higher discharge of Ni from the on-land storage site compared to the marine. The flux of nickel from the sea deposits in the Jøssingfjord and Dyngadypet corresponded to 30% of the leakage from the land deposit.

Preface

This thesis is the final product of the two-year master programme of the Mineralogy and Geochemistry at the Department of Geosciences, The Faculty of Mathematics and Natural Sciences, University of Oslo. This thesis uses geochemical knowledge to investigate an environmental case at an industrial site in southern Norway. Helge Hellevang was the main supervisor of the thesis.

Investigating and evaluating an objective that is relevant to the current circumstances has been very awarding and motivating. NYKOS (New Knowledge on Sea Disposal) is a very interesting research project, and working close with NIVA (Norwegian Institute for Water Research) at this has been truly educational, although this thesis is only a minor contribution.

Being able to work close to, and with, experienced and inspiring people has given this thesis a lot, both from the mining company Titania AS and NIVA.

Acknowledgements

I would first and foremost like to thank my main supervisor Helge Hellevang, University of Oslo. The door was always open whenever I had questions about my research or writing. He consistently allowed for this thesis to be my own work, but always steered my in the right direction whenever needed.
I would also like to thank my co-supervisors, Morten T. Schaaning (NIVA), Per Aagaard (UiO) and Mona Schanke (Nordic Mining). Although, a special thank to Morten T. Schaanning who has been involved and encouraging from the first day. Additionally, Ann Heidi Nilsen and Elise Opsal at Titania AS for good help and continuously advice.

Furthermore, I would like to thank the professors and staff at Department of Geosciences for all help completing this thesis. Firstly, Berit Løken Berg for help and guidance with the SEM analyses. Beyene Girma Haile for sample preparation for XRD analyses and then Thanusha Naidoo for running the XRD machine. Mufak Said Naoroz for grain size analysis and ion chromatography. Siri Simonsen and Magnus Kristoffersen for help with the QICPMS analyses. Marit Villø for help in NIVA's laboratory with the preparations of the DGT-probes prior to analyses. Joachim Johansen and the crew at Trygve Braarud for obtaining the box-cores used for the experimental setup. Titania AS with sample material and data.

I must express a special thanks to Linda Lorraine Fauske for invaluable cooperation and help throughout the last two years on the master's programme.

Finally, this thesis would not been possible without the love and support from my friends and family. Thank you for the continuous encouragement throughout my years of study, and through the process of writing this thesis.

Thank you!

Hedvig Eikeng Sterri

Table of contents

1 Introduction

1.1 Thesis outline

This thesis will first introduce the current status of the mining industry, globally and at Titania AS, and the aim of study. Then the study area will be presented to introduce the ore body itself, the Norwegian mining company Titania AS and the up to date legislation. Subsequently, relevant theory and previous work will be presented. Furthermore, the methodology and materials will be explained to provide insight to the path of retrieving the results. The results chapter hereafter follows methodology. The findings will then be interpreted, compared and evaluated in the discussion chapter. Finally, summary and the conclusion are presented along with recommendations for further work.

1.2 The mining industry

As both the world's population and the individual consumption increase, the demand for mineral resources increase correspondingly (Vogt, 2013). Mineral resources are key constituents in today's society, with its industry, urban megacities and rapid growth. Mining at a global scale has accelerated, as the need for more environmental friendly and renewable solutions are required. The world needs to address the pressing issue created by the burning of fossil fuels over many decades, and the role of mineral resources in the process of a green shift is not to be ignored. An example is solar panels, which require over a dozen metals and minerals in the production (U.S Geological Survey, 2016) . These are mined from ore bodies all over the world, with Asia being the largest producer from 1984 to 2012. Over the mentioned time period, the worldwide mineral production has increased by 79 % (Reichl et al., 2014).

The demand of raw material from the mining industry is increasing, thus production increase correspondingly. This calls for best practice guidelines and up-to-date legislation that take into account placement of the colossal amount of mine waste being produced. Safe storage of these vast amounts of waste is one of the main problems from an environmental perspective, but is also an immense economic burden of industrial mining (Ramirez-Llodra et al., 2015).

The reason why mining activity produce such large volumes of waste is due to the fact that the targeted metal from the ore usually constitutes only a small part of the total rock volume. The waste is the unprocessed overburden and the processed tailings. Tailings are the residuals after several processes and steps are conducted, such as crushing, milling and grinding. These processes usually utilize chemicals that may, in certain concentrations, be toxic. Mine tailings usually also contain heavy metals such as Ni, As, Cu, Pb, Cd, Se and Hg as well as residues of process chemicals (Ramirez-Llodra et al., 2015). The share of the ore that becomes waste varies, but is about 60% for Cu and up to 99.99% for Au (Vogt, 2013).
Despite the fact that mining in some cases may not be very environmentally friendly, it is a necessity, as mentioned above. It is a shame that the legacy of poor waste treatment and management has shaped the mining industry disproportionally, so that new projects are easily rejected as a result of the bad reputation (Franks et al., 2011). Although Norway could afford to import the minerals and elements needed and hence not take a direct part in the mineral industry itself, it is important to avoid the unfortunate "not in my backyard" -way of thinking. This means that, as Norway possesses one of the largest ilmenite ore bodies worldwide, it would be somewhat ignorant to not exploit this resource. A crucial element to this is that Norway has a proper set of guidelines and legislation that will ensure the most environmentally friendly solution possible. On the contrary, other countries have created an immense environmental impact as a direct result of failure of tailings storage and management. A very unfortunate example is Mount Polley copper mine disaster in 2014, in British Columbia, Canada. Here, the mine tailings pond breached and released 10 million cubic meters of water and 4,5 million cubic meters of tailings into Polly Lake (Allen and Voiland, 2015).

Mining activity has played a central role in the economic growth of Norway for several hundred years. In the beginning and until the 1970's, the sulphide minerals were in focus. At later times, minerals and metals have become dominant, both nationally and globally. This as a result of increasing demand and good market prices (Sørby et al., 2010).
The industry experienced an extensive growth in the 16th and 17th centuries. However, the mining production only reached industrial scales 100 years ago. In the 20th century, many mines were closed, but the number of individual operations in Fennoscandia has increased since the end of

World War 2. At present times, Norway is the worlds largest producer of olivine (45%) and the third largest of nepheline syenite (15%) (Sandstad et al., 2012).
There are 40 major metallogenic areas in the Norwegian part of the Fennoscandian shield. Of these, 11 show potential for ferrous metals such as Fe, Ti and V. These areas are of different genetic types of metal deposits, but Tellnes in the Rogaland Anorthosite Province is of mafic intrusion- hosted $Ti - Fe \pm V$ origin (Sandstad et al., 2012).

1.2.1 Disposal methods

The aim of safe storage and disposal of tailings is to ensure that the tailings are, to the fullest extent possible, physically stable and chemically inert in the context of geographical position, isolation and local/ regional climate (Franks et al., 2011, Ramirez-Llodra et al., 2015). The disposal of waste rock and tailings can be done in several ways; with the characteristics of the mining site often deciding which methods is used. Hence, the disposal method is site specific. Ritcey (2005) identified the possibilities of waste disposal in the following way:

- Land- based storage
- Backfill to the mine
- Deep lake disposal
- Marine disposal
- Reprocessing for secondary metal recovery

The latter is doubtfully a possibility, as reprocessing does not address the issue of disposal. This goes for backfill as well, as it often requires an additional disposal method (Lottermoser, 2007). Each of the alternatives has certain advantages and disadvantages. These will depend on the specific ore, process and site location (Ritcey, 2005). On a worldwide basis, most industrial- size mines dispose tailings in conventional dams (Shimmield et al., 2010, Vogt, 2013). The structures are often termed “tailing ponds” or “tailings dams” (Kossoff et al., 2014). Long- term physical stability is a well-recognized problem for on-land storage (Franks et al., 2011).

Subsea tailings disposal is also an alternative, whether it is in rivers and lakes, or in the sea. Marine disposal of mine tailings are often classified into groups according to the depth at which the tailings are disposed. Ramirez-Llodra et al. (2015) define three groups:

- Coastal tailings disposal (CTD)

- Submarine tailing disposal (STD) (<100m)
- Deep- sea tailing placement (DSTP) (>100m)

Depositing mine tailings into shallow coastal waters was a common procedure, until the environmental impact of depositing tailings within the euphotic mixed zone was understood (Ellis, 2001). This zone is in the upper part of the water column, containing oxygen and the process of photosynthesis. Due to the impact of such disposal, the development of method utilizing a pipe to lead the tailings below the euphotic surface-mixing zone was engaged (Ramirez-Llodra et al., 2015). In Norway, however, there is a fourth alternative; the fjords. This type of marine disposal is debatable, but offers an alternate option, as on-land storage may be difficult due to for example characteristics such as rough topography.
This thesis will concentrate on two disposal settings: land-based storage and marine disposal. There are, as mentioned, challenges connected to each of the storage methods on a general basis. Norway´s topographic and geographic setting influences the choice, as valleys, fjords and steep mountains are commonplace and somewhat limits terrestrial storage due to the potential lack of space.

1.2.2 Mobilization of pollutants in disposal environments

When the decision on whether to store the mine tailings on land or in the marine environment are to be made, the mobilization of pollutant is of great significance. The physical and chemical properties of tailings are site specific and key to understanding the potential environmental impact and worst-case predictions. Grain size is one of the most important physical properties. This is due to the increase in ratio between surface area and volume, as the extraction processes decrease the grain size considerably. Reduced grain size has implications for both on-land and marine storage.

Mobilization in an on-land storage environment

There are generally two types of on-land storage, either the tailings are placed in a closed dam facility, or a more open system where water can drain through the tailings masses. Hence, these two types have different challenges connected to them. A closed system will reduce the weathering of the tailings considerably, especially if the tailings surface is beneath the water

table. A dam that is not closed will allow for water and air to penetrate the tailings surface and drain through the system, potentially leaching out contaminants. The possible weathering zone is no longer limited to the tailing surface (Iversen and Aanes, 2011).

A consequence of the above mentioned grain size reduction is the increased surface area per volume, which implicates that grains become kinetically prone to oxidation and the release of sorbed contaminants (Kossoff et al., 2014). Mineral processing changes the geochemical properties, and promotes mobilization and dissolution of minerals. Fresh tailings weather when exposed to oxic conditions, and secondary minerals form. The ones that will form will depend on the interaction between local conditions and source mineralogy (Kossoff et al., 2014). Oxic conditions may also lead to oxidations of sulphides, which furthermore can cause acid mine drainage (AMD). The residence time of the water draining through the tailings dam is also of considerable significance, as this may influence/determine a reactions outcome and whether or not precipitation can occur.

pH has a major influence on the mobility of trace metals, as acidic conditions increase the mobilization (Appelo and Postma, 2005).

Mobilization in a marine storage environment

Grain size is also of importance when deposing mine tailings in marine environments, as the small grain sizes are harder to settle. Due to this, mine companies has advanced the disposition technique by the use of a pipe that directs the tailings deeper down in the water column. This promotes a quicker and more predictable settling of small grains that are easily and potentially widely distributed. Additionally, by mixing tailings with seawater instead of freshwater, the density increases further. Dissolution rates will influence the magnitude of impact in marine environments. If dissolution takes place before the mineral grains have settled or at least reach bottom layers, there is an increased risk for spreading in the euphotic zone. Any discharge into this zone can spread widely with dispersion, dilution and possibly decomposition (Ellis, 2001). Bioturbation from animals such as the polychaetes, marine worms, are also of concern. This is as bioturbation causes disturbance in the sediment column, adding oxygen and providing tunnels for contaminant fluxes.

1.3 Legislation

The extractive industry is bound to act within certain rules and legislation according to the Norwegian Law and the EEA- agreement set by the European Union (EU). The framework that the industry must accommodate is, from Sørby et al. (2010):

The Pollution Control Act

This act of 13th of March 1981 nr.6 has as purpose to protect the environment against pollution and waste. Any addition of solids, liquids and gases to the surrounding water, air or ground is regarded as pollution to the environment. Waste comprise of objects or substances that are endangering or impose as a risk to nature and the given setting. Any violations must be in cooperation and authorized by the government (Miljødepartementet, 1981).

Directive 2006/21/EC on the management of waste from extractive industries

The directive ensures safe management of waste resulting from extractive industries, from the extraction itself to treatment and storage. As a facility operator needs permit to run, this directive lays down the rules for granting such permits (European Parliament, 2006).

BAT: Best available technique, and BREF: Reference documents containing information on BAT

The authorities decide what is the Best Available Technique for each site, by evaluating the local environmental setting. This means that the is BAT for one operating facility may be the contrary for another (Sørby, 2016). To coordinate the information on the site specific BAT's, have documentation and relevant experiences been gathered and sent in to the Joint Research Centre's directorate B- Growth and Innovation, by European Commission. Sustainable Production and Consumption (SUSPROC), will carry out the BREF on Management of tailings and waste-rock in mining activity, to enlighten problems, to prevent or reduce the environmental and human effects and to share knowledge (JRC DIR.B, 2015).

Due to these acts and directives, the Norwegian extractive industries are obliged to conduct thorough investigations, risk assessments and waste management plans to the authorities before

any permits are given. This will hopefully ensure, to the best ability, an environmentally friendly production and extraction.

1.4 Aim of study

When deciding what is the best practice of mine tailings management for the specific site, several factors must be considered. A very important aspect is the long-term stability and maintenance. Due to this, the overall objective of this thesis was to compare transport of heavy metals in both a marine and an on-land setting.
The broad objective hence encompasses two separate, yet interrelated, settings:

On- land storage site of mine tailings
Titania AS provides data from the landfill, which has been monitored over several years. The candidate will also gather data in form of water samples in and surrounding the tailings dam to further laboratory analyses. The on-land tailings dam is not a closed system, so water drained from the dam will reach the surroundings. This happens in a controlled manner in line with government regulations, with nickel as the primary pollutant. Transport by air and water will be examined, and quantifying to the best of ability is the prime objective.

Marine storage site of mine tailings
In cooperation with the Norwegian Institute for Water Research (NIVA), box core experiments in a fjord- environment setup will be conducted to measure metal fluxes and pore water concentrations from the Titania tailings. Investigating and potentially quantifying the leaching of metals from tailings is the prime objective.

Based upon the transport of contaminants, presumably one of the storage options will stand out as the best future storage option for mine tailings at Titania AS. The aim is to investigate and evaluate on-land and marine storage of mine tailings with focus on contaminant transport.

2 Background

2.1 Introduction

The area of study is situated in the southwest of Norway in Sokndal, Rogaland, figure 2.1. Here, Titania AS mines the Tellnes deposit. The host rock is an ilmenite-rich norite, and the product is ilmenite ($FeTiO_3$). The ilmenite is further processed into ilmenite concentrate that is a crucial feedstock for the production of white pigment (Nilsen, 2015).

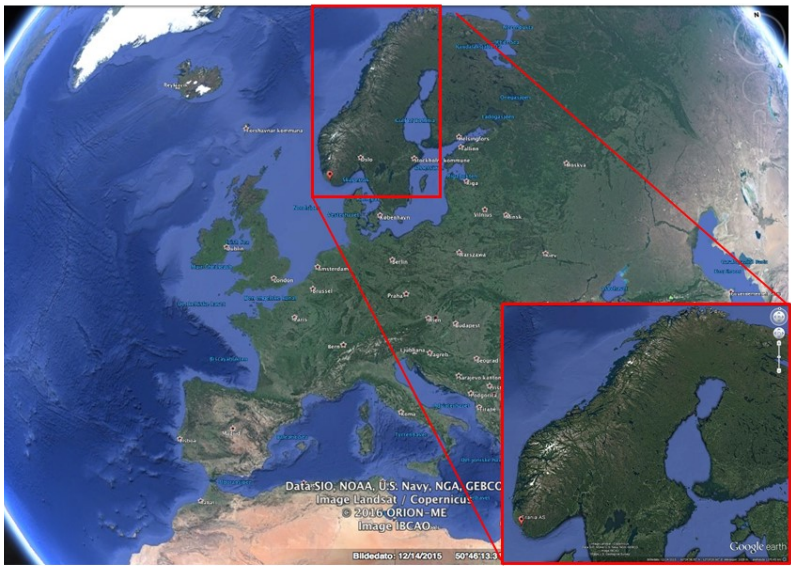

Figure 2.1: The Tellnes deposit mined by Titania AS is situated in Sokndal, southwest in Norway. Picture modified from Google Earth

2.2 Mining in the Sokndal area

Many of the known ore deposits were formed during the Caledonian rifting, subduction and collision 600-390 Ma, but the Tellnes deposit in which Titiania AS mines, is a part of the Rogaland Anorthosite Province. This province covers 1000 km^2 in the southwestern Norway. It intruded the Sveconorwegian orogenic belt of Baltica approximately 930- 920 Ma (Korneliussen and Robins, 1985, Diot et al., 2003).

2.2.1 Titania AS

A mining company that has experience with both marine and on- land storage is Titania AS, which started its production of ilmenite in 1902. Titania is situated in Sokndal in the southwest of Norway, where the mining area and the area of tailings disposal are close by, figure 2.2.

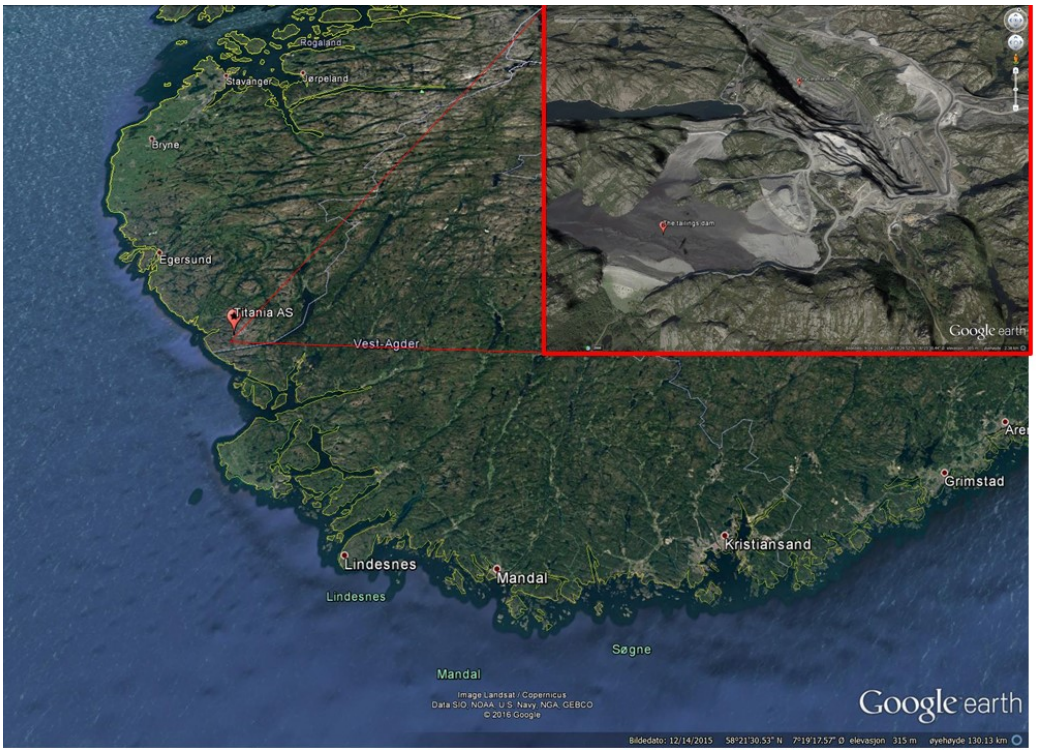

Figure 2.2: The mine area and tailings dam placement between the cities of Egersund in the north and Lindesnes in the south.

Titania AS is Europe's largest extractor of ilmenite (Neeb et al., 2012). Ilmenite is utilized as white pigment in for example paint, paper and cosmetics. Previously, Titania disposed mine tailings into the nearby fjord and coastal system, Jøssingfjord and Dyngadypet. Due to environmental organizations and legislation decided by the government, the storage placement changed into an on-land setting in 1994.

With the on-land option the Norwegian Environment Agency has imposed regulations for discharge of certain elements of primary concern. Nickel is one of these elements, and the discharge amounts can be seen in table 2.1, from Sørby and Storbråten (2016):

Table 2.1: Discharge of Ni with source and recipient

Source	**Recipient**	**Component**	**Permit** (kg/ 24 h)
On-land storage site	Logsvassdraget	Nickel (Ni)	1.5
On-land storage, open-pit mining, ore dressing plant and drying plant	Jøssingfjord	Nickel (Ni)	6.0
Old on-land storage site at Sandbekk	Sandbekk river	Nickel (Ni)	1.5

Titania has many years of experience in mine tailings management, as the company has had both marine and on-land storage. In the beginning, Titania utilized the on-land disposal option for the tailings produced. Then, the marine option was chosen. The waste was deposited first in Jøssingfjord, and then later in Dyngadypet when the first site was filled up. This caused a lot of debate in the media, with environmental organisations together with the Norwegian Institute for Marine Research trying to get the government to force on-land storage instead. The debate and disagreement went on for about a decade before the final decision was made in 1993, which stated that hereby the mine tailings must be stored in an on-land dam. This is the option used at the present, but the storage dam will be full within the next eight to ten years. Hence, a thorough evaluation of the alternatives must be carried out in order to make the best decision possible.

2.2.2 The Tellnes mineral deposit

The "Rogaland Anorthosite Province" comprises three anothosite plutons, where Tellnes is situated in the easternmost pluton Åna-Sira anorthosite massif (Charlier et al., 2015). The Tellnes deposit makes the core of the Tellenes- Sokndal area, which is a world-class titanium deposit. It produces more than 800 000 tons of ilmenite concentrate, which corresponds to 6-7 wt.% of total production of Ti-minerals in the world by TiO_2- content (Sandstad et al., 2012, Charlier et al., 2007).

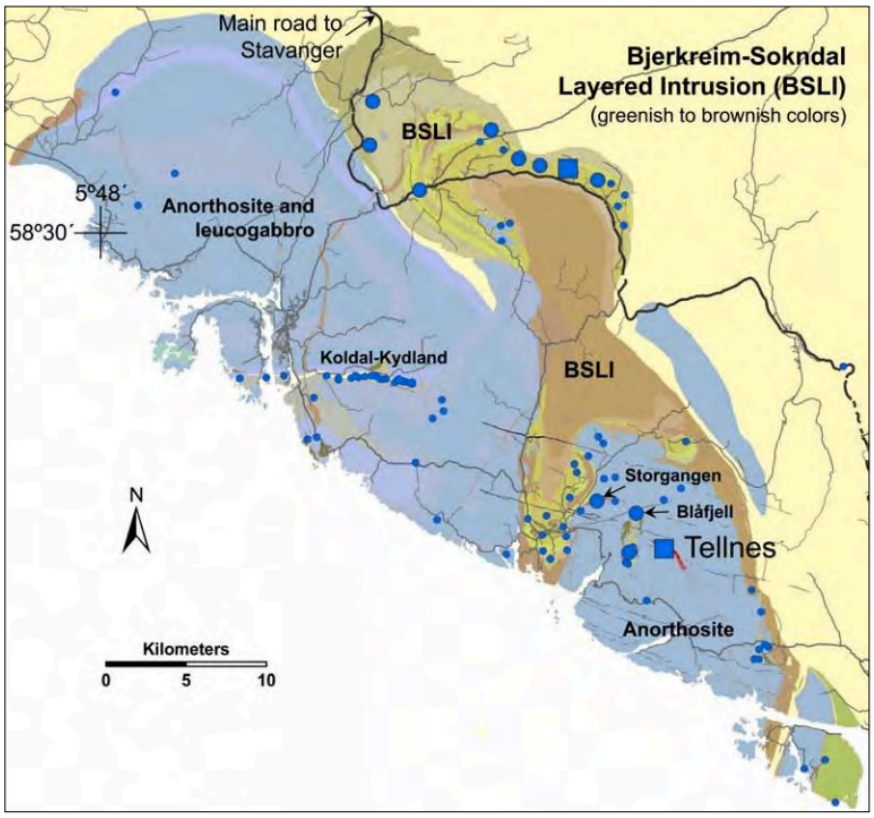

Figure 2.3: Map from Sandstad et al. (2012), where the components of the Åna-Sira massif can be seen in the southeast. The most known deposits in this massif is Blåfjell, Storgangen and Tellnes.

The Rogaland Anorthosite Province contains several Fe-Ti oxide occurrences, and the Åna-Sira massif comprises of three of the most known deposits: Blåfjell, Storgangen and Tellnes, figure 2.3. They have different economic importance, which has changed over time from coarse grained lump ore to a more fine-grained ore (Krause et al., 1985). Tellnes is by far the largest, and the body is a trough-shaped, 3 km long and 600 m wide intrusion that plunges eastwards at depth. The composition is fairly homogeneous, but complex. Its average modal composition comprise 53 vol.% plagioclase (An45-42), 29 vol.% hemo-ilmenite, and 10 vol.% orthopyroxene, together with biotite and accessary amounts of olivine, magnetite, clinopyroxene, apatite and sulphides (Sandstad et al., 2012). From an economical point of view, the major and trace metal composition is very important for industrial ilmenite, especially the pollutants Mg and Cr (Charlier et al., 2007).

The Tellnes ilmenite is characterized as a hemo- ilmenite. This influences the TiO_2 content of the ore body in at least two ways. A significant hematite component will decrease the TiO_2 content relative to the stoichiometric ilmenite (52,89% TiO_2), and the MgO- solid solution with FeO in the crystal lattice of the ilmenite is also a TiO_2- reducing factor (Korneliussen and Robins, 1985). Nonetheless, there are some benefits being a hemo- ilmenite as well. Hemo- ilmenites are very suitable for the sulphate process in the TiO_2 pigment production as hematite lamellae dissolves more easily in acids than homogeneous ilmenite (Sandstad et al., 2012). The intrusion is interpreted as a result of gravity-induced subsidence of a sub-horizontal sill with jotunite as a parental magma. However, it is difficult to distinguish if the parental magmas have been produced by melting mantle or by melting mafic lower crust. Nevertheless, the Rogaland Anorthosite Province yield high initial $^{187}Os/^{188}Os$, which indicate a crustal source (Charlier et al., 2015).

Titania AS has analysed the ore mineralogy and gangue and got the following compositions, see table 2.2 and 2.3.

Table 2.2: Ore mineralogy analysed by Titania

Ore mineralogy

Mineral	Formula	Weight%
Ilmenite	$(FeO,MgO)TiO_2$ (Hem_{13})	39,9
Orthopyroxene	$(Mg,Fe)SiO_3$ (En_{77-75})	8,6
Clinopyroxene	$(Ca(Mg,Fe)AlFe^{3+}Ti\{(Si,Al)_2O_6\}$	6,5
Plagioclase	$(NaAlSi_3O_8)(CaAl_2Si_2O_8)$ (An_{45-42})	36,9
Biotite	$K(Mg,Fe)_3\ \{AlSi_3O_{10}\}\ (OH,F)_2$	4,2
Spinel	$(Mg,Fe,Zn)Al_2O_4$	1,5
Magnetite	Fe_3O_4 (ilmeno-magnetite)	1,5
Apatite	$Ca_5(PO_4)_3(F,Cl,OH)$	0,6
Sulphides*	$FeS_2Fe_{1-x}S,(Fe,Ni)_9S_8,CuFeS_2$	0,3

*FeS_2 occurs as pyrite and marcasite, $Fe_{1-x}S$ – Pyrrotite, $(Fe,Ni)_9S_8$ – Pentlandite, $CuFeS_2$ – Chalcopyrite

Table 2.3: Gangue mineralogy analysed by Titania

Gangue mineralogy

Mineral	Weight (%)
Plagioclase	50
Pyroxene	10
Biotite	7
Silicates (other)	5
Ilmenite	15
Apatite	0.5
Sulphides	0.2

The sulphides in the Tellnes ore appear as aggregates in intergrowths where the main minerals are either pyrrotite ($Fe_{1-x}S$) or pyrite ($FeS_{2)}$. Other minerals that are present but rare are pentlandite ($(Fe,Ni)_9S_8$), chalcopyrite ($CuFeS_2$), millerite (NiS), siegnite (Ni_2FeS_4) and violarite ($(Co, Ni)_3S_4$ (Mellgren, 2002).

2.2.3 Mineral processing at Titania AS

To finally be able to extract the economically valuable minerals, the crude ore must endure several steps in the industrial mining process, figure 2.4. First of all, the ore body is crushed into smaller and smaller pieces; until the grain-size is small enough that ilmenite appears as individual grains. Furthermore, the mineral separation phase can be performed, in order to the fullest extent possible separate and hence concentrate the mineral of economic value from the gangue, which has no/little economic value. This can be done by several different techniques, but at Titania the processes are 75% gravimetric separation and 25% flotation. Flotation is a versatile method that is used to separate ore minerals from gangue minerals, which Titania uses. The particles are physically separated by the differences in the ability of air bubbles to selectively connect to specific mineral surfaces. The air bubbles attract the hydrophobic particles that rise to the surface, where they can be collected (Ramirez-Llodra et al., 2015). When conducting the

flotation method, chemicals and oils such as tall oil, kerosene and sulphuric acid are added to affect the surface of the mineral grains to obtain the hydrophobic effect mentioned above. This was the original separation method used, but this is reduced to only about 30%. At the present, the majority of the separation is done by gravitational separation followed by dehydration, which results in a reduction of chemicals used and released to the environment (Sæland, 2007). Gravity separation is a technique that separates the heavy minerals (ilmenite) from the lighter (plagioclase, orthopyroxene) with water and the effect of gravity. Hence, the specific gravity of components is used for separation. Moreover, CaO is used in the thickeners, after the flotation process. This is to separate out the water that is lead to the process water (Tellenesvannet), while the settled fine particles are sent to the tailings dam. The extracted concentrate of ilmenite, magnetite and sulphide are transported to the drying plant, close to the loading pier. In close proximities to this area, there are separate silos containing the ilmenite, the sulphides and the magnetite. The drainage system ensures circulation of the process water.

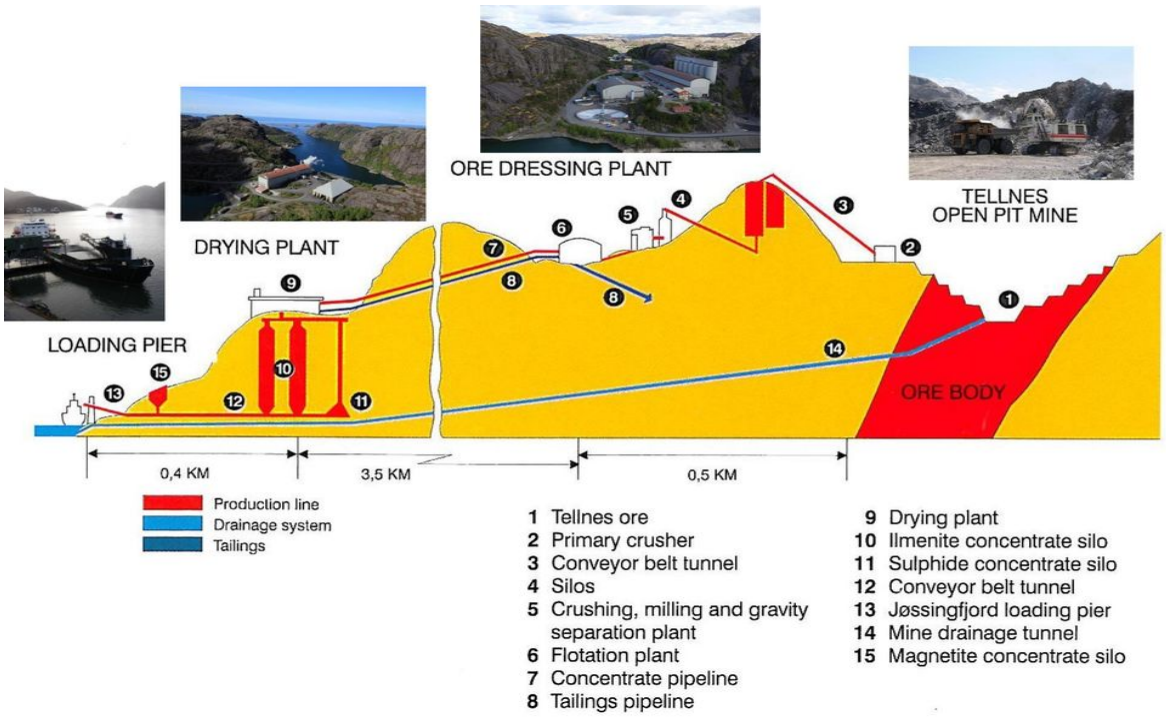

Figure 2.4: An overview of the processes at the Tellnes plant. Figure from Nilsen (2015). The numbers indicate the steps in the process from ore to concentrate.

2.3 The storage sites

An overview of the storage sites are presented in figure 2.5. The on-land storage sites are Sandbekk from 1916 to 1965 and Tellenes from 1994 until present. The marine storage sites are the Jøssingfjord site from 1960 to 1984 and later Dyngadypet from 1984 to 1994.

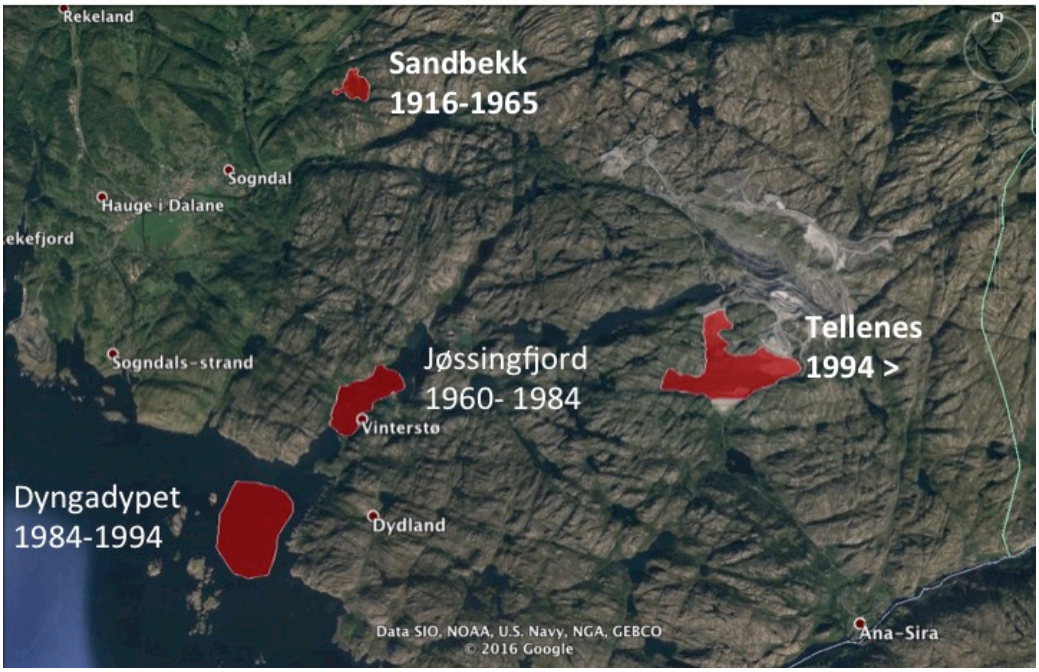

Figure 2.5: The storage sites in which Titania has placed their tailings. First at on-land at Sandbekk (1916-1965), then marine in Jøssinfjord (1960-1984) and Dyngadypet (1984-1994), and finally back on land at Tellenes (1994- until present). Map modified from Google Earth.

2.3.1 On- land storage sites

Since Titania AS started the mineral ore extraction in 1902, several different disposal settings and sites has been utilized to handle the mine tailings. The initial storage site was the Sandbekk landfill (1916-1965), where the coarse gangue material was piled up in large heaps while the more fine-grained gangue was released into the Sokndal River (Sæland, 2007). The Sandbekk landfill contains approximately 6 million tons mine waste.

Since 1994, the Tellenes on-land storage site was used for the mine tailings. The landfill covers 1,3 km^2. Titania still use the Tellnes landfill to store the mine tailings, but predictions state that it will reach its capacity within 2025 (Nilsen, 2014).

2.3.2 Marine storage sites

From 1960 to 1994, Titania AS switched over to the marine tailings disposal technique; storing the mine waste at the bottom of Jøssingfjord and later at Dyngadypet, figure 2.6. Jøssingfjord was filled up quite readily as the amount of waste deposited was 2 million tons per year, and consequently the depth was reduced from 70 m to 25 m from 1960 to 1984. Then, as Jøssingfjord was filled to capacity, Titania was permitted to deposit at Dyngadypet, a basin a bit further outwards from the fjord. Over the ten years Dyngadypet was used to dispose tailings (1984-1994), the basin depth was reduced from 170m to 140m (Ibrekk et al., 1989, Sørby et al., 2010). The Tellnes landfill was opened in 1994, when the government decided that Titania could no longer use the marine disposal technique. This was due to the larger area of tailings spread than was predicted in advance. This was said to have consequences for the aquatic life in the upper areas of the water column, as for example shrimps were found to have black particles in their gills that lowered their economic value. The large spread occurred because at that time, seawater was not mixed with the tailings. This is done to achieve a density of the suspension that exceeds the seawater density, so that the tailings plume will sink towards the basin bottom. Additionally, the mix was not de-aired to remove all air bubbles (Sørby et al., 2010)

Before deciding to store mine tailings in the nearby coastal areas of Titiania AS, and continuously during disposal, investigations of the water bodies in the area have been conducted. This has been done to determine the spread of contaminants, the influence on the marine fauna and the degree of water turbulence. After the change of disposal site, Titania AS is still obligated to regularly review the affected area.

The Jøssingfjord is originally a sill fjord that opens out at the Dyngadypet, which is at a deeper depth than the Jøssingfjord. A sill fjord is a fjord that is partly separated from the outer basin by a threshold, usually caused by a reduction of erosion by the glaciers mouth (IMR, 2013).

Outside the Dyngadypet basin, lays the Dyngadypet- Sirevåg area, which is an open coastal area. Table x summarizes the water body classification of the placement sites used by Titania AS and the surroundings (Trannum, 2016).

Table 2.4: Water body classification from Trannum (2016)

	Classification	Water residence time	Current	Water column
The Jøssingfjord	Protected coast/fjord	Moderate	Weak	Partially divided
Dyngadypet	Deep basin (170m)	Moderate, only one passage out of the basin	Dominated by coastal flow, NW direction	Unknown
Dyngadypet-Sirevåg	Open, exposed coast	Short	Weak	Permanently mixed

The water body characteristics are of great importance when mine tailings are disposed in the marine/fjord setting. A water body that experiences turbulence and strong currents through water column will not be suitable for storage of mine tailings as the constant movement may cause severe spread and flux of contaminants (Sørby et al., 2010, Ramirez-Llodra et al., 2015).

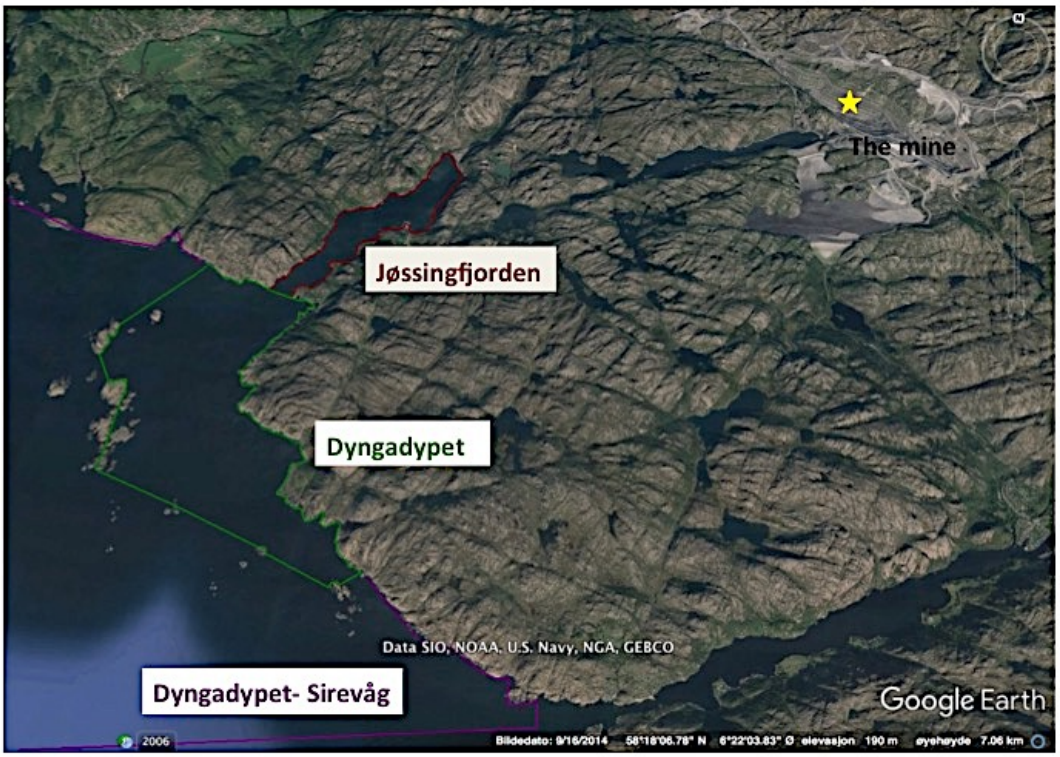

Figure 2.6: The water bodies used as marine storage sites. Jøssingfjord and Dyngadypet were the two disposal sites, but Dyngadypet-Sirevåg that is the open coastal areas outside the sites must also be evaluated. Map from Google Earth, modified after vann-nett.no

3 Theory and previous work

3.1 Introduction

This master's thesis includes certain theoretical considerations in order to describe the contaminant transport in different mediums. Chapter 3 will provide these considerations, comprising elaboration factors that play a vital role in transport. The focus will be especially on the pollutants Ni and Cu.

3.2 Geochemical considerations

This section's aim is to introduce important geochemical consideration regarding the reactions and properties of the tailings at Titania. This is a substantial aim, as the system is very complex with several unknown factors. However, the basic concepts of the main processes and influences on the system will be presented.

3.2.1 Solubility and the solubility product, K_{sp}

Solubility is defined as the upper limit of solute that can be dissolved in a solvent at the point of equilibrium. Le Chaterlier's principle is important in this matter, as it can be used to explain the main factors that affect solubility. This is as Le Chaterlier's principle says that the amount of stress on a system can be predicted, as the system will shift to alleviate the stress. The solubility of minerals is strongly linked to the principles of equilibrium and the law of mass action. The law of mass action states that for a reaction

$$aA + bB \leftrightarrow cC + dD \tag{3.1}$$

the distribution of equilibrium is given by

$$K = \frac{[C]^c\,[D]^d}{[A]^a[B]^b} \tag{3.2}$$

here, the K is the equilibrium constant and the bracketed quantities are activities (effective concentrations). At equilibrium the amount of products and reactants remain the same at a macro

level, however the reaction does not stop. The transfer of particles still occur, hence equilibrium is dynamic. The law of mass action allows for concentration calculations of the given reaction (Appelo and Postma, 2005).

For solid solutions, the solubility product can then be explained like the following: An ionic compound X_nY_m is slightly soluble in water. To form a saturated solution, some solid dissolves

$$X_nY_m(s) \leftrightarrow nX^+(aq) + mY^-(aq) \quad (3.3)$$

When the solution is saturated, the mixture achieves equilibrium at a given temperature.

$$K_{sp} = [X^+]^n \times [Y^-]^m \quad (3.4)$$

K_{sp} is the solubility product of the ionic compound, and shows the interaction between the ions in the given solution. Hence, more soluble salts having higher K_{sp} values, while less soluble salts having lower K_{sp} values. K_{sp} are affected by temperature (King, 1959).

The solubility product of the present mineral phases will hence play a key role to how the reactions will occur in the mine tailings being deposited. An insight in this can therefore indicate which mineral phases easily dissolve, and which precipitates out and remains stable. One could imagine the precipitation of a stable compound that includes for example Ni would be of value, in such a way that the pollutant would be bound up in a mineral. The metal sulphides all have relatively low K_{sp} values, denoting low solubility and are generally insoluble in water, table 3.1 (Sampaio et al., 2009). However, in oxidizing environments S can oxidize to SO_4, which then will dissolve more easily.

An increase in Ni^{2+} concentration would result from for example NiS dissolving during the mining processes at Titania. Then, the chemical pathway of Ni and to which compound it is precipitated with will be of great importance to predict the subsequent leaching of Ni. Ni could again form the relatively insoluble NiS depending on the presence of S, and if pH conditions would allow it. Another option is the soluble compound $NiSO_4$, which easily could release the Ni again when the solubility product is exceeded.

Table 3.1: solubility product constants of metal sulphides at standard conditions (25°C, 1atm) from (Sampaio et al., 2009).

Metal ion	Log K_{SP} (metal sulphide)
Hg(II)	-52,4
Ag(I)	-49,7
Cu(I)	-48,0, -48,5
Cu(II)	-35,1
Cd(II)	-27,7 -25,8
Pb(II)	-27,0, -27,5
Zn(II)	-23,8
Ni(II)	-20,7
Fe(II)	-17,3

However, by the oxidation of pyrite (the steps are further investigated in section 3.2.3) sulphate is produced. Sulphate is a salt, and hence much more soluble than sulphides. Furthermore, Ni bound as nickel sulphide, (NiS), is more or less insoluble in water, whereas Ni bound as nickel sulphate, ($NiSO_4$), is reported with the solubility of 65.5 g/100 mL at 0°C (EuropeanCommission, 2011). Table 3.2 display reactions involved in the breakdown of common sulphide minerals (Konhauser, 2006).

Table 3.2: Reactions involved in the breakdown of common sulphide minerals. From Konhauser (2006)

Mineral	**Reactions**
Chalcopyrite	$4CuFeS_2 + 17O_2 + 2H_2SO_4 \rightarrow 4CuSO_4 + 2Fe_2(SO_4)_3 + 2H_2O$
Covellite	$CuS + 2O_2 \rightarrow CuSO_4$
Chalcocite	$5Cu_2S + 0.5O_2 + H_2SO_4 \rightarrow CuSO_4 + Cu_9S_5 + H_2O$
Bornite	$4Cu_5FeS_4 + 37O_2 + 10H_2SO_4 \rightarrow 20CuSO_4 + 2Fe_2(SO_4)_3 + 10H_2O$
Sphalerite	$ZnS + 2O_2 \rightarrow ZnSO_4$
Galena	$PbS + 2O_2 \rightarrow PbSO_4$
Arsenopyrite	$4FeAsS + 13O_2 + 6H_2O \rightarrow 4FeSO_4 + 4H_3AsO_4$
Stibnite	$2Sb_2S_3 + 13O_2 + 4H_2O \rightarrow (SbO)_2SO_4 + (SbO_2)_2SO_4 + 4H_2SO_4$
Millerite	$NiS + 2O_2 \rightarrow NiSO_4$
Molybdenite	$2MoS_2 + 9O_2 + 6H_2O \rightarrow 2H_2MoO_4 + 4H_2SO_4$

3.2.2 Temperature and pH

Temperature

Temperature is important for reaction rates, diffusion, solubility and dissolution, and will all be affected in their own way.

Temperature affects solubility of solids depending on whether the reaction is endothermic or exothermic. Bearing in mind Le Chaterlier's principle, the temperature effect in both situations can be predicted. From Grønneberg et al. (2013):

- Endothermic reaction, $\Delta H > 0$. Increasing the temperature will produce stress on the reactants side; hence the system will shift towards the product side to relieve this stress. This will result in more of the solid being dissolved when equilibrium is again restored, thus giving increased solubility.
- Exothermic reaction, $\Delta H < 0$. Increasing the temperature will produce stress on the products side; hence the system will shift towards the reactants side to relieve this stress. This will result in less of the solid being dissolved when equilibrium is again restored, thus resulting in decreased solubility.

The rate of most reactions is highly temperature dependent. As seen by the Arrhenius equation from Appelo and Postma (2005) , the rate constant changes with temperature

$$\ln k = \ln A - E_a/RT \tag{3.5}$$

where A is the pre-exponential factor, E_a is the activation energy (kJ/mol), R is the gas constant and T is absolute temperature. The activation energy is here important. It differs significantly for chemical reactions and transport. The activation energy is very high for diffusion in solids (500 kJ/mol), which implies an evident effect for small temperature increase from 10°- 20°C (Appelo and Postma, 2005). Temperature usually has an impact, and will in most cases increase the rate, as the molecules will have more thermal energy.

pH

Sulphides (S^{-2}, HS-) are very reactive with metal ions over a broad pH range. This is taken advantage of in the sulphide precipitation industry to remove lead, copper, nickel, cadmium, zink etc. from wastewaters and polluted waters in near proximity to industrial sites such as a mine-processing site (Huisman et al., 2006).

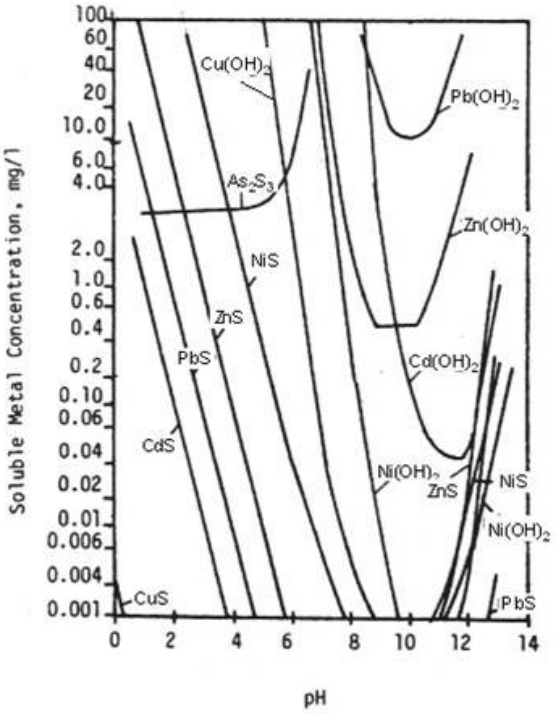

Figure 3.1: The equilibrium concentrations of metal sulphides and metal hydroxides as a function of pH. The sulphides react over a broader pH range than the metal hydroxides (Huisman et al., 2006).

Figure 3.1 displays the equilibrium concentration of metal sulphides and metal hydroxides. It is evident that the metal sulphides react over a broader pH range than the metal hydroxides, potentially leaving lower effluent concentrations. Hence, the precipitation of NiS can be done without interfering with other metal sulphides if it is not desired (Huisman et al., 2006). If pH is held at high levels (pH >10), the metal sulphides presented in figure 3.1 will not precipitate from solution.

On the surface of oxides and hydroxides, the surfaces gain a pH dependence due to sorption of protons and other ions in solution (Appelo and Postma, 2005). The general trend is that cations

will sorb at high pH, while anions will sorb at low pH. Furthermore, basic solutions will mobilize anions, while acidic mobilize cations.

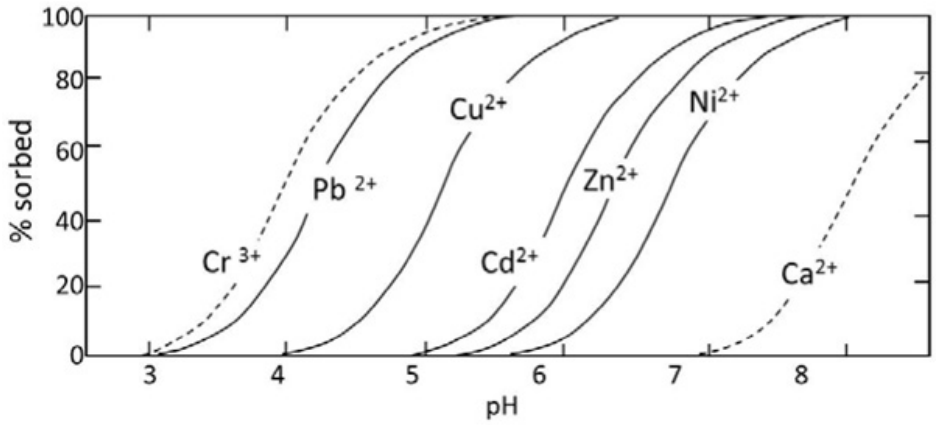

Figure 3.2: Adsorption of heavy metals on ferrihydrite as a function of pH (Stumm and Sulzberger, 1992)

Figure 3.2 shows adsorption of heavy metals on ferrihydrite as a function of pH as found by Stumm and Sulzberger (1992). All metals show no sorption at low pH, and increasing sorption with increasing pH. This may indicate that the protons are competing with the metal ions for the sorption sites (Appelo and Postma, 2005).

The pH is hence crucial to the mineral phase to where the heavy metals may be attained. At low pH levels, heavy metals are no longer sorbed, and hence are released to the surrounding environment.

Oxidation of sulphides are acid producing processes, as will be further described in section 3.2.3. Consequently, this will lower the pH of the system. The overall pH of a system is a function of several parameters, such as the access to oxygen or Fe^{3+} that drive oxidation processes, the buffer capacity of other minerals present (or added) and the reactants that are prone to oxidation, such as sulphides (Mellgren, 2002).
The buffer capacity, or alkalinity, is known as the water's capacity to resist changes in pH (Appelo and Postma, 2005). The main sources of alkalinity in natural systems are rocks that contain carbonate, bicarbonate and hydroxide compounds, and the main contribute to alkalinity in seawater is bicarbonate and carbonate. The average pH of seawater is measured to be 8.1- 8.2

(Doney et al., 2009, Marion et al., 2011). The seawater's buffer capacity is an important factor in the marine disposal setting, where the buffer capacity does not allow for the same pH drop by oxidization processes.

3.2.3 Acid mine drainage (AMD) and oxidation processes

Some ore bodies contain sulphides along with the mineral/ element of economic value. The sulphide bearing ores can generate acids when in contact with an oxidizing environment, and this is called Acid Mine Drainage (Parbhakar-Fox and Lottermoser, 2015). Although the ore that Titania mines is not particularly sulphide rich, the concept of AMD must be investigated due to its severe consequences. As mentioned, at Titania the tailings are placed in a tailings dam, and although manually watered, it has access to oxygen. The potential AMD- processes are of highest magnitude when tailings are exposed to weathering by oxygen. Formation of AMD when the sulphide-containing tailings are covered in water is considered negligible (Mellgren, 2002).

Pyrite is a common example of an iron sulphide present in waste rock of mines, and can be used to predict the steps leading to acid mine drainage. The overall process is described by the reaction from Appelo and Postma (2005):

$$FeS_2 + {}^{15/4}O_2 + {}^{7/2}H_2O \rightarrow Fe(OH)_3 + 2SO_4^{2-} + 4H^+ \quad (3.6)$$

The strong acid generation of pyrite oxidation is evident as 4 moles of H^+ are produced per 1 mole of pyrite. As long as pH>2, $Fe(OH)_3$ will form as seen in reaction 3.6 above.
There are several steps in the process of pyrite oxidation, whereas oxidation of disulphate to sulphate by O_2 is the first step:

$$FeS_2 + {}^{7/2}O_2 + H_2O \rightarrow Fe^{2+} + 2SO_4^{2-} + 2H^+ \quad (3.7)$$

Next, oxidation of ferrous iron to ferric iron by oxygen occurs:

$$Fe^{2+} + {}^{1/4}O_2 + H^+ \rightarrow Fe^{3+} + {}^{1/2}H_20 \quad (3.8)$$

Subsequently, hydrolysis and precipitation of ferric complexes and minerals:

$$Fe^{3+} + 3H_2O \rightarrow Fe(OH)_3 + 3H^+ \quad (3.9)$$

The oxidation rate of sulphide- containing tailings depends on several factors and the combination of them. The factors comprise, as stated by Mellgren (2002) the following:

- Exposed surface area
- The concentration of ferric iron (Fe^{3+})
- Bacterial activity and mediation
- pH and oxygen concentration, section 3.2.2
- Temperature and activation energy, section 3.2.2

As grain size is drastically reduced through the mining process, the surface area to volume ratio is increased. This meaning more exposed surface area, and hence the reaction rate increase (Kossoff et al., 2014, Lottermoser, 2007).
The ferric iron resulting from the oxidation of ferrous iron (eq. 3.8) is recognized as a stronger oxidant that O_2, even at neutral pH values (Lottermoser, 2017). If the ratio Fe^{3+}/Fe^{2+} is high and there is available oxygen the oxidation rates will increase.

Bacteria can mediate the rates of sulphide oxidation as well. Two bacteria types would be of particular interest in the on-land setting are acidophilic bacteria that oxidize the sulphides, or sulphate reducing bacteria. However, in the on-land storage site at Titania there might not be suitable environment for either bacteria type. This is as the pH is not low enough for the acidophilic bacteria and there is no organic carbon source for the sulphate reducing bacteria (Mellgren, 2002).
However, the sequence of redox zones divided into distinct biogeochemical zones are bacterial mediated. This is an important sequence in the marine disposal setting, as microbial processes are crucial when the oxygen is readily depleted in the upper sediments, figure 3.3.

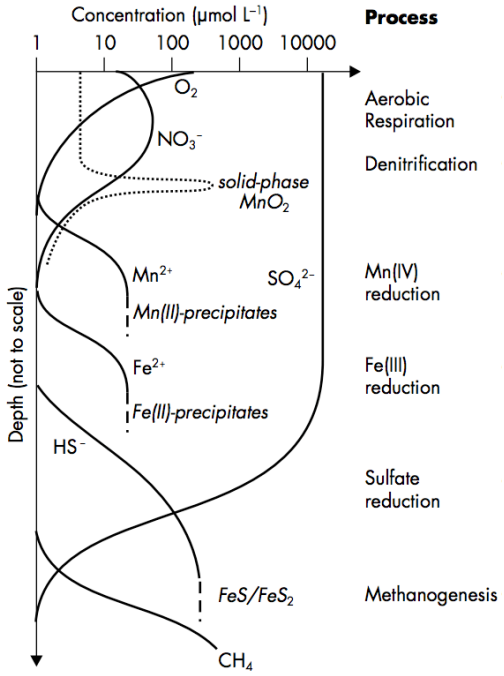

Figure 3.3: Redox sequence in sediments showing the dominant microbial community growing at a particular depth (Konhauser, 2006).

Figure 3.3 displays the microorganisms that are metabolically active at certain depths. The sediments are broadly explained as *oxic*, *suboxic* and *anoxic* by the levels of dissolved O_2 in the pore waters (Konhauser, 2006). The highest redox potential occurs when there is an O_2-abundance, however O_2 is readily depleted in the sediment column. Nitrate is the second most effective oxidant, and denitrifying bacteria consume nitrate and release N_2. As the nitrate concentration decreases, Mn and Fe oxides become abundant. Mn^{2+} and Fe^{2+} are stable in solution. Furthermore, sulphidic conditions are brought about by the bacterial reduction of sulphate to H_2S. Finally, formation of CH_4 (Appelo and Postma, 2005).

When Mn^{2+} and Fe^{2+} are stable in solution, upward migration may occur bringing the ions closer to the sediment surface and in a more oxic environment. The reduced species of Mn and Fe are oxidized by the following reactions

$$Mn^{2+} + {}^{1/2}O_2 + H_2O \rightarrow MnO_2 + 2H^+ \qquad (3.10)$$

$$Fe^{2+} + {}^{1/4}O_2 + {}^{5/2}H_2O \rightarrow Fe(OH)_3 + 2H^+ \qquad (3.11)$$

Hence, Mn^{2+} and Fe^{2+} are oxidized and precipitates as MnO_2 and $Fe(OH)_3$, which is acid producing (Rincón-Tomás et al., 2016, Schaanning et al., 2017).

3.3 Transport of metals

The transport of metals in sediments occurs by aqueous diffusion and advection, and is affected by dispersion and chemical interactions with the solid. These processes will be presented below from Appelo and Postma (2005).

Diffusion

Diffusion is a very slow process in stagnant water. It occurs by spreading of solutes (contaminants) due to concentration differences, as a result of Brownian motion. It causes the solutes to spread out from its source following a Gaussian distribution. Diffusion follows Ficks' law: the contaminants move towards a zone of lower contaminant concentration. Ficks' first law relates the flux of a chemical to the concentration gradient (Appelo and Postma, 2005):

$$F = -D \frac{\partial c}{\partial x} \tag{3.12}$$

where F is the flux (mol/s/m^2), D the diffusion coefficient m^2/s and c the concentration (mol/m^3). The effective diffusion coefficient (D*) accounts for transport through porous media.

Dispersion

Dispersion is the second important transport mechanism. Dispersion is a process that spread solutes due to flow of water, and it tends to level out special differences in concentration. It is driven by the concentration gradient, as a function of average flow velocity and its variability. There are two variations of dispersion;

- Longitudinal: in the direction of flow
- Transverse: perpendicular to flow

The dispersion term is defined as the sum of mechanical dispersion and diffusion. Mechanical dispersion is mixing that occurs as a result of local velocity variations around the mean velocity of flow, meaning spreading by the water itself (Appelo and Postma, 2005). The hydrodynamic

dispersion coefficient, D_L, is the combination of mechanical dispersion and molecular diffusion (simply called diffusion).

$$D_L = D_e + \alpha_L v \tag{3.13}$$

where D_L is the hydrodynamic diffusion coefficient, D_e is the effective diffusion coefficient, (m^2/s) α_L is the dispersivity (m), and v is velocity (m/s).

3.4 Previous work

There are several reports and investigations done by the Norwegian Environment Agency, various consulting companies and educational institutions prior to this thesis. However, many of these have had a specific aim of a subpart of the total system. The titles of the most used work, and hence the literature in which this thesis has been based upon, will be presented below. Additionally, the thesis has been constructed by numerous other sources that can be found in the bibliography.

The Norwegian Environment Agency

- Sørby and Storbråten (2016) *Tillatelse til virksomhet etter forurensingsloven for Titania AS*
- Miljødirektoratet (2017) *Revisjonsrapport: Revisjon ved Titania AS*

NIVA (Norwegian Institute of Water Research)

- Ibrekk et al. (1989*) Miljøkonsekvensutredning: Landdeponi og sjødeponi, Titania A/S*
- Schaanning et al. (1992) *Konsekvenser av utslipp fra tørkeanlegget ved Titania A/S*
- Sørby et al. (2010) *Bergverk og avgangsdeponering: Status, miljøutfordringer og kunnskapsbehov*
- Trannum (2016) *Overvåking av marin bløtbunnsfauna for Titania A/S i 2015*

Geode Consult AS

- Ettner and Sanne (2016) *Tiltaksorientert overvåkning, resultater 2015. Titania AS*

Norwegian University of Science and Technology (NTNU)

- Myran (2007) *Rapport Støvnedfall Titania, Åna-Sira*

MSc theses

- Mellgren (2002) *Dissolved nickel in the Lundetjern land deposit- Identification of main causes and methods for treatment*
- Gravdal (2013) *Stability of heavy metals in submarine mine tailings: a geochemical study*

4 Materials and methods

4.1 Introduction

This chapter will explain and justify the methods used in this thesis. As there are several options when obtaining results, choosing the right methods are important to achieve the most scientific correct outcome. This chapter will hence describe the equipment and techniques used in the on-land and marine setting.

The sample material for the on-land setting comprises dust filters quantifying wind-blown material, water samples representing the dam and the surrounding mine area and a material sample of the mine tailings. For the marine setting, box cores containing sample material from Titania AS were observed and then used to measure metal flux, pore water concentrations, bioturbation and the redox conditions.

The methods used in this thesis consists of Scanning Electron Microscope (SEM), grain size distribution, x-ray diffraction (XRD), ion chromatography Quadropole Inductively Coupled Plasma Mass Spectrometer (QICPMS), box cores, electrode measurements of pH, Eh and Es, the Diffusive Gradients in Thin films- technique (DGT) and metal flux measurements.

4.2 Collecting sample material

The sample material used in this thesis has both been gathered in field as well as supplied by Titania AS and NIVA. The total material collected encompasses nine water samples from the tailings dam and the surrounding streams and lakes, and one solid sample from the tailings dam itself. Most of the water samples were gathered and analysed twice, November 2016 and April 2017. Titania AS provided with two dust filters placed in the closest village Åna-Sira, as well as monitoring data with continuous measurements of trace metal content from the outlet zones and climatic data of the area.

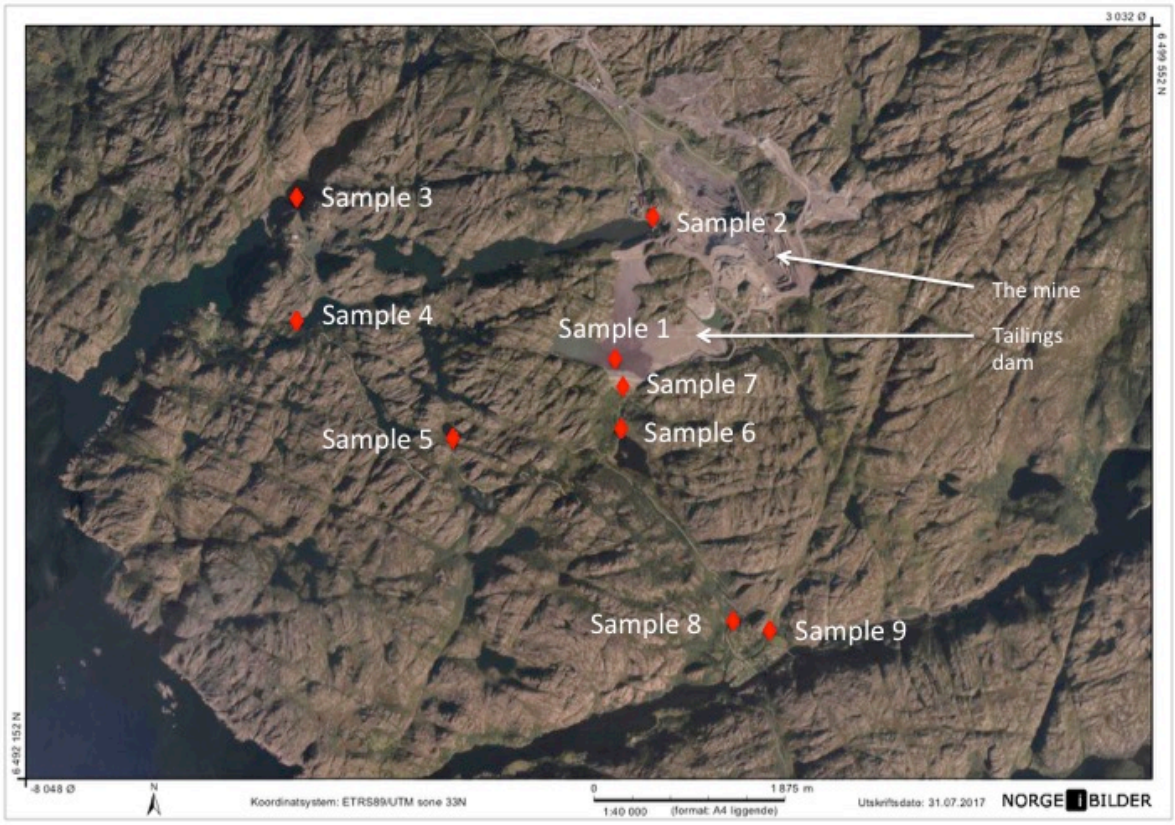

Figure 4.1: Map with an overview of the water samples taken at, and around, the tailings dam at Titania AS. Modified from Norgeibilder.no

The aim of gathering the water samples was to investigate the entire water system adjacent, and on, the mine tailings dam. Hence, nine samples were taken for further analysis to inspect element concentrations and distribution. From figure 4.1 above, the locations of the water samples can be seen. These locations were chosen to ensure capturing the drainage pattern of the tailings dam and to analyse the water bodies that is not directly affected by the tailings dam. The plastic centrifuge tube with cap were washed in the water sample to avoid contamination, and then properly sealed and marked. This procedure was followed for all nine samples, and the measurements were done twice (November 2016 and April 2017) at the same locations.

Collecting the solid sample from the tailings dam is similar to the above-explained technique, only at a bigger scale with a larger container. This material was used for the box-cores in the

marine setting experiment as well, to demonstrate and calculate the effect of these tailings in seawater with benthic fauna present.
The water samples were collected November 23 2016 and then secondly at 20th of April 2017. When collecting the samples in April, there was no production at Titania AS, which consequently made sample 1 and 2 unattainable.

4.3 Methods applied for the on-land disposal setting

After collecting the samples in the field, and retrieving the dust filters from Titania AS, they were prepared so that they met the requirements for the given machines used. Dust filters were examined by SEM (Scanning Electron Microscope) and the solid sample was the basis for grain size distribution and XRD (X-ray diffraction), while the water samples were the basis for ion chromatography and QICPMS (Quadropole Inductively Coupled Plasma Mass Spectrometer). These methods will be presented in this chapter.

4.3.1 Scanning Electron Microscope (SEM)

To analyse the dust filters provided by Titania AS the Scanning Electron Microscope (SEM) was used. SEM produces an image of the given sample by scanning the sample with a beam of electrons. As the incident beam interacts with the sample, information on the topography and composition is obtained (Andersen, 2015b).
As the material is windblown, the grain size was presumed to be quite small and spread throughout the filters cover. SEM was hence a thought to be a good choice for exploring, tracing and identifying the windblown material.

For topography and morphology SEM uses the secondary electrons (SE) which penetrates the surface $\sim 100nm$. For analyses of the chemical composition electrons that penetrate the specimen deeper and hence are of high energy were used, these include backscattered electrons (BSE), X-ray mapping and cathodoluminescence. In addition to the SEM image-display system, there is an additional tool that has the analytical capability so that quantitative analyses can be conducted. This tool is named EDS, energy dispersive X-ray spectroscopy. The basic principle is based on

the fact that when the incident beam interacts with the atoms in the specimen, shell transitions occur and an X-ray that is characteristic of the parent (specimen) element is generated. This permits elemental analysis, as well as a map which shows the elemental distribution in a sample surface (Andersen, 2015b).

Sample preparation

A part of the filter was mounted on a sample holder that fits the arrangement in the sample chamber. Two samples were prepared from each filter, resulting in a total of four specimens arranged for analysis with SEM- EDS. This was done, as each dust filter should have one specimen coated with gold and one with carbon. Coating is added to make the specimen conductive. For quantitative analysis the carbon-coated specimens was used, as this type of coating does not interfere with the compositional signal. To obtain the best images of the specimen, the gold-coated specimens were used. The SEM system was held at a high- vaccuum setting.

The two gold- coated samples, one from each filter, was then used to investigate the grain size distribution by manual counting of grains. This method was then thought to be representative for the filter itself. The method developed in this study to do this was to:

- Selected four random locations on each sample, thus four locations on each filter
- Classify the grains by size intervals
    - <10 μm
    - 10- 50 μm
    - 50-100 μm
    - >100 μm
- Each location was set to a zoom of 100x, 500x and 1000x
    - 100x: get an overview of the sample, was able to count a variety of grains but the small grains were hard to separate out
    - 500x: smaller grains were easier to locate and count
    - 1000x: the smallest grains became visible
- Calculated the number of grains in each size interval per area

This method is graphically displayed in figure 4.2.

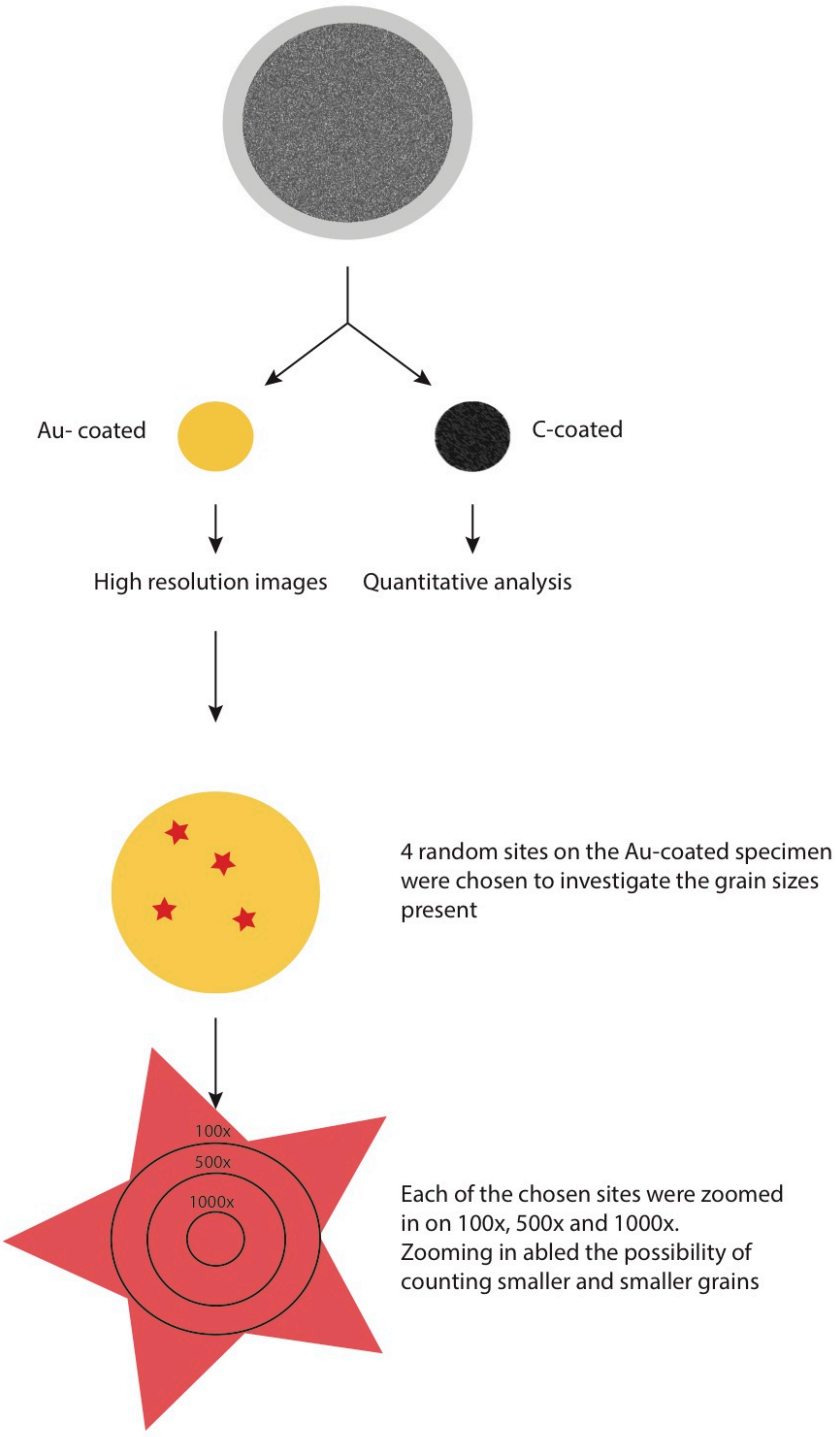

Figure 4.2: A graphical illustration of the method used to analyse grain size distribution in the dust filters. The cold-coated specimens were used where four random sites were chosen for further investigation. Each of these sites was zoomed in on in 100x, 500x and 1000x. Grains were counted in each zoom-view and categorized into the intervals of <10, 10-50, 50-100, >100 μm.

Dust filter localities

The two dust filters were provided by Titania, and represents the period 4. - 31.08.2016. The filters positions can be seen in figure 4.3, below. Both are situated in Åna-Sira, a small village southeast of the Titania mining site. Filter 9353 will hereafter be named filter 3, and filter 9354 will be named filter 4. Filter 3 has a longer distance to the mine area than filter 4, which is placed in upper Åna-Sira.

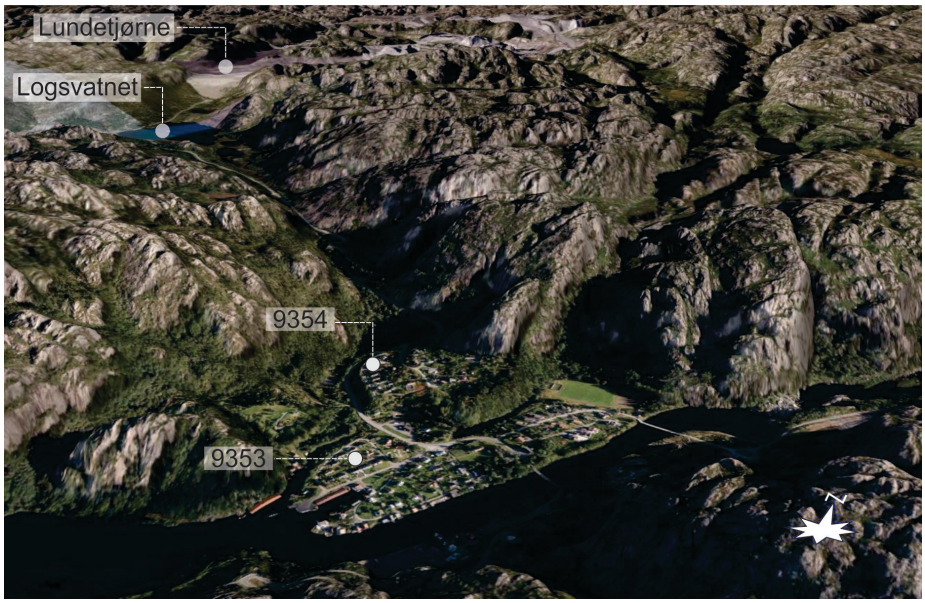

Figure 4.3: Image of the dust filter placements in Åna-Sira. Filter 9354 is called filter 4 in this thesis, and filter 9353 is called filter 3. Filter 4 is placed closer to the tailings dam than filter 3. Picture from Elise Opsal, Titania AS.

Senior Engineer Berit Løken Berg helped with and performed the analysis and elemental composition at the Department of Geosciences at University of Oslo. The equipment used was a Hitatchi SU5000 FE-SEM (Schottky FEG) and Dual Bruker X-Flash30 EDS System, and HR EBSD system with argus.

4.3.2 Grain size distribution

In order to determine the grain size of the material gathered from the tailings dam at Titania AS, a grain size distribution analysis was conducted. This can give an indication on the amount of tailings prone to wind transportation, and the general size of the tailings being disposed by air.

The grain size distribution is done by laser diffraction. The Beckman Coulter LS13 320 can determine grain distribution within the area of 0,4 μm – 2000 μm. The method is based upon the principle of diffraction of light when hitting a surface (BeckmanCoulter, 2009). In this case, when the light from the laser hits the surface of the particle it is diffracted in an angle representing the size of the particle. Hence, laser diffraction measures the angular variation in the intensity of light scattered when the beam of light passes through the particle. Essentially, small particles scatter light at a high angle, while large particles scatter light at a small angle. Each particle will create a specific pattern, and the intensity will depend on the number of particles in the given size interval (Cyr and Tagnit-Hamou, 2001).

From the total solid material collected, 100ml was submitted for analysis within a plastic tube. The laser diffraction analysis was run, providing a cumulative distribution. The grain size distribution is then determined by grain volume. The grain size distribution was done twice, from two different sample volumes of the same sample. The result was the mean of these two.

Mufak Said Naoroz preformed the grain size distribution analysis at the Department of Geosciences at University of Oslo.

4.3.3 X- ray powder diffraction (XRD)

X-ray diffraction (XRD) is an analytic technique to determine atomic and molecular crystal structure. The technique is primarily used for phase identification and information on unit cell dimensions. XRD was chosen to identify and quantify the mineral phases in the samples from the solid tailings, and the suspended material in the water column in the tailings dam.

X-ray diffractometers usually consist of a sample holder, an X-ray tube, an X-ray detector and a goniometer to measure and detect X-ray angles.

The incident beam of monochromatic X-rays is generated in the X-ray tube by directing high-energy electrons at a metal target (Cu-target). When the filament electrons achieve sufficient energy to kick out an inner shell electron of the Cu-target, characteristic X-ray spectra are created as an electro from a higher energy orbit move in to replace the ejected electron. The diffractometer use (in this case) the $K\alpha_{1\text{-}2}$ lines from Cu. The characteristic X-rays are filtered to produce the monochromatic X-rays needed for X-ray diffraction. These X-rays are then directed towards the sample. The sample holder is held in a horizontal position, while the source (x-ray tube) and detector are rotated in opposite directions along the same circle. The X-ray detector then detects a range of angles simultaneously, in the instrument used a 3° window (Andersen, 2015c). XRD analysis relies on basis of Braggs' law, which states:

$$n\lambda = 2d\ sin\theta \tag{4.1}$$

where n is order of reflection, λ is wavelength, d is interplanar spacing of the crystal and θ is the angle of the incident beam. This law relates wavelength to diffraction angle and the lattice spacing in a crystalline sample. When the geometry of the incident X-rays strike the sample satisfy Braggs' law, constructive interference and an intensity peak occurs. This signal is detected and converted into a count rate that is the input to a computer that can read and interpret it (Dutrow and Clark, 2016).

Sample preparation

Before analysing with XRD, sample preparation is a crucial step. In order to obtain correct results, the sample preparation must be conducted with the following characteristics from 9Andersen (2015c):

- Homogeneous
- Even grain size
- Random grain orientation
- Flat- top surface

One sample was from the solid mine tailings and the other was the solid residue from the water surfacing the mine tailings dam. The solid residues from the filtered water sample and solid mine tailings were named S-1-W and S-1-S respectively. S-1-W was from liquid sample 1 at location 1 in the on- land disposal dam. The sample contained a lot of solids. To analyse this water sample by ICPMS and ion chromatography, the solids had to be removed.

- Centrifugation so that the suspended solids settled at the bottom of the plastic tube.
- The liquid was removed and transferred to another plastic tube by a syringe. Left in the original plastic tube was some liquid and the residual solids
- Leftover liquid was further removed by vacuum filtration. This technique uses the vacuum effect created to filter the sample through a filter, leaving the solids
- The solid residue on the filter was then left to dry in the oven at 50°C for 24 h.

The next step for preparing the samples was to utilize the micronizer in order to minimize and homogenise the sample to the optimal condition. The micronizer is a wet crushing tool and is usually used in the final step to obtain ultra-fine grain size, typically <10μm. The procedure went on in the following order:

- Crushed sample S-1-W by hand in a mortar before inserted in the jar used for the micronizer
- S-1-W: 1 grams sample and 5mL of ethanol were added to the jar, as well as 48 agate rods stacked neatly
- S-1-S: 3 grams sample and 8 mL of ethanol as well as 48 agate rods stacked neatly
- Both samples were crushed for 12 minutes
- After using the micronizer, the samples were placed in the oven for 24 h at 60 °C to dry

The dried samples were then ready to be mounted on sample holders. The sample holders were cleaned with ethanol and a special paper tissue without fine particles to avoid risk of contamination. After the sample material was placed on the sample holder, a glass slide was used to remove excess powder and to create a surface as smooth as possible. This is done to avoid preferential grain orientation. After this procedure, sample S-1-W and S-1-S were ready to be analysed by X-ray powder diffraction.

The XRD results came in .raw files that were firstly worked with in DIFFRAC.EVA, and then finally in SiroQuant by the Rietveld-method (Hillier, 2000).

Beyene Girma Haile performed micronizing and X-ray diffraction on the two samples at the Department of Geosciences at University of Oslo. The equipment used was a McCrone micronizing mill and a Bruker D8 Advance. The instrument uses a 2.2 kW Cu Kα radiation source, λ= 1.5418 å.

4.3.4 Ion chromatography

Ion chromatography is used for water analysis, and is able to measure major cations and anions. Paull and Nesterenko (2013) states that the definition of ion chromatography is as "high-performance liquid chromatography of small charged and polar solutes, predominantly based on ion-exchange and electrostatic interactions with an oppositely charged stationary phase". From this, the ion chromatography is a method of separating ions and polar solutes based on their affinity to the stationary phase i.e. the ion exchanger. This is possible as ionic species separate differently depending on their type and size. This method is useful for determining the major ion/anion composition of the water samples taken.
Before the ion chromatography was conducted, the water samples were filtered through a $0{,}45\mu m$ filter and marked accordingly to the sample names and locations. This was done to remove sedimentary and particulate matter as well as avoiding microbial reactions prior to the analysis.

Mufak Said Naoroz performed the analyses at the Department of Geosciences at University of Oslo with Dionex ICS-1000/2000 Ion Chromatography system.

4.3.5 Quadrupole Inductively Coupled Plasma Mass Spectrometer (QICPMS)

Mass spectrometry represents a wide range of analytical methods to separate and measure charged ions and molecules (Andersen, 2015a). Mass spectrometry is a quantitative analysis of the trace elements in rocks, minerals and water, which is exactly according to this thesis's aim.. Mass spectrometers generally consist of an ion source, a mass analyser and a detection system. This is true for the QICPMS as well, but the mass analyser is special: it is a quadrupole mass analyser.

QICPMS uses an argon plasma source to convert the sample atoms into ions. These ions are focused before let into the quadrupole mass spectrometer where ions are separated by their mass to charge (m/z) ratio. The quadrupole mass filter only lets a certain ratio pass at a time. The m/z ratio- setting is rapidly changed so all ions in the sample can be analysed. The ions that were let through the mass spectrometer will end up in the detection system that catches and counts the received ions and then passes the information through to the computer system. Finally, the software will calculate the concentrations based on a standard (Thomas, 2001).

Sample preparation

The water samples underwent preparation in advance of the QICPMS analysis. Firstly,

- 10ml of the original samples were filtrated through 0,45μm filters over in new tubes to remove sediments and particulate matter and prevent microbial reactions altering the sample
- Two drops of 1% HNO_3 was added into each tube of filtrated sample

As the amount of trace elements were expected to be low, only the sample from the tailings dam needed dilution. Sample 1 was hence diluted 4 times. Along with the nine samples was one blank sample (1% HNO_3) prepared as well, to function as a reference in the analysis. To check the QICPMS measurements before analysing the samples, a known standard is used. This has known concentrations of elements, and here the Trace Metals in Drinking Water (TMDW) solution is used for this calibration.

Siri Simonsen and Magnus Kristoffersen at the Department of Geosciences at University of Oslo performed the analyses with a Bruker Aurora elite Quadrupole Inductively Coupled Mass Spectromenter (QICPMS). A total of 7 elements were analysed: Cu, Cr, Co, Cd, Pb, Ni and Zn.

As the samples are expected to contain the elements lying in the middle of the spectrum (Ni, Cu, Zn etc.) a collision gas were introduced. If not, molecules would potentially be ionized and atomised so that molecules instead of ions would be let through the system. The collision gas splits these molecules. Although this lowers the overall concentration of the other elements, this is not a problem as the Bruker Aurora Elite is sensitive enough.
When the system for the QICPMS was set up, the chosen Ni isotope was the 60- and 62- isotope. The 58- isotope is more abundant, but is likely to inflict with the 58- isotope of Fe and was consequently not used.

4.4 Methods applied for the marine disposal setting

To investigate the marine setting, NIVA's research facility at Solbergstrand, Norway was used. Firstly, box-cores were collected with the boat Trygve Braarud at the Drøbak straight, figure 4.4. The box cores were then placed under observation over time with mine tailings from Titania AS on top at Solbergstrand. The fjord sediments were collected at a depth of 193m. However, the first liners were gathered at a location a few hundred meters away, but the boat captain decided together with NIVA to drive further to avoid taking samples in a downhill site.

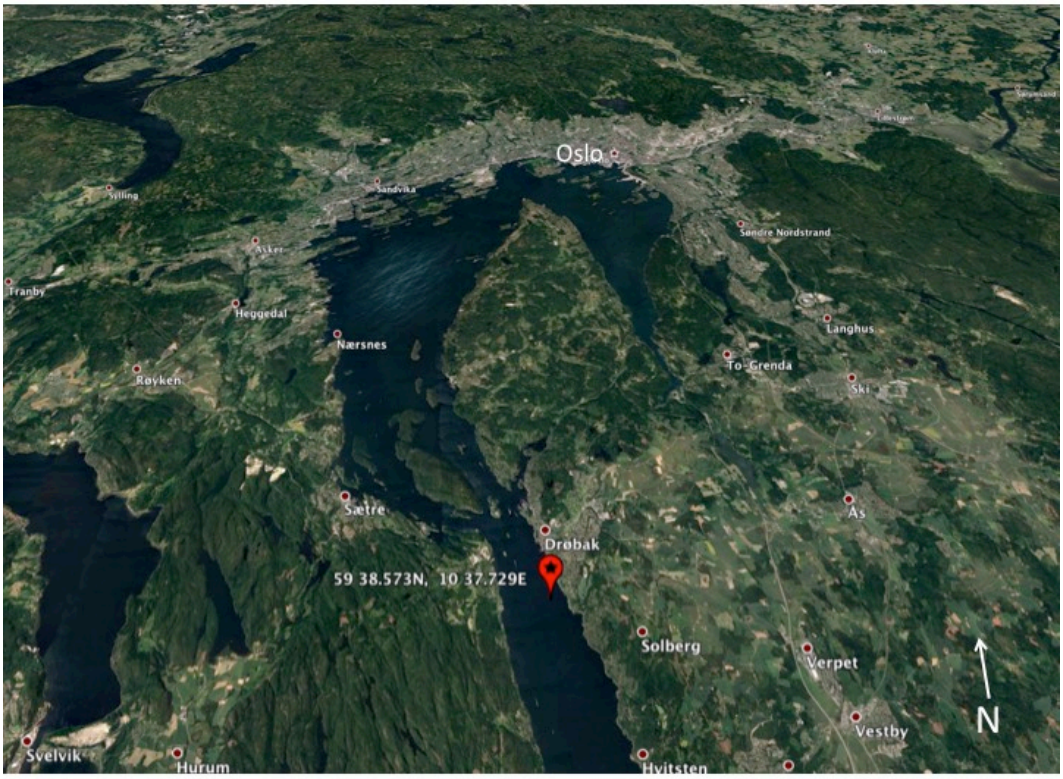

Figure 4.4: Sample location from where the box-cores were taken to provide the experiments with "uncontaminated" fjord bottom sediments. The location is marked with a red point, and is in the Drøbak straight. The majority of samples were collected at a depth of 193m.

These box cores were the basis for exploring metal ions in water by Diffusive Gradients in Thin films (DGT) and flux from sediments to the water column. The measurements were all conducted in a depth context, so that profiles from the sediment surface and downward could be created with the given parameters.
As mentioned in the previous chapter, solid material from the mine tailings dam at Titania AS was gathered in field for both on-land and marine application.

4.4.1 Box core sampling and liners' setup

On the 16th of March Trygve Braarud and its crew set out to sample box-cores in the outer Oslofjord, see figure 4.4. Together with the boat crew was Morten Schaanning and Joachim Johansen (NIVA), and the students Linda Fauske and Hedvig Sterri (candidate). The fjord bottom was of soft muddy sediment, with 10-20 cm overlying water. 11 cores were sampled, and then placed in mesocosm tank with 60cm water at NIVA's research facility at Solbergstrand, located in the Drøbak Strait.

NIVA has created polycarbonate boxes that fit the box- corer that's named liners. They are made of clear, hard plastic and are of size 0,1m^2. When the liner was mounted within the box-corer, a lift lowered the box-corer towards the fjord bottom to gather fjord sediments without disturbing the sedimentation layers or the sediment surface. To do this the corer tube penetrates the seabed as the corer reaches the bottom. As the main cable is redrawn, the closing grab is placed in position to close the corer tube. Then the box- corer is redrawn up on the ships'/boats deck, figure 4.5. The box-corer used was from KC-Denmark A/S Research equipment.

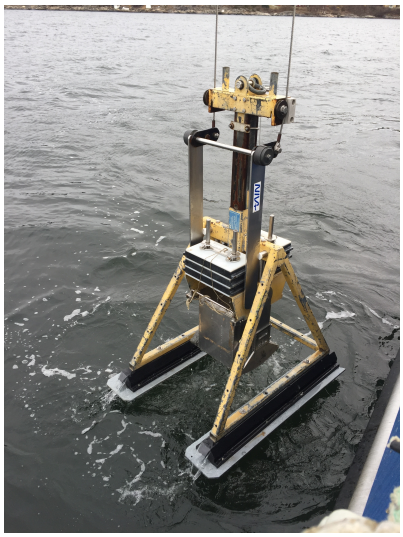

Figure 4.5: The box-corer with a liner on the way up containing sediments from the fjord bottom at approximately 193m depth.

Figure 4.6: The box-corer reaching the boat deck with help from the boat crew and NIVA.

Figure 4.7: The liner being removed from the box-corer tube by Morten Schaanning and Joachim Johansen from NIVA.

As the box-corer is raised from the seabed and on-board the boat, the liners are extracted from the corer- tube, figure 4.6 and 4.7. These liners were, as the boat reached the Research Facility at Solbergstrand, transported into the building and placed in a mesocosm tank. The liner's receives a steady supply of seawater from 60m depth in the Oslo fjord by a Watson- Marlow multichannel peristaltic pump, and continuously aeration input in the water above the liner's, figure 4.8. This water has a salt content of 34 PSU and a temperature of 10 °C.

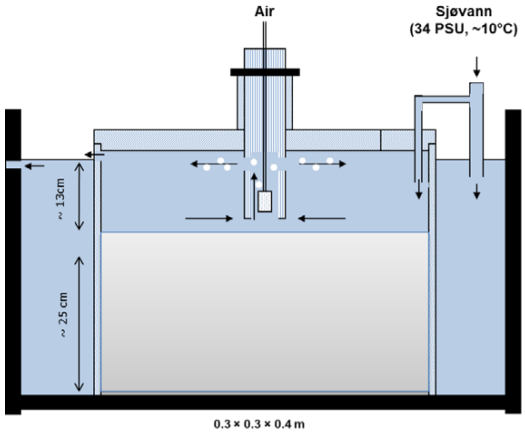

Figure 4.8: A schematic drawing of the liner's installation in the mesocosm-tank at Solbergstrand (Ruus et al., 2012).

As NIVA is conducting this box-core experiment as a part of a larger project (NYKOS- New Knowledge On Sea Diposal), 11 liners were gathered to have enough to test tailings from the industrial mining companies Titania and Nussir, along with liners used for control. The Nussir liners were not used in this thesis for other than an analysis done to evaluate the methods used. Two additional liners were taken as well, in precaution of an unfortunate event. The liners had two different fill-levels of sediments; three liners had a lower level than the others, liners number 16, 20 and 10. The high-filled were then the liners numbered 3, 14, 1, 9, 32, 21, 18 and 4.

On the 17th of March, the liners containing fjord sediment, seawater and tailing slurry was added. It was added in the liners following the setup that can be seen in the conceptual drawing in figure 4.9. The intention was to add a 2cm thick layer of tailings on the fjord sediment surface without disturbing the layering or the surface itself. The tailings from Titania were delivered to NIVA in a large plastic barrel containing 1/3 tailings and 2/3 water. It was partly frozen due to storage in a garage. Firstly the water was drained off, and replaced with seawater, then thawed with a heat rod up to 30° in the overlying seawater. The wet density of the tailings was 2 g/cm^3, so 4kg per liner should yield a nominal thickness of 2cm.

To preserve the sediment surface and sedimentation layers, the tailings were mixed with seawater in 1L plastic bottles to create thinner slurry before pouring gently into the overlying water of the receiving liners. The tailings settled rapidly on the sediment surface in a fairly even layer of the intended thickness.
After the setup with liners and tailings were completed, water was flushed through at the speed of 2ml/min was connected to each liner. Aeration was near the water surface the first two days to reduce potential sediment disturbance and transport out of the liners, for then to be moved downwards to the tailings surface from that point on.
The tailings from Titania AS was distributed into the liners numbered 20, 4 and 14, while tailings from Nussir AS was placed in 16, 21 and 18. Liners number 32, 10 and 1 were set up as control, and number 3 and 9 were extra.

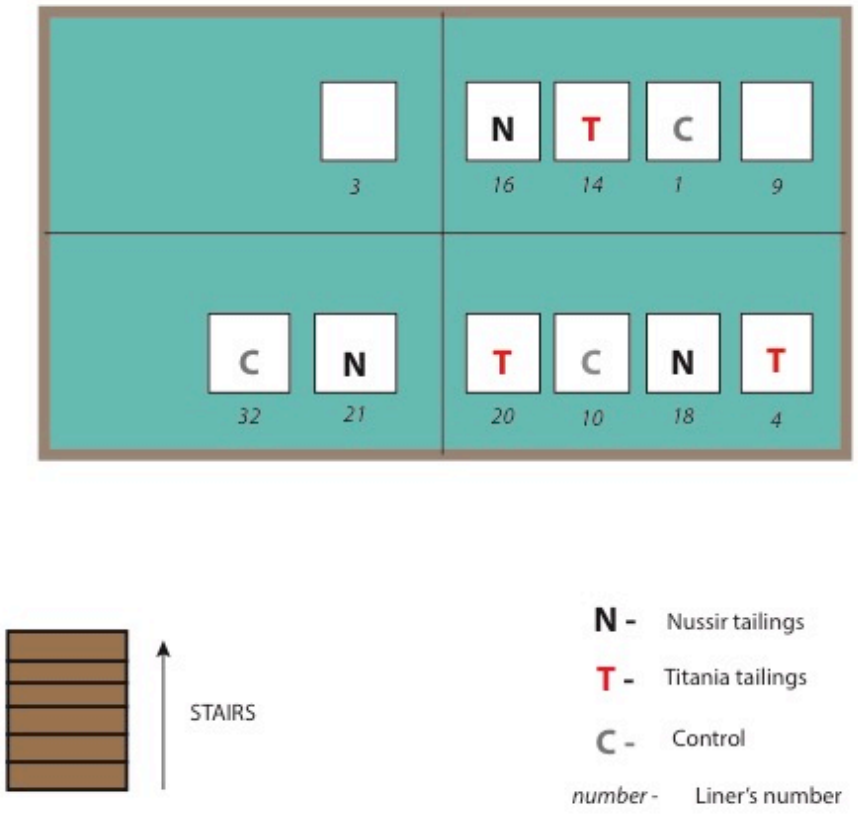

Figure 4.9: Conceptual overview of the mesocosm-tank at Solbergstrand Research station at Solbergstrand. 3 liners underwent each treatment: Titania, Nussir or control. The liners are marked with the letters that correspond to their treatment.

There are both natural variances and analytical uncertainties connected to this method. Firstly, the box-core sampler cannot grab the exact same sediments when sampling. Although the samples with the same treatment are treated as replicas, they may not be in real life. Natural variances occur over small distances as well, and hence the fjord bottom sediments are a function of these. Furthermore, the mesocosm setup should ideally create an equal environment with respect to temperature and water flow, but spatial variances could occur.

4.4.2 Electrode measurements of pH, E_h and Es

Electrode measurements were carried out in order to investigate the levels of pH, E_h (redox potential) and Es (sulphide content) beneath the sediment surface in the liners. These measurements provided with important information about the conditions from the sediment surface to a 7.5 cm depth.

Senior researcher at NIVA, Morten Schaanning, developed the setup used to measure pH, Eh and Es, figure 4.10. This setup allows for combined measurements of the three parameters on one reader, in a depth context. Prior to analysis, the reference electrode were marked with the depth that were to be analysed: 0-0,5, 1-15, 2-2,5, 3-3,5, 4-4,5, 5-5,5, 6-6,5, 7-7,5cm, figure 4.11. Additionally, the pH electrode was calibrated with pH 7.00 and pH 4.001 solutions.

Figure 4.10: The reference electrode is marked with the depth intervals for analyses.

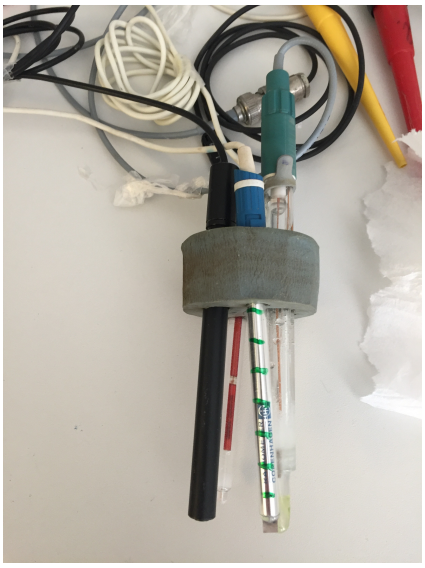

Figure 4.11: The electrode setup. The black electrode measured Es, the red measured Eh and the see-through measured pH.

The electrode-setup was then utilized in each of the 11 liners in the mesocosm-tank, submerged down to the given depths mentioned above. This was done carefully as not to break the electrodes. The black electrode measured Es (sulphides), the red measured E_h (redox potential),

the metal electrode with the depth markings were the reference electrode and the see-through with blue top is the pH-electrode, figure 4.11.

The electrode measurements were conducted in agreement with the Norwegian Standards Associations report NS 9410 ((NSA), 2007), in line with appendix E, E.1- E.5. As the half-cell potential on the reference electrode is 185 mV, this needs to be added to the measurements before the final results for E_h and Es can be reported, as follows

$$E_h = E_h' + 185\ mV \tag{4.2}$$

where E_h' is the measured value of redox potential. This is also true for Es:

$$Es = Es' + 185\ mV \tag{4.3}$$

where Es' is the measured value of sulphides.

4.4.3 Diffusive Gradients in Thin films (DGT)

The technique of diffusive gradients in thin films (DGT) is used for in situ measurements of labile metal ions in water. It is a fairly new technique, but has been proven useful due to its simplicity and wide applicability (Garmo et al., 2003). DGT samplers take advantage of the diffusion theory for calculations of concentrations. The sampler's core, the absorbent, is an iminodiaceate chelating resin (Chelex), overlain by a diffusive layer consisting of diffusive hydrogel, finally covered by the filter membrane (Davlson and Zhang, 1994). Figure 4.12 below displays the concept, as the metal ions in solution are diffusing through the diffusive gel via the DBL (Diffusion Boundary layer), to further sorb to the Chelex resin gel (Pesavento et al., 2009).

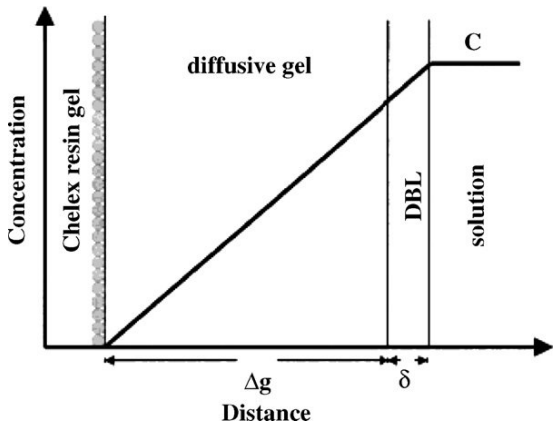

Figure 4.12: Schematic figure of the concentration gradient where the DGT is in contact with an aqueous solution. C is concentration and DBL is Diffusive Boundary Layer. (Pesavento et al., 2009).

The system is based on the principle that ions will diffuse through the filter and furthermore through diffusive gel, and then binding onto the absorbent. The Chelex (absorbent) is known for binding a large number of metal ions selectively in the presence of high concentrations of alkali metals, as for example in seawater (Garmo et al., 2003)

The liners at Solbergstrand research facility were used as the base for the marine analysis. Nine DGTs were placed into the liners, three for Titania AS's tailings, three for Nussir AS's tailings and the last three in the control liners. The probes were left to absorb for 24 hours before collection and prepared for further analysis. The probes were placed so that the whole window of catchment was below the sediment surface of the liner. Due to this, downwards on the DGT represents depth in the sediment column in the liners. As the reactions occur mostly near the sediment surface, the Chelex gel was analysed with decreasing frequency at increasing depth. Further, the probes were analysed at the laboratory at NIVAs location in Oslo. The procedure of detaching the Chelex from the overlying layers was done in the following way; firstly the DGT was washed to remove sediment grains and particles with clean paper. Then, a scalpel was used to cut loose the catchment area, containing all three layers: the membrane, the diffusive layer and the absorbent, from the frame. In agreement with NIVA, cut intervals downward the DGT (representing depth) was done at 0-5, 5-10, 10-15, 15-20, 20-30, 30-50, 50-70, 70-90 and 90-130mm. After dividing up the incisions, the outer layers were removed, leaving the Chelex gel. Each Chelex-bit was then placed within a sample holder that was pre-cleaned with 1% nitric acid (HNO_3). With all the gel pieces placed in respective sample holders, 1ml of 1% nitric acid was

added in each and left to stand for three days before thinning. The last step was adding 10 ml deionized water, and removing the Chelex gel by pouring the solution over in a clean sample container leaving the gel-bit behind in the old container. Finally, the metal concentrations from the DGT were to be analysed by Q-ICPMS.

4.4.4 Flux measurements

Flux measurements were carried out 20th, 24th and 26th of April. Water samples from the input and outlet of each liner were taken to analyse for Pb, Cd, Co, Cu, Zn and Ni. The metal flux from each liner were calculated by the following equation:

$$F = (C_i - C_o) * Q/A \quad (4.4)$$

where F is flux (μg m^{-2} h^{-1}), C_i is concentration in the input water (μg L^{-1}), C_o is the concentration in the outlet water (μg L^{-1}), Q is the water flow rate in the given liner (L h^{-1}) and A is the area of the liner.

There are uncertainties connected to flux measurements: If the difference between input water and output water is small, the fluxes often show a larger variance. This means that small fluxes have larger uncertainties in measurements than large fluxes.

5 Results

5.1 Introduction

The means by which the transport of metals is driven is a key factor. This is as the surrounding environments in the on-land and marine disposal sites are contrasting. The results in the following chapter were, based on this, and divided into on-land and marine disposal sections respectively. The on-land site contains solid material from the mine tailings dam, dust filters that capture windblown particles, and liquid samples from both the tailings dam itself together with rivers and creeks adjacent and bordering the dam. The marine part contains the box core experiments, where mine tailings from Titiania were placed on top of uncontaminated fjord bottom sediments to examine the pore water chemistry, the pH and Eh- environment, diffusion of contaminants and potentially, the effect of benthic fauna on the system.

5.2 On land: the disposal site and surroundings

5.2.1 Tailings mineralogy

The mineral phases present in the samples S-1-S and S-1-W from section 4.3.5, analysed with X-ray diffraction can be seen in figure 5.1 below. It is evident that the most dominant minerals are ilmenite, orthopyroxene and plagioclase. Some sulphides are present as well, though in lesser amounts, such as pyrite and millerite. S-1-W is the suspended solids collected in the water stream in the tailings pond, a direct flow from the pipes that bring the tailings into the pond. These are filtrated particles from water sample 1. The composition shows strong connections to the S-1-S, with ilmenite, orthopyroxene and plagioclase as main minerals. However, silicates play a stronger role in the water suspended particles (S-1-W), with more than double the amount than in S-1-S.

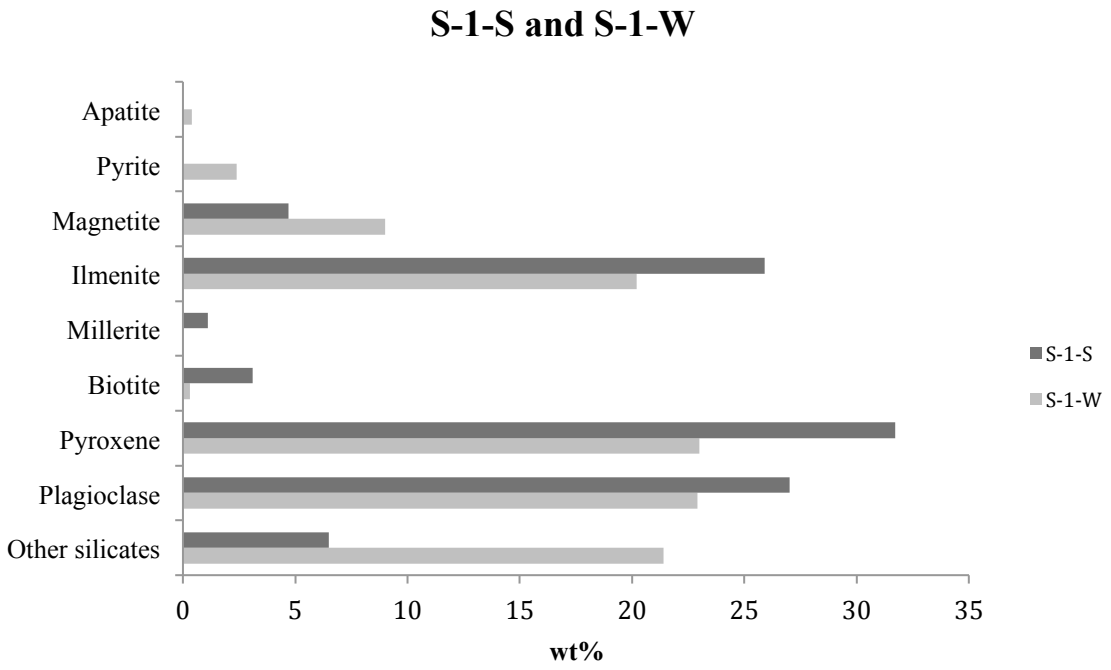

Figure 5.1: Sample S-1-S was taken from the solid tailings. The dominant mineral phases were ilmenite, pyroxene and plagioclase. Sample S-1-W was taken from the suspended solids in the water stream in the tailings pond. Ilmenite, pyroxene, plagioclase and silicates were dominant mineral phases

In, addition, the grain size distribution was investigated to predict how the tailings are prone to aeolian transport. The grain size distribution of a sample of the tailings can be seen in figure 5.2. The peak of the curve is at ~ 200 μm, and the majority of grains are within the size interval 60-600 μm. The statistics provides with more detailed information. From the statistics presented below the curve the mean is 225 μm, while the median is 188 μm. As mean > median, the curve is right skewed. Thus, there are many grains with a lower particle diameter than the mean value, and furthermore one could say that there are many grains with small particle diameters and few with large. This is supported by the skewness value being >1, meaning a right-skewed data (Moore et al., 2014). Note x-axis scale, as the shape of the curve might be slightly deceiving.

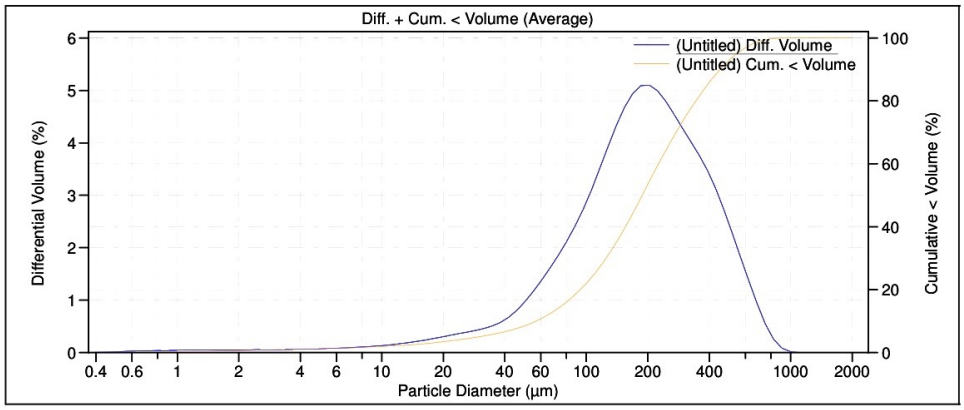

Volume Statistics (Arithmetic)	Average of 2 files	(Untitled)
Calculations from 0.375 µm to 2000 µm		
	Mean	S.D.
Mean:	225.0 µm	2.554
Median:	188.0 µm	0.850
S.D.:	158.0 µm	5.949
Skewness:	1.114	0.073
Kurtosis:	1.147	0.301

Figure 5.2: Grain size distribution of a sample taken in the tailings pond. Most grains lie within the interval 60-600 µm. The mean is 225µm, but since the median is lower it indicates that the majority of grains are small (<225µm) while some large grains stretches the curve, note the x-axis scale.

5.2.2 Windblown material

As some particles are transported from the tailings dam by wind, Titania has been monitoring this potential pollution path by dust filters set up in the near-by village, Åna-Sira. First, the gangue material was analysed by X-ray diffraction (XRD) to examine mineral phases both in the solid material itself and in the filtered solid material suspended in the tailings dam water. These results were compared to the mineral phases presented by Titania. A grain size analysis was also conducted, due to the great importance of size when it comes to aeolian transport. Furthermore, the filters were then analysed by scanning electron microscope.

The scanning electron microscope (SEM) with the element-mapping tool was used in order to examine the dust filters. The images produced showed the filter fibres in the background, with grains of various sizes and densities spread throughout the filter. The visibility of the filter fibres implies that the grain abundance was not immense. Grains occurred in sizes ranging mostly from >10 µm to 100 µm, however small grains were more abundant than large. Figure 5.3 shows this.

Both filters show the same trend, increased abundance with decreased grain size. The filters deviate from each other at category 50-100 µm, the next largest grain category, where filter 4 showed a higher value than filter 3.

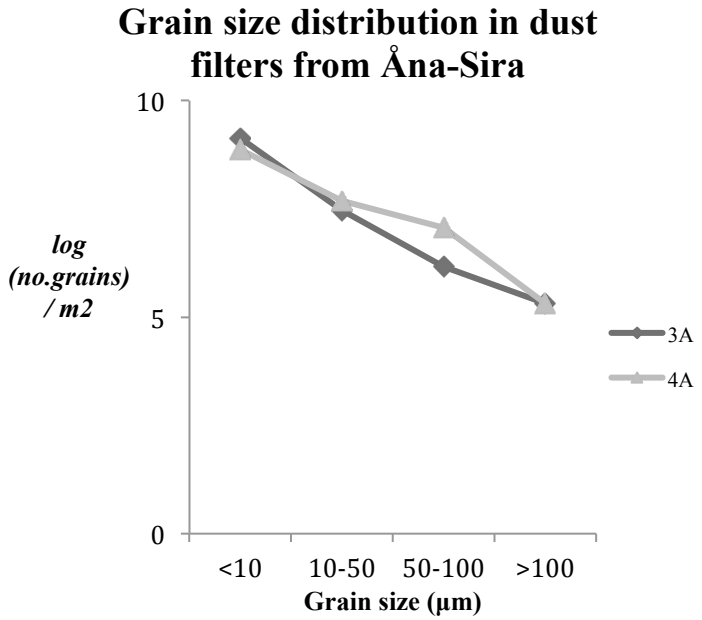

Figure 5.3: The grain size distribution from the dust filters (3 and 4) in Åna-Sira. The figure shows the trend of a decreased abundance with increasing grain size.

The general elemental/mineralogical trend in both filters was that grains either were windblown material consists of plagioclase grains and ilmenite grains. Naturally, the two filters had similarities, as both collects from the same source at near proximities to each other. However, elements maps from spots on both filers will be presented, along with pictures from various places on the filters to appropriately represent the filters composition.

An element map from a sample of filter 3 can be seen in figure 5.4. *A* depict the sample as seen the scanning electron microscope, with a 50x zoom. The white grains are the grains with highest density. Furthermore, the element map presents the option of showing the most abundant elements and their placement. In this case, the most abundant elements (in this frame) were S, Ti

and Fe, as seen in *B* and more thoroughly in *C*. There was not much Ni present in this sample, but it is evident that Ni follows the Fe-Ti-S rich grains, as seen in *D*.

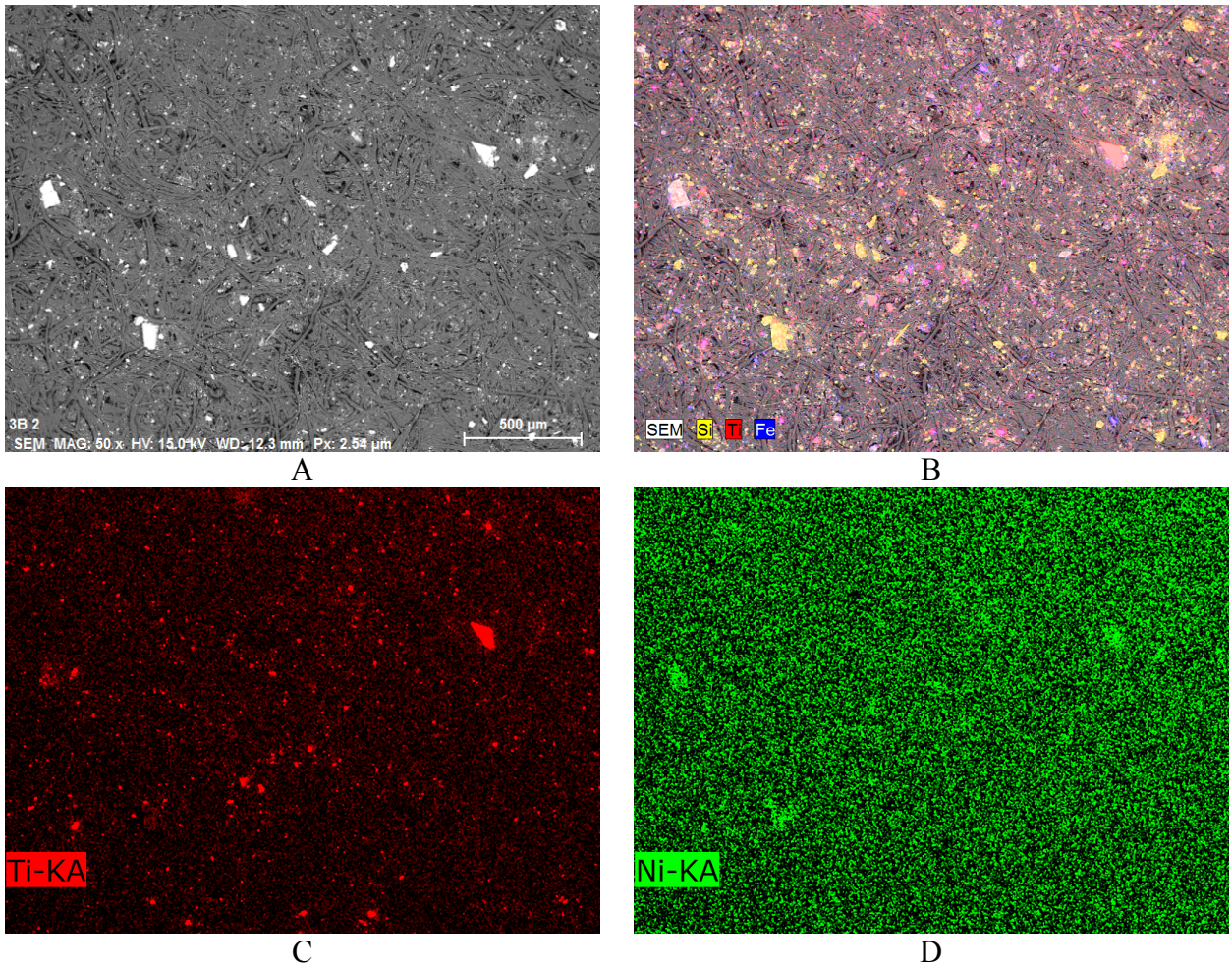

Figure 5.4: Element map obtained from a section in filter 3. *A* shows the image obtained where the brightness of the grains reflects the density. *B* shows the element map with the distribution of Si, Ti and Fe togheter. *C* shows where in the section the grains contain Ti, and *D* shows where Ni is present.

Figure 5.5 is from filter 4. The SEM picture is taken with 500x zoom. The overall composition can be seen in *B*, but is unfortunately misleading, as the red colour of Ti is too similar to the purple colour of Al. The Al is situated with the Si- grains as can be seen in *C*, while the Ti- Fe grain is the large grain in the upper right corner as seen in *D* and *E*. Ni is also here situated alongside with the Ti-Fe grain. The Ti-Fe grains are denser than the Si-Al grains.

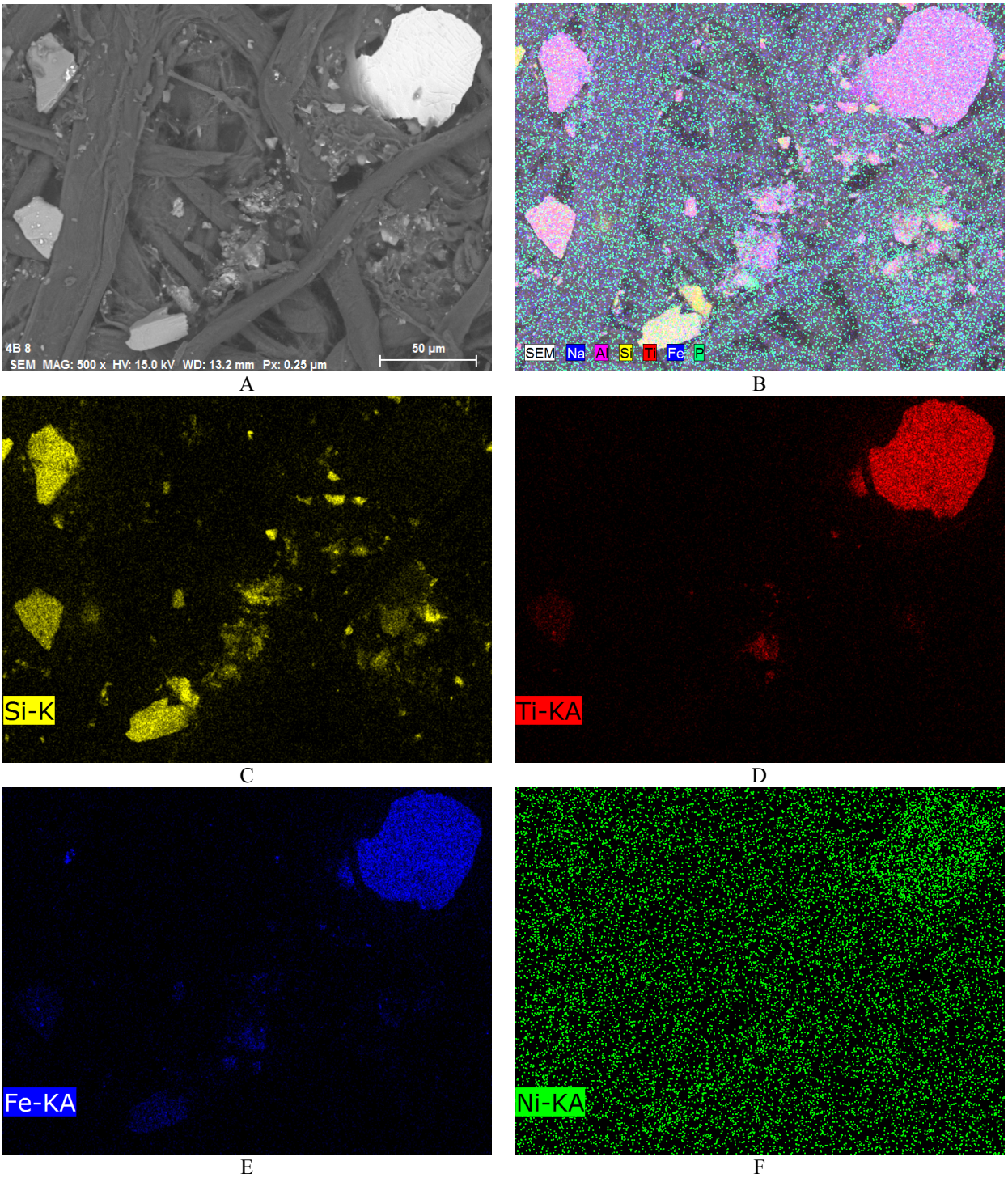

Figure 5.5: Element map obtained from a section in filter 4. *A* shows the image obtained where brightness grains reflects density. *B* shows the element map with the distribution of Na, Al, Si, Ti, Fe and P. Unfortunately, colours of Al and Ti are very similar. *C* displays the distribution of Si and it is evident that it is present in most small grain in this section. *D* shows Ti , and this clarifies what is Ti and what is Al from *B*. *E* shows Fe, and the grain coincides with the Ti-grain in the upper right corner. *F* shows Ni and is, in this section of filter 4, bound to the Fe-Ti grain.

Mineralogical composition of the windblown particles

From the SEM-pictures and element maps, it seemed like the main two types of grains in the filters were ilmenite and plagioclase. The element mapping indicated that the smallest grains were most abundant, and that they consisted of plagioclase and pyroxene. The larger, and less abundant grains were ilmenite.

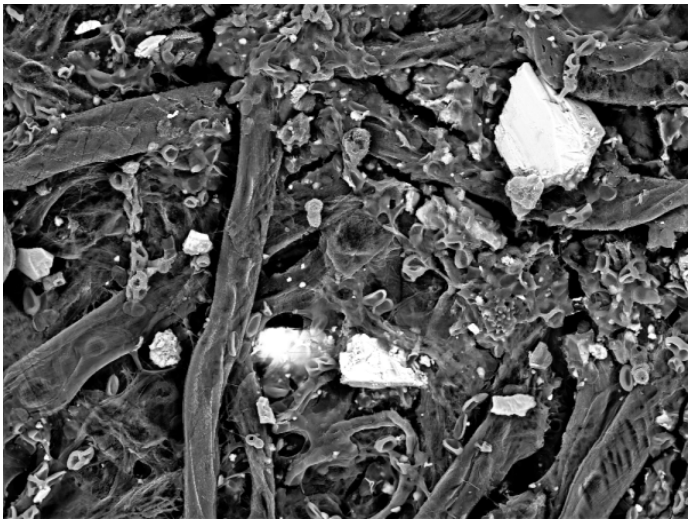

Figure 5.6: Picture taken from filter 3, gold coated specimen. Magnification 500x. The brighter the grains appear, the denser are they are.

This picture, figure 5.6, is a good representation of the filters grain distribution and content. The big grain to the upper right may, as stated above, be an ilmenite grain. The other rather large grain in the lower centre of the picture seems to show the same density as the large one in the upper right. As the SEM-pictures show the brightness as the grade of density, this supports the claim that these might rather be ilmenite than plagioclase. One could then further assume that the smaller, and less bright, grains were plagioclase and/or pyroxene grains. Figure 5.7 below shows the element mapping for this picture.

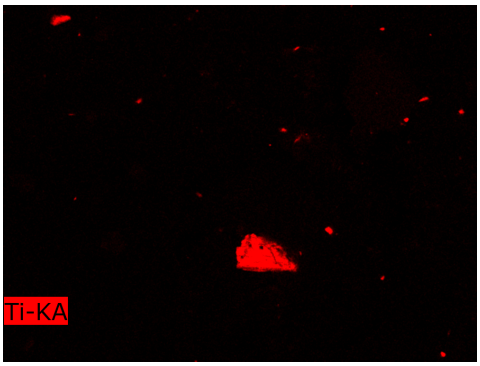

A

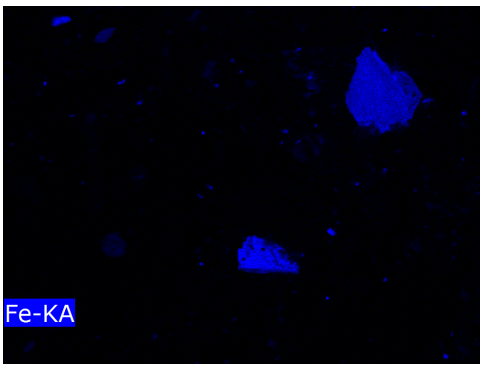

B

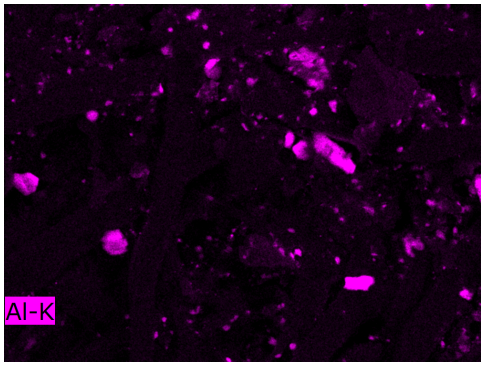

C

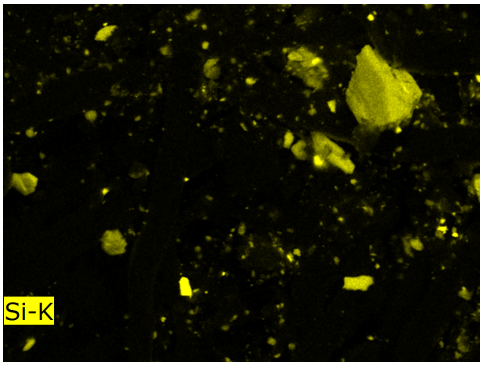

D

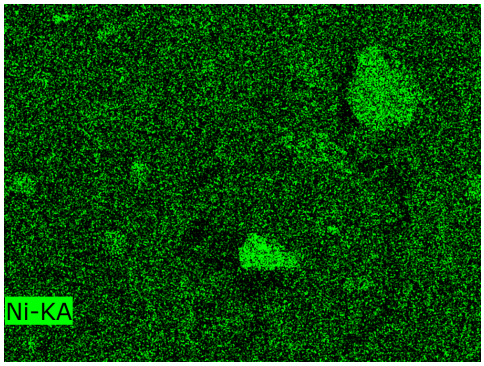

E

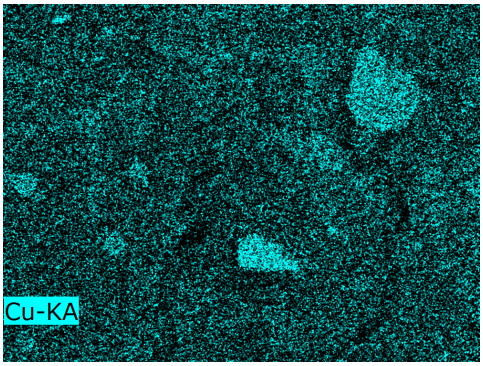

F

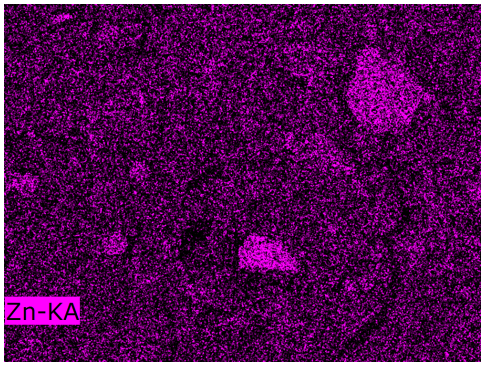

G

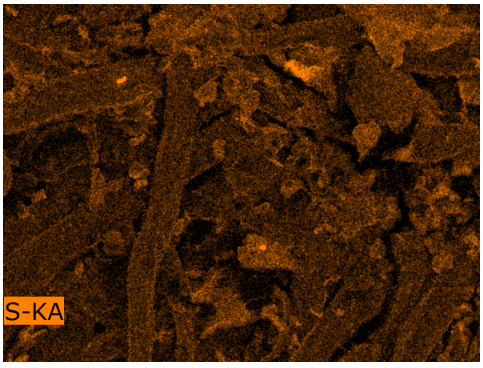

H

Figure 5.7: Images produces by SEM element mapping displays the element distribution of Ti, Fe, Al and Si in the grain within the frame. In *A* it is evident that Ti is only present in one grain, not in both the two densest grains. From *B*, Fe is present in both the two densest grains, and indicates that the grain in the upper right is not $FeTiO_2$, but holds a composition without Ti. From *C*, Al is present in most of the small grains, and together with *D*, most of them holds an Al-Si composition. *E*, *F* and *G* display the distribution of heavy metals in the grains. *H* displays the S content.

Figure 5.7 shows a selection from the element mapping. Starting with the upper right grain, that is visible in *B* and *D*, indicating presence of Fe and Si, along with Mg and heavy metals in form of Ni, Cu and Zn in small amounts. This could then possibly be a pyroxene, where on the heavy metals have attached. Furthermore, the other dense grain in the lower centre is highly likely an ilmenite grain, as it is not appearing with other elements than Fe and Ti, except for the heavy metals Ni, Cu and Zn in small amounts. Moreover, looking at the smaller and more abundant grains, in *C* and *D* these become well defined. Most of these also contain Ca, in addition to Si and Al, along with small amounts of Na. This may point to plagioclase with both endmembers present (Na and Ca).

5.2.3 Water chemistry of streams and lakes adjacent to the on-land storage site

The water samples 1-9 are described in the following section by the data gathered by ion chromatography, QICPMS and pH measurements. Each sample was studied individually, but placed in a context of standard lake element concentration of the southwestern Norway and drinking water regulations. These were plotted together with the ion chromatography analyses and QICPMS- analyses for each sample.

The drinking water regulations are from the Ministry of health and care services with limit-values for substances that can reduce drinking water quality and be harmful to human consumption. The lake element concentrations were gathered from NIVA's national lake investigations of water chemistry 2004-2006 (Skjelkvåle, 2008). The water samples were gathered twice, one in November 2016 and secondly in April 2017, hence the results describe them as sample A and B respectively.

Table 5.1 and 5.2 below shows the cation/anion (ion chromatography) analyses and the trace element (QICPMS) results for all 9 samples, along with pH measurements

Table 5.1: Ion chromatography analysis and pH measurements of water samples 1-9. All results are in mg/L. Reference values are Lake element concentrations from a report done by Skjelkvåle (2008).

Sample	Date	pH	Na	K	Mg	Ca	F	Cl	SO_4	Br	NO_3	PO_4
1	23.11.16	7,50	15,5	6,4	26,8	106,5	1,06	10,3	234,7	*n.a*	1,7	1,6
2	23.11.16	7,26	9,88	3,49	2,93	15,02	0,08	10,2	43,3	*n.a.*	3,6	*n.a.*
3	23.11.16	6,50	10,4	4,03	6,9	28,4	0,2	11,6	89,9	*n.a.*	1,6	0,5
4	23.11.16	5,54	6,3	1,3	0,8	0,7	0,1	13	2,82	0,46	1,2	0,25
5	23.11.16	5,64	4,78	1,38	0,57	0,47	0,06	9,59	1,88	0,46	1,18	*n.a.*
6	23.11.16	6,35	7,76	1,11	2,98	9,50	0,09	13,25	24,45	*n.a.*	1,09	*n.a.*
7	23.11.16	7,50	18,86	5,10	30,33	113,18	0,75	9,72	211,21	*n.a.*	0,66	0,75
8	23.11.16	6,71	8,10	2,29	6,70	21,83	0,17	11,27	57.80	*n.a.*	1,06	*n.a.*
9	23.11.16	5,64	4,81	1,80	0,59	0,60	0,14	9,91	2,05	*n.a.*	1,56	*n.a.*
Ref.*		**5,31**	**0,99**	**0,11**	**0,18**	**0,62**	**-**	**1,6**	**2**	**-**	**0,081**	**0,003**

*Lake element concentrations from Skjelkvåle (2008)

Table 5.2: Q-ICPMS analysis results of water samples 1-9, where A represents the sample taken in November 2016 and B in April 2017. Also the pH measurements are given. The drinking water standard is given as context, and is the regulations given by the Ministry of health and care services. All concentration values are given in μg/L.

Name	Sample	Date	pH	Cr	Co	Ni	Cu	Zn	Cd	Pb
1	1	23.11.16	7,5	0,021	0,59	48,81	0,52	29,63	0,0046	0,02
2	2	23.11.16	7,26	0,052	2,41	30,93	1,9	191,45	0,03	0,053
3 A	3	23.11.16	6,5	0,84	2,81	59,40	2,77	240,52	0,022	0,06
3 B	3	20.04.17	*5,5**	0,79	0,09	23,3	1,1	0,66	*<0,02*	*<0,03*
4 A	4	23.11.16	5,54	0,04	1,03	3,08	0,67	150,81	0,08	0,50
4 B	4	20.04.17	*5**	0,04	0,25	1,31	0,32	2,07	0,04	0,25
5 A	5	23.11.16	5,64	0,06	0,59	1,22	0,56	115,37	0,08	0,72
5 B	5	20.04.17	5*	0,057	0,25	1,32	0,48	4,12	0,06	0,67
6 A	6	23.11.16	6,35	0,13	0,06	19,79	0,38	20,65	0,04	*<0,03*
6 B	6	20.04.17	*5,5**	0,11	0,08	27,91	0,59	5,63	*<0,02*	*<0,03*
7 A	7	23.11.16	7,5	6,46	0,61	259,95	1,54	1,31	*<0,02*	*<0,03*
7 B	7	20.04.17	*7**	1,39	14,40	433,39	81,47	0,76	*<0,02*	*<0,03*
8 A	8	23.11.16	6,71	0,03	0,25	29,85	0,59	53,73	0,02	0,05
8 B	8	20.04.17	*5,5**	0,035	0,064	17,40	0,20	0,93	0,01	0,06
9 A	9	23.11.16	5,64	0,09	0,40	0,65	0,31	94,52	0,06	0,35
9 B	9	20.04.17	*5**	0,06	0,063	0,38	0,22	9,86	0,03	0,17
Drinking water std.				**50**	**-**	**20**	**100**	**100**	**5**	**10**

* pH measurements April 2017 done by pH test strips, and does not provide with an accurate measurement

Sample 1

Sample 1 was collected from the southern part of the tailings dam, as seen in figure 5.8. The sampled water was from a stream running on top on the disposed tailings, following the discharge pattern from north to south, finally ending up in the tailings dam. Accordingly, sample 1 is as close as possible to direct outlet of tailings.

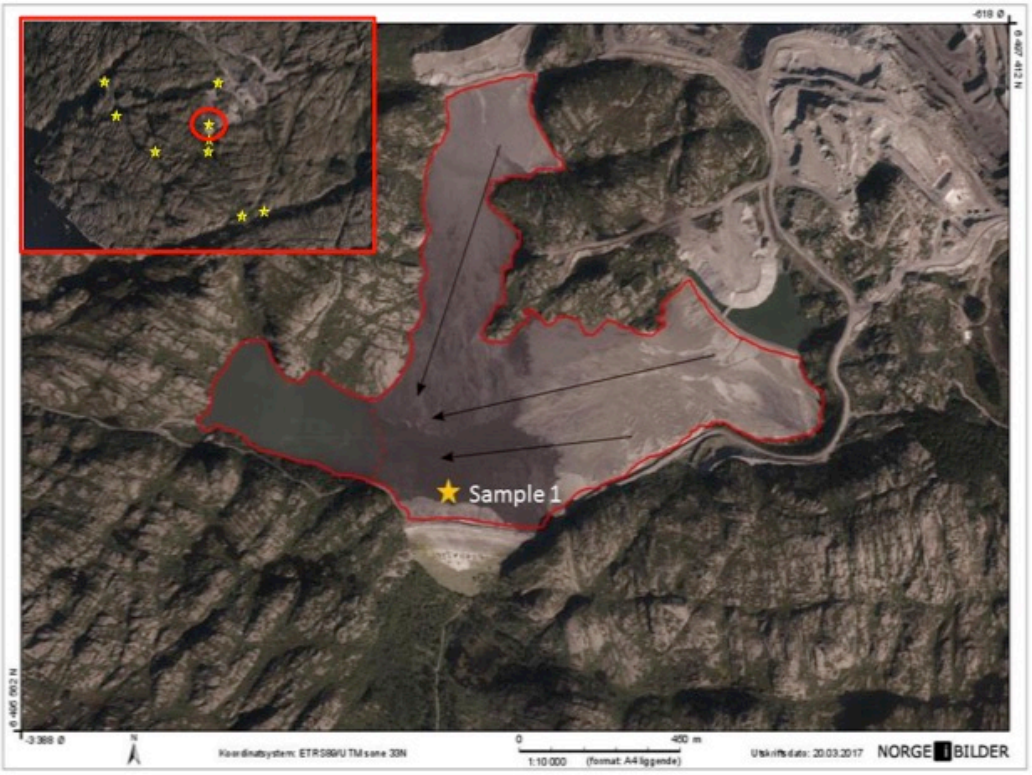

Figure 5.8: Sample 1 was taken in the tailings pond, in the water flow from the outlet point further north in the tailings dam.

The pH measured was 7.5, and is not diluted into natural waters. The overall levels for the cation/anion analysis showed a spread in concentrations, with SO_4 as the anion with highest concentration and F as the lowest. Ca was the dominating cation, with far higher concentration than the other ions. The reference columns are barely visible; as the reference values are very low compared to the highest measured concentrations in the samples, figure 5.9.

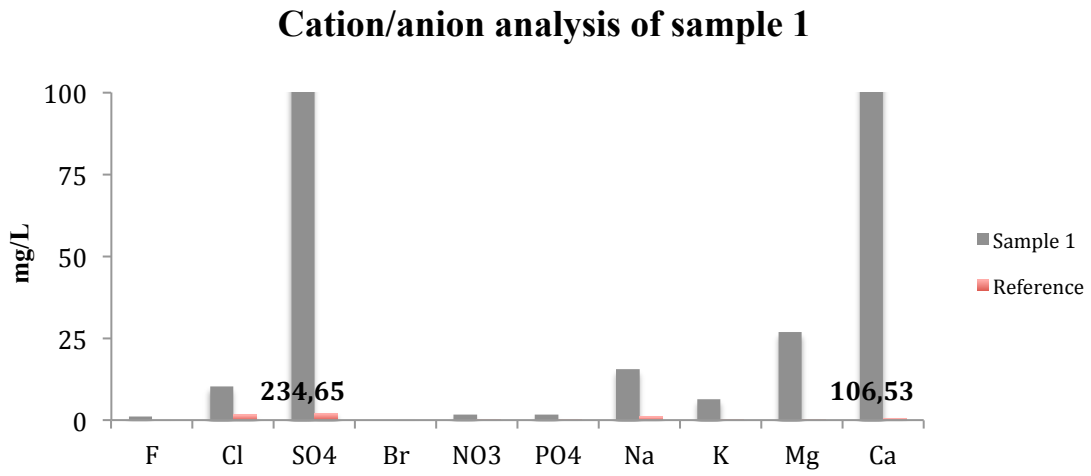

Figure 5.9: The cation/anion analysis of sample 1 showed SO_4 and Ca as the dominant ions. All values highly elevated above the reference values of lake element composition in the south of Norway.

From the trace metal analysis, figure 5.10, the two elements with the highest concentrations were Ni and Zn, with values 48,81 and 29,63 µg/L respectively. Other heavy metals were at concentrations ~2-3 orders of magnitude lower, indicating the dominance of Ni and Zn.

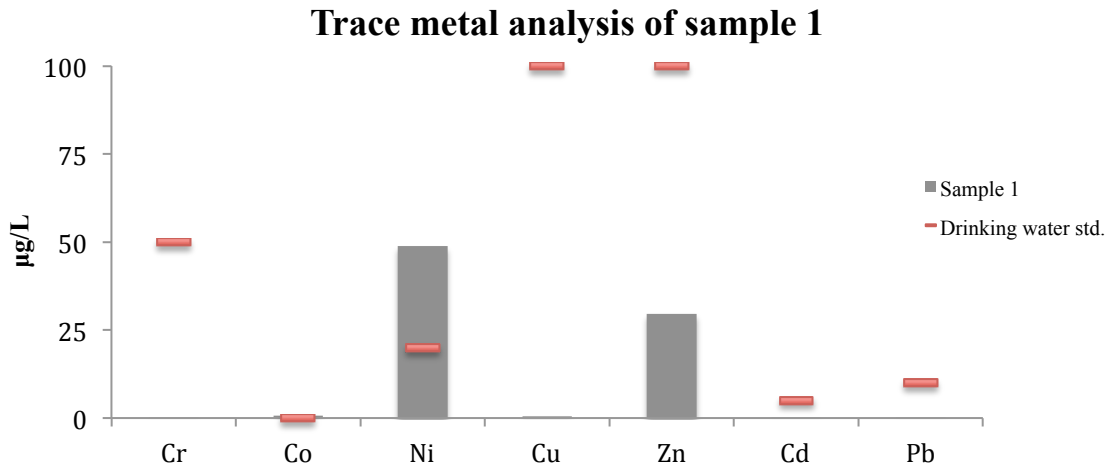

Figure 5.10: Trace metal analysis of sample 1 showed Ni and Zn as the dominant metals. However only Ni was above the drinking water standard.

In the context of drinking water standards the element analyses by ICPMS show results for sample 1 that are within the acceptable range, except Ni that clearly exceeds the limit.
It was not possible to get a second measurement of sample 1 in April 2017 due to the mine being inoperative at the time.

Sample 2

Sample 2 was collected at the mining site, at the end of Tellenesvatnet approximately 1,4km from the tailings dam, figure 5.11. The pH measured was 7.26. This water is being used as process water, and has been recycled to further use.

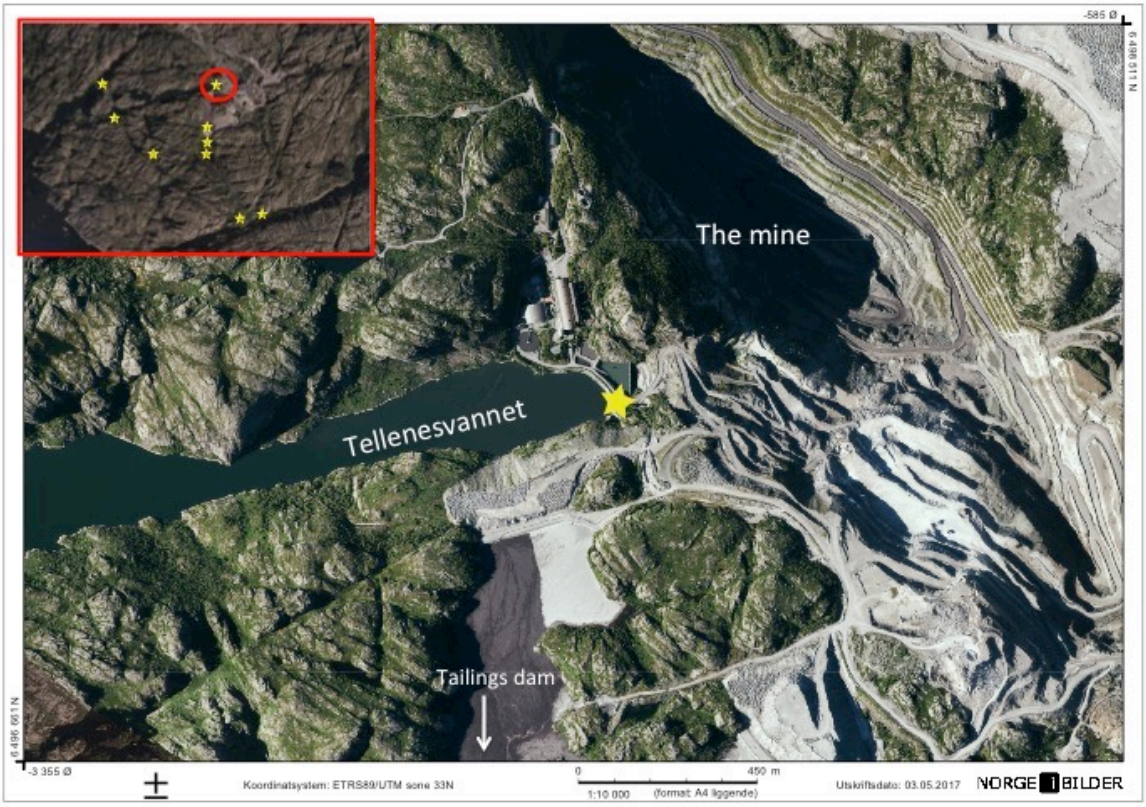

Figure 5.11: Sample 2 was taken in the end of Tellenesvannet, which is used as process water. It is adjacent the mine itself, and the sample location is north of the tailings dam.

The cation/anion analysis results can be seen in figure 5.12. The values in sample 2 were generally lower than in sample 1. The dominating ions were still SO_4 and Ca.
The trace metal analysis provided results within the same range as sample 1, although with the notable exception for Zn, figure 5.13. Ni showed also here values above the drinking water limit, with a concentration of 30,9 µg/L.

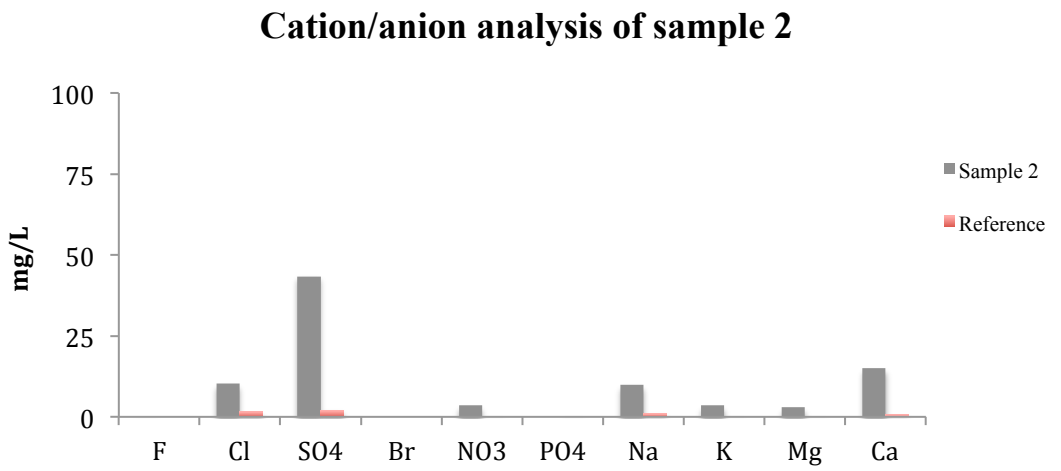

Figure 5.12: The cation/anion analysis of sample 2 showed SO_4, Ca and Cl as the dominant ions. All values elevated above the reference values of lake element composition in the south of Norway.

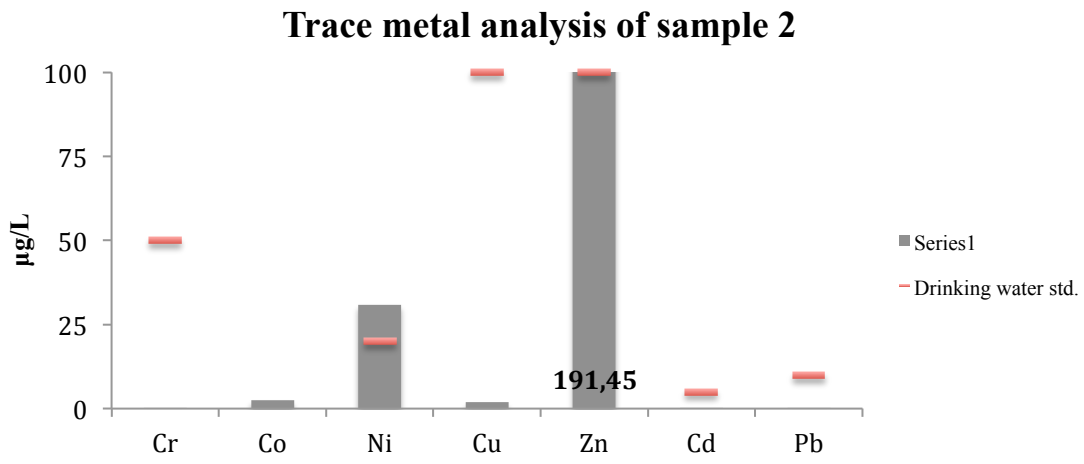

Figure 5.13: Trace metal analysis of sample 2 showed Ni and Zn as the dominant metals. Both were above the drinking water standard.

It was not possible to get a second measurement of sample 2 in April 2017 due to the mine being inoperative at the time.

Sample 3

Sample 3 was collected inland from the Jøssingfjord approximately 3,8km from the tailings dam, in a small creek close to Helleren, figure 5.14. The creek is downstream the drying plant at Titania, situated on the nearby hill to the southeast. The pH measured in sample 3 was 6.5, hence lower than sample 1 and 2.

Figure 5.14: Sample 3 was taken in a small creek draining from the drying plant. The sample location is close to the Jøssingfjord, and approximately 3,8km from the tailings dam.

The cation/anion analysis gave the results given in figure 5.15. The values in sample 3 show generally low values, with the exceptions of SO_4 and Ca. However, in the context of the reference values for lakes in the southwest of Norway, the concentrations found in sample 3 all compound exceed the values.

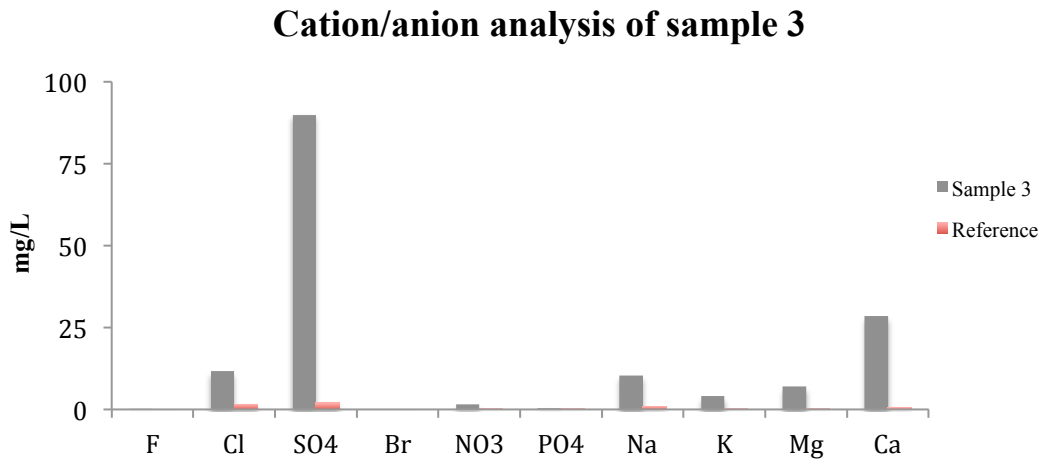

Figure 5.15: The cation/anion analysis of sample 3 showed SO_4 and Ca as the dominant ions. All values elevated above the reference values of lake element composition in the south of Norway, except PO_4 and NO_3.

The data achieved from the trace metal analysis of sample 3 can be seen in figure 5.16. The trace element concentrations were to some extent similar to sample 2, except for the increase of Zn and Ni concentrations. From table 5.2 above, Ni concentration was almost the double of that measured in sample 2 (30,93 µg/L). Both 3A and B showed Ni values above drinking water standard.

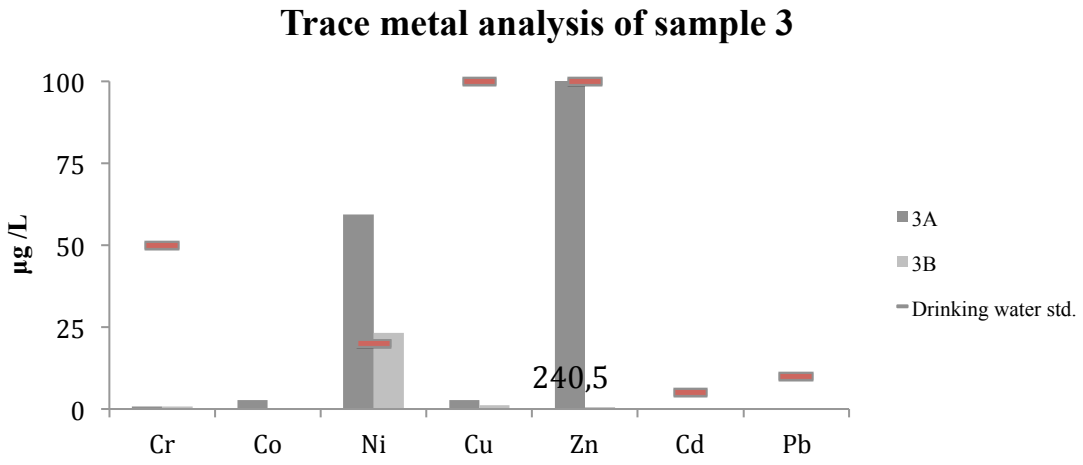

Figure 5.16: Trace metal analysis of sample 3 showed Ni and Zn as the dominant metals. Both were above the drinking water standard.

The values for sample 3 shows that most elements are within range of the drinking water standards, except Ni and Zn. Note that the second (April 2017) measurement showed a dramatic decrease in Zn values compared to the first (November 2016) measurement.

Sample 4

Sample 4 was collected downstream of the drying facilities of Titania AS, as the southwestern corner of the small lake called the Nedre Liavatn, approximately 3 km from the tailings dam, figure 5.17. This small lake is situated southwest from the Tellenesvatnet and southeast from the drying plant. The measured pH was 5.54, which was lower than for samples 3, 2 and 1.

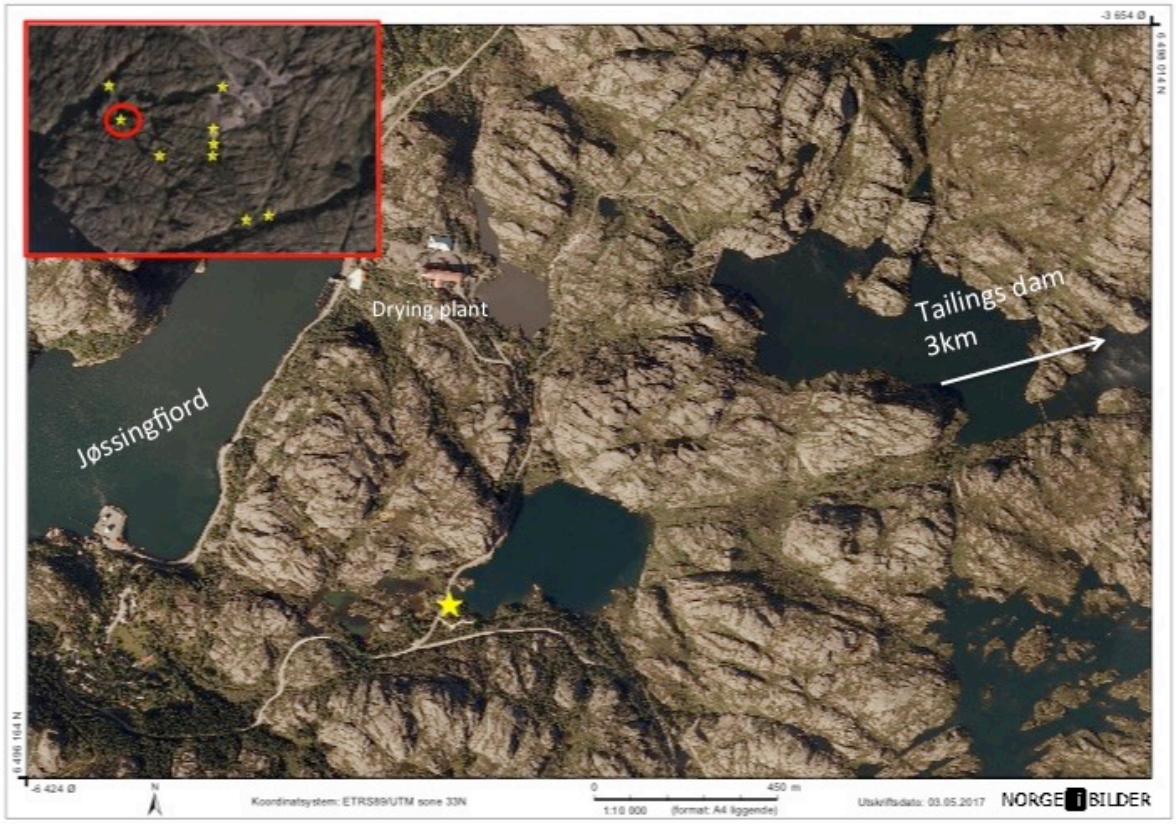

Figure 5.17: Sample 4 was taken in the south western corner of a small lake, in proximities of the Jøssingfjord and drying plant. The tailings dam is 3km from here, in a westward-direction.

The cation/anion analysis can be seen in figure 5.18. Sample 4 values are overall low, and in contrast to sample 3, even SO_4 and Ca are within the same range as the other cations and anions. Note the change in scale from 100 mg/L to 10 mg/L. In sample 4, Cl and Na were the ions with highest concentrations, but they both were below 15 µg/L. Ca, Mg, K, PO_4, NO_3, Br, SO_4 and F all had concentrations that were close to the reference values of lakes in southwest of Norway.

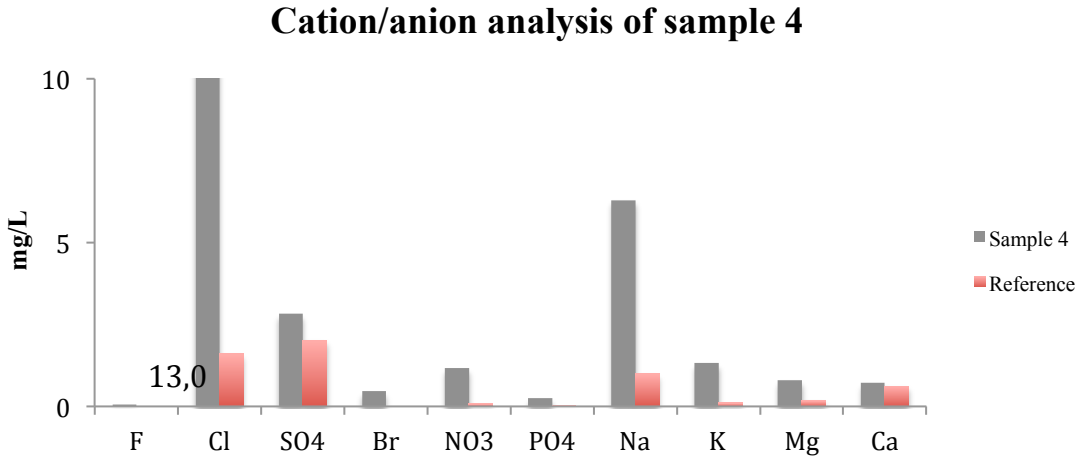

Figure 5.18: Note the scale. The cation/anion analysis of sample 4 showed Cl and Na as the dominant ions. All values elevated above the reference values of lake element composition in the south of Norway, however in a closer range than sample 1,2 and 3.

The trace metal results for sample 4 are presented in figure 5.19. The Zn concentration was still high, although lower than sample 3.Ni that in the previous samples (1,2,3) were high, was in sample 4 remarkably lower with only 3,08 and 1,31 µg/L in the first and second measurement, respectively. Note that the second (April 2017) measurement showed a dramatic decrease in Zn values compared to the first (November 2016) measurement.

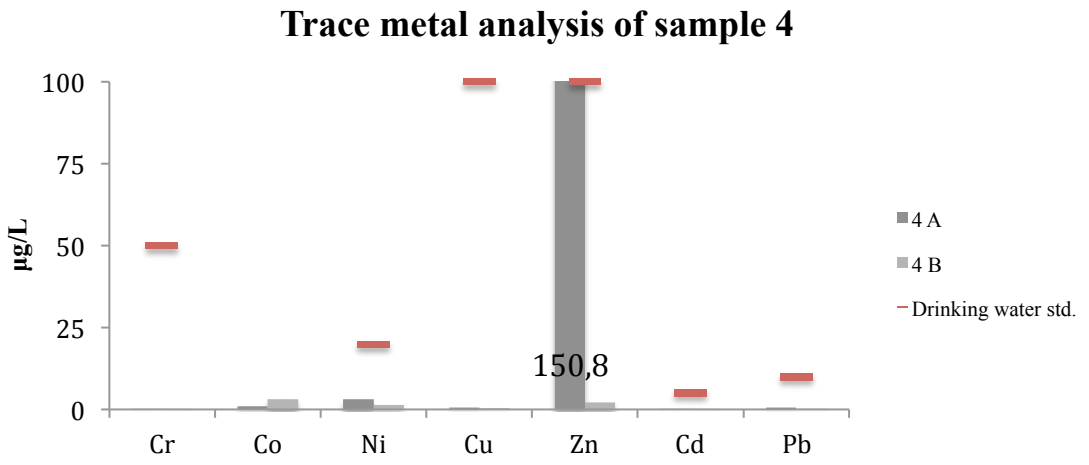

Figure 5.19: Trace metal analysis of sample 4 showed Zn as the dominant metal, with minor components of Ni and Co. Zn was above the drinking water standard

Sample 5

Sample 5 was collected in the south-western direction from the tailings dam, in a small pond called Måketjørn, figure 5.20. The sample location is about 2 km away from the tailings dam and the measured pH was 5.64.

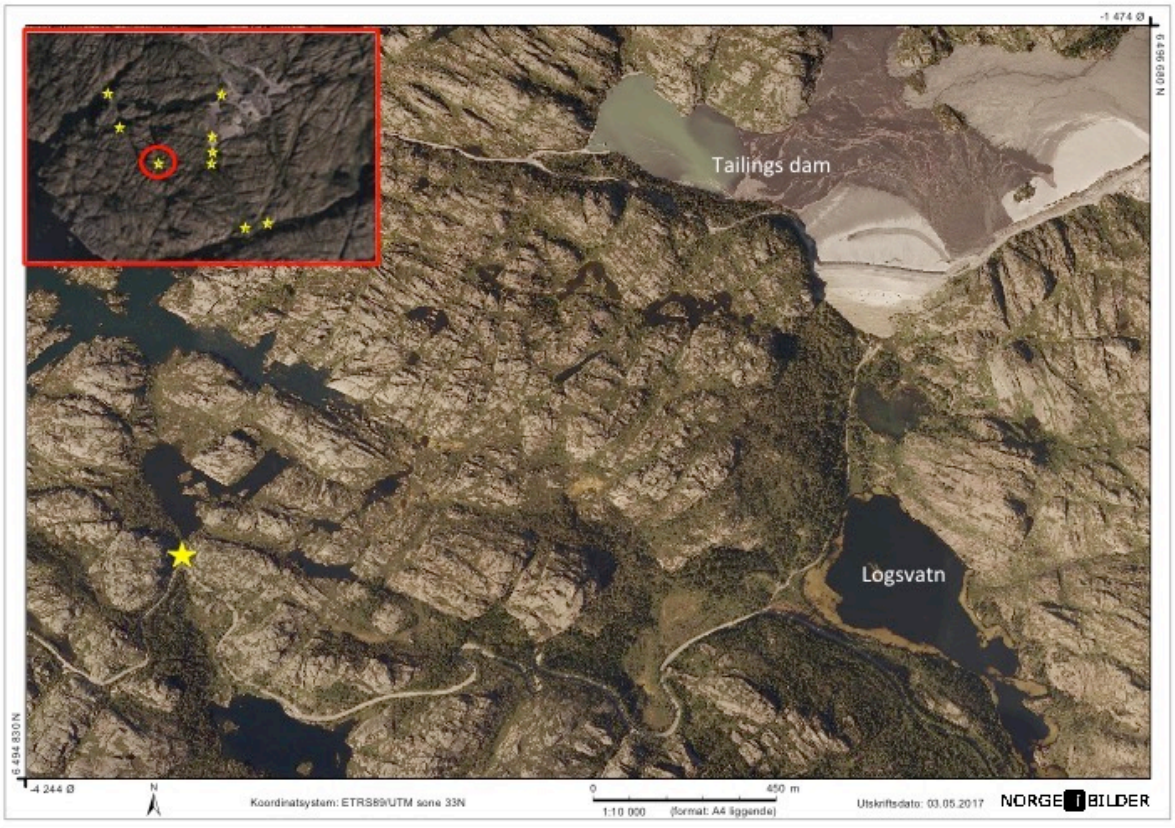

Figure 5.20: Sample 5 was taken in the southern part of a small lake 2km away from the tailings dam.

Cation/anion analysis of sample 5 gave generally low concentrations of both cations and anions, figure 5.21. Note the change in scale from 100 mg/L to 10 mg/L. Na and Cl was the most abundant ions.

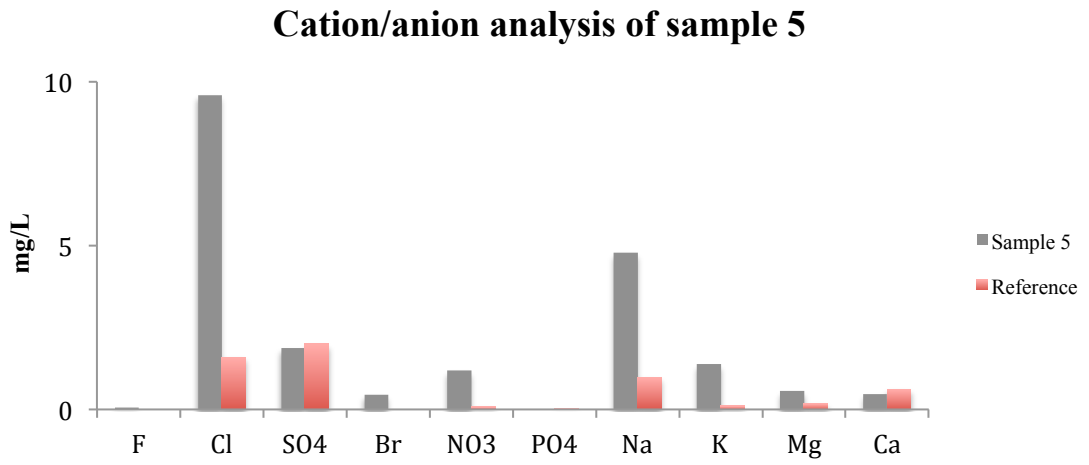

Figure 5.21: Note the scale. The cation/anion analysis of sample 5 showed Cl and Na as the dominant ions. All values elevated above the reference values of lake element composition in the south of Norway, except SO_4 and Ca.

The trace element analysis for sample 5 is presented in figure 5.22 below. Zn remained the element with highest concentration compared to the other elements. Note that the second (April 2017) measurement showed a dramatic decrease in Zn values compared to the first (November 2016) measurement.

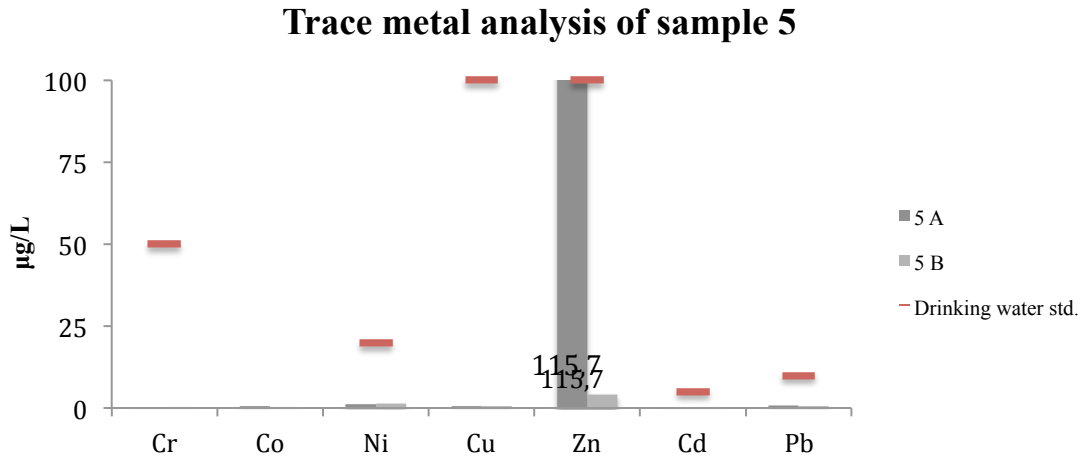

Figure 5.22: Trace metal analysis of sample 5 showed Zn as the dominant metal. Zn was above the drinking water standard

Sample 6

Sample 6 was collected in the lake downstream of the tailings dam wall, called Logsvatnet, figure 5.23. Sample 6 was taken at approximately 1km from the tailings dam. The tailings dam leak drainage water in the direction of the Logsvatn that are pumped back up to the dam and then further let out into the Jøssingfjord. The pH measured in this sample was 6.35.

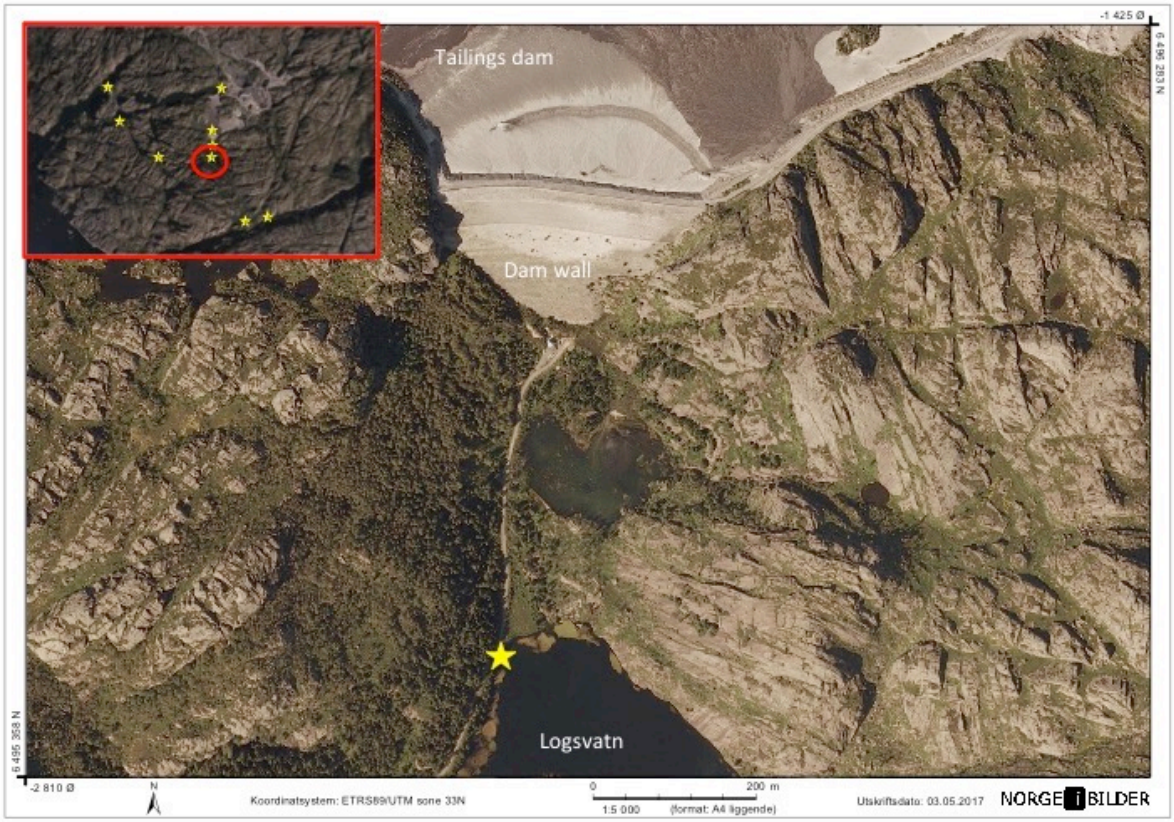

Figure 5.23: Sample 6 was taken in the northern end of Logsvatn, a lake downstream the tailings dam.

The cation/anion analysis showed highest concentration of SO_4, while Ca, Na and Cl are within the same range around 10 mg/L, figure 5.24.

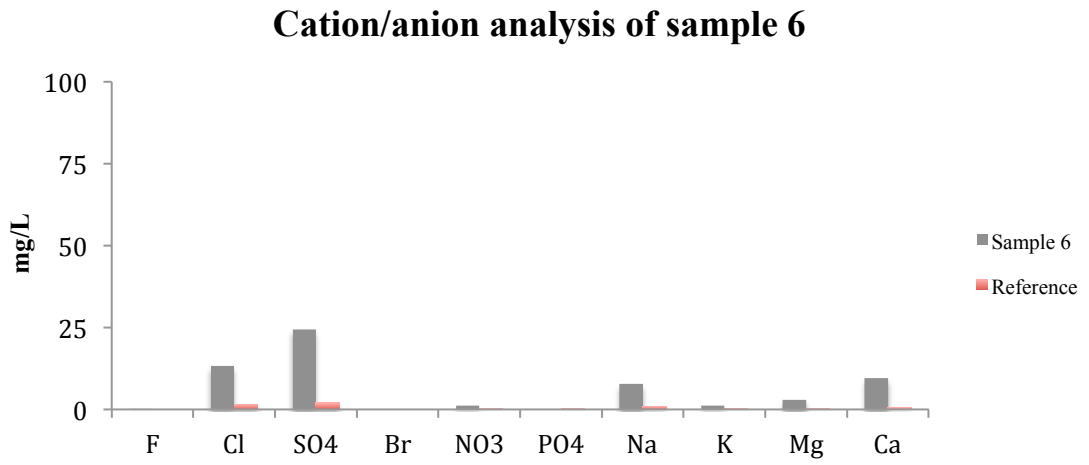

Figure 5.24: The cation/anion analysis of sample 6 showed SO_4 and Cl as the dominant ions. All values elevated above the reference values of lake element composition in the south of Norway, except PO_4 and Br that was *n.a*.

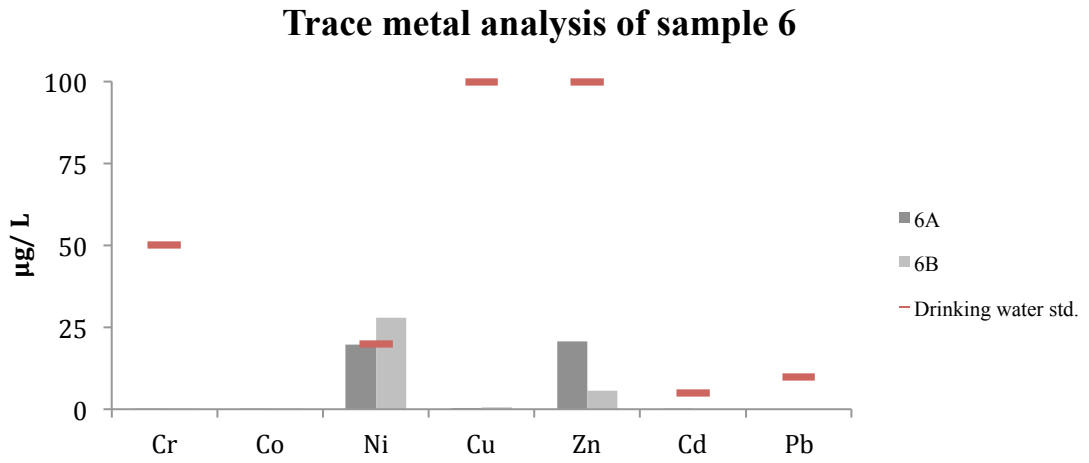

Figure 5.25: Trace metal analysis of sample 6 showed Ni and Zn as the dominant metals. Ni was above the drinking water standard with 27,9 µg/L in 6B, and just below in 6A with19,8 µg/L.

The trace metal analysis for sample 6 gave the results in figure 5.25. Zn and Ni were the elements that had the highest concentrations. Zn was within range of drinking water standards, while Ni was slightly below in 6A and above in 6B with 29,7 µg/L.

Sample 7

Sample 7 was collected from the outlet ejected from the tailings dam in front of the dam wall, see figure 5.26. This water is drainage water from the tailings. pH was measured to 7.5 in sample 7, and was taken approximately 500m from the tailings dam.

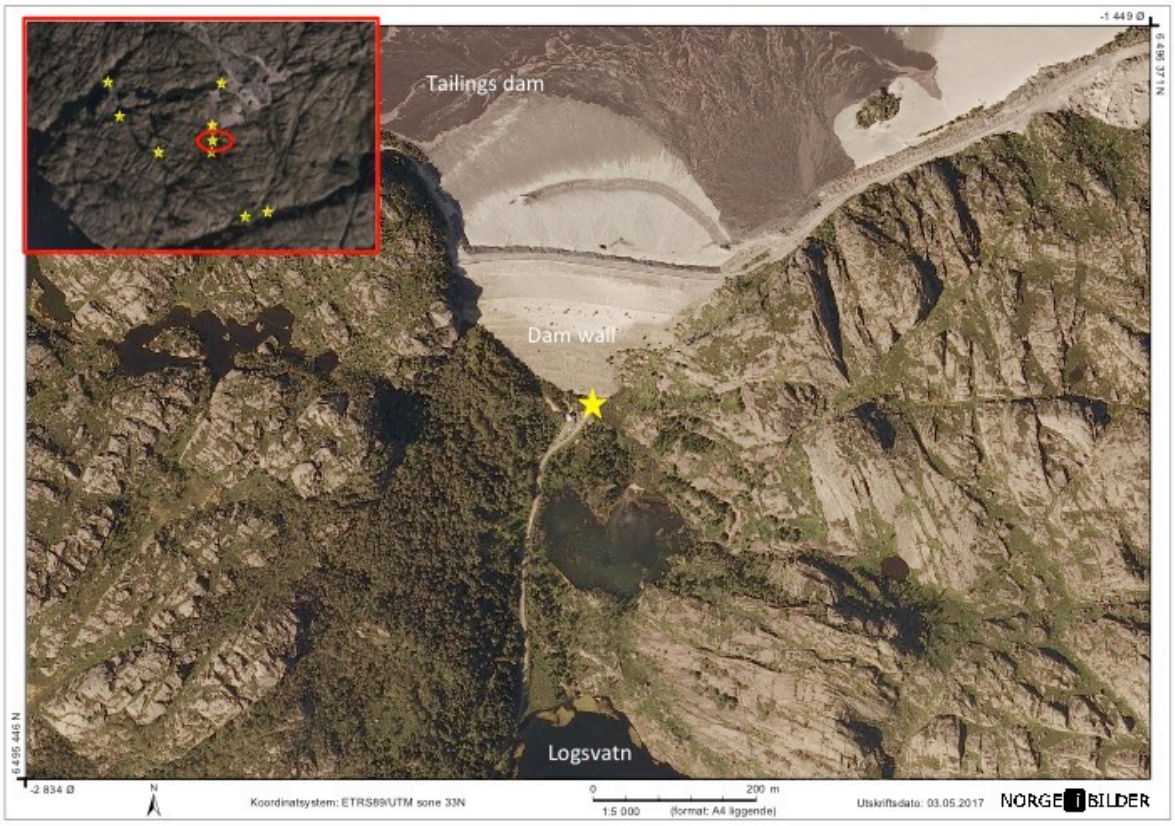

Figure 5.26: Sample 7 was taken just below the tailings dam, from the direct outlet point from the dam.

Cation/anion results showed highest values for SO_4 and Ca, but also Mg and Na had higher concentrations in sample 7 than in the other samples. All values exceed the reference values by far.

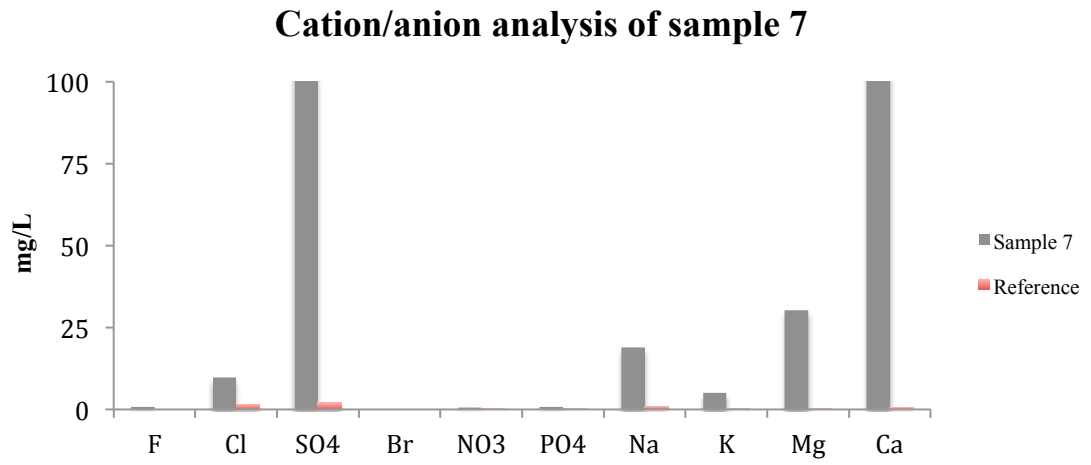

Figure 5.27: The cation/anion analysis of sample 7 showed SO_4 and Cl as the dominant ions, and they both exceed the scale of 100 mg/L. All values elevated above the reference values of lake element composition in the south of Norway, except Br that was *n.a*.

The trace metal results from sample 7 revealed Ni and Cu as the dominant metals, with the second measurements giving the highest values, figure 5.28. Ni was here measured with the highest values of all samples so far, with 7A as 259,9 and 7B 433,4 µg/L. Cu was measured in 7B with 81,5 µg/L, but only 1,5 in 7A. All other metals had concentrations below drinking water standards.

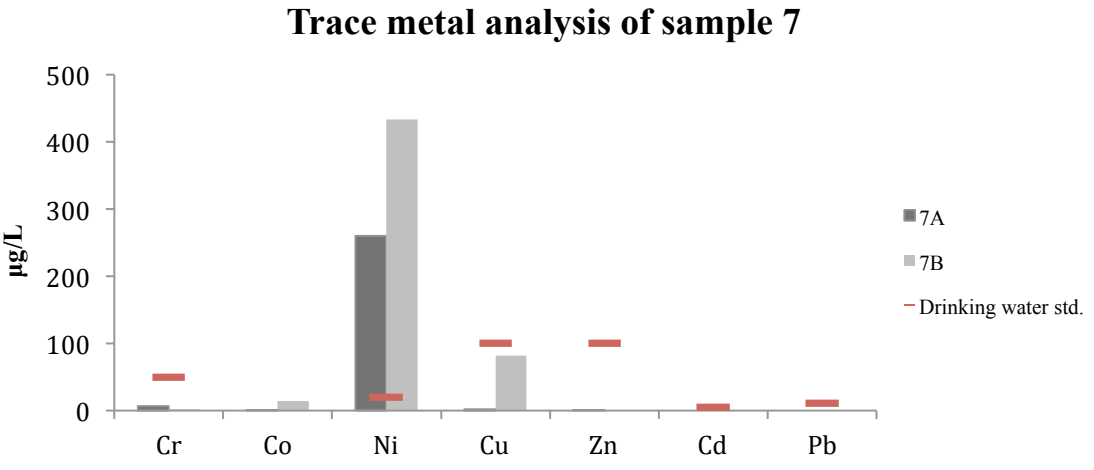

Figure 5.28: Trace metal analysis of sample 7 showed Ni and Cu as the dominant metals, with minor values of Co. Ni was highly above the drinking water standard at both measurements. Note the scale. Cd and Pb below detection limits.

Sample 8 and 9

Sample 8 and 9 was both collected in the small nearby village, Åna Sira, see figure 5.29. Sample 8 from a creek downstream the tailing dam, and sample 9 in a small river draining an area east of the dam.

Sample 8 was taken approximately 3km from the tailings dam and sample 9 was 3,4 km away. pH measurements from these samples showed 6.71 and 5.64 respectively. Hence, a higher pH was obtained from the creek downstream the tailings facility.

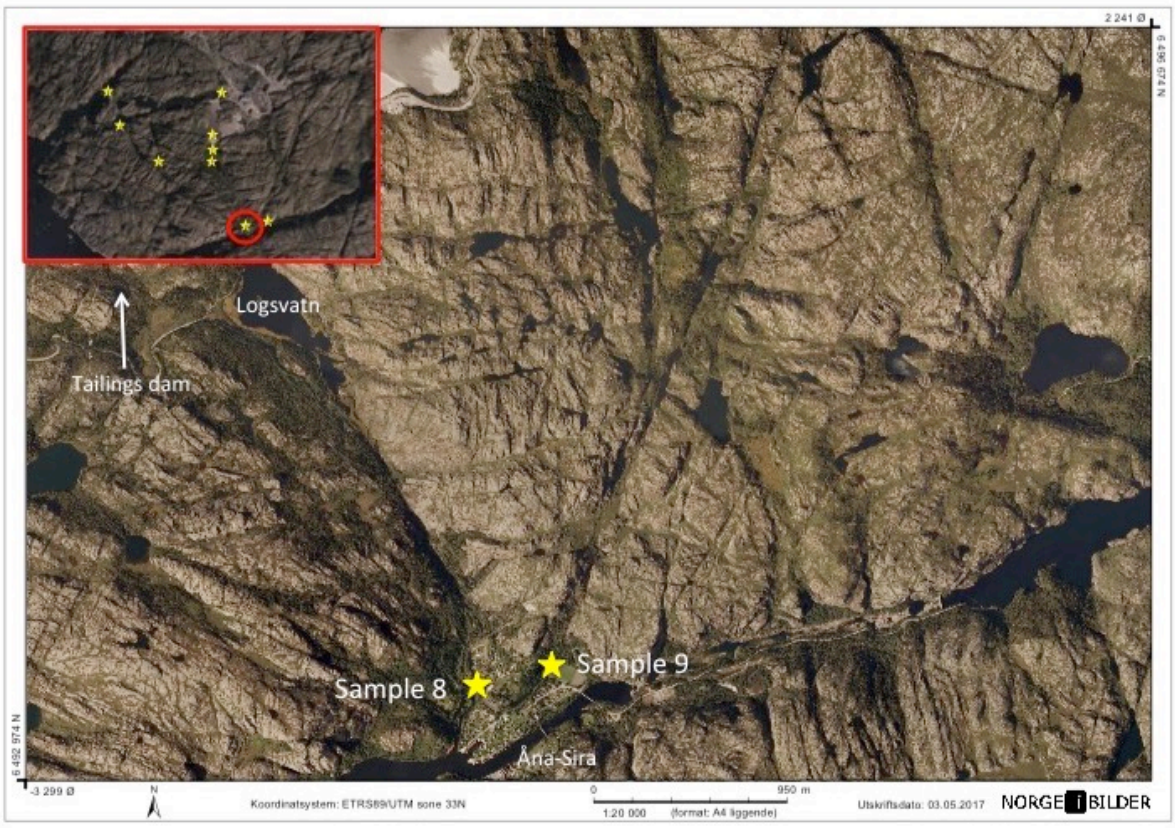

Figure 5.29: Sample 8 was taken in the northern part of the small village Åna-Sira, south- southeast of the tailings dam. Sample 9 was taken further east, in a small creek near the local football field.

The cation/ anion analysis of sample 8 showed that SO_4 was the dominating anion, while Ca and Mg were the most abundant cations, figure 5.30.

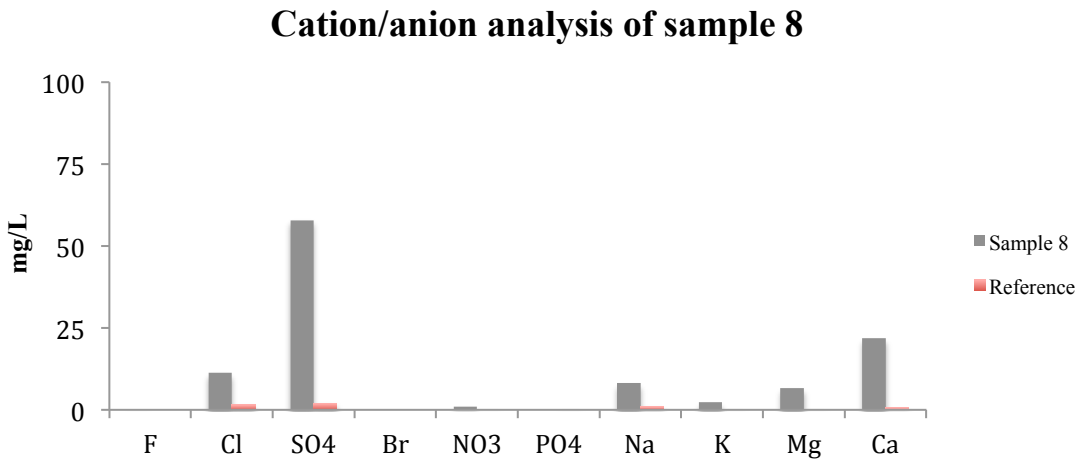

Figure 5.30: The cation/anion analysis of sample 8 showed SO_4 and Ca as the dominant ions. All values elevated above the reference values of lake element composition in the south of Norway, except PO_4 and Br that was *n.a*.

Trace metal analysis of sample 8 had overall lower concentrations of elements than sample 7, but Zn and Ni were still the elements of highest concentrations, figure 5.31. The first measurement done in November 2016 continues to provide with lower concentrations of Ni and especially Zn.

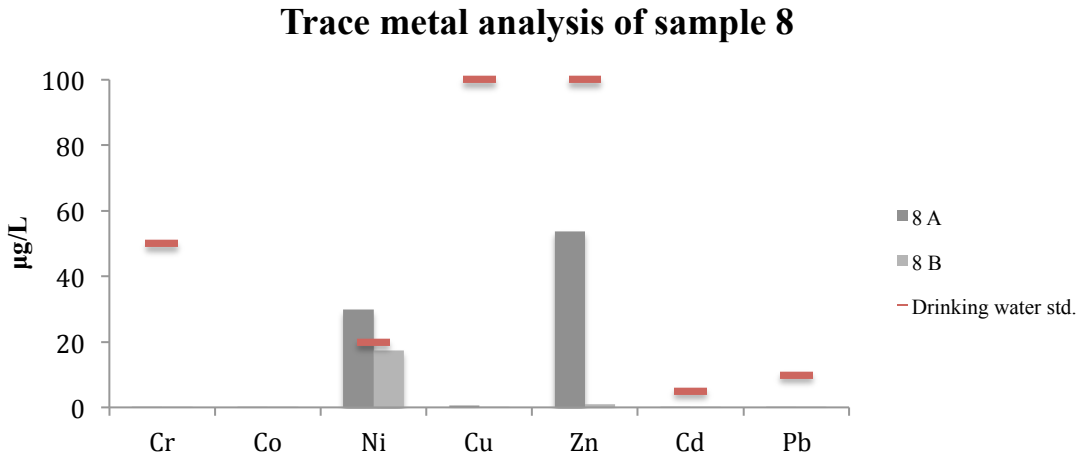

Figure 5.31: Trace metal analysis of sample 8 showed Ni and Zn as the dominant metals. Ni was above the drinking water standard in the first measurement, but was below the limit of 20 µg/L in the second.

The cation/anion analysis of sample 9 gave over all low concentrations of all ions, figure 5.32. Cl and Na were the most abundant with 9,9 and 4,8 µg/L, respectively.

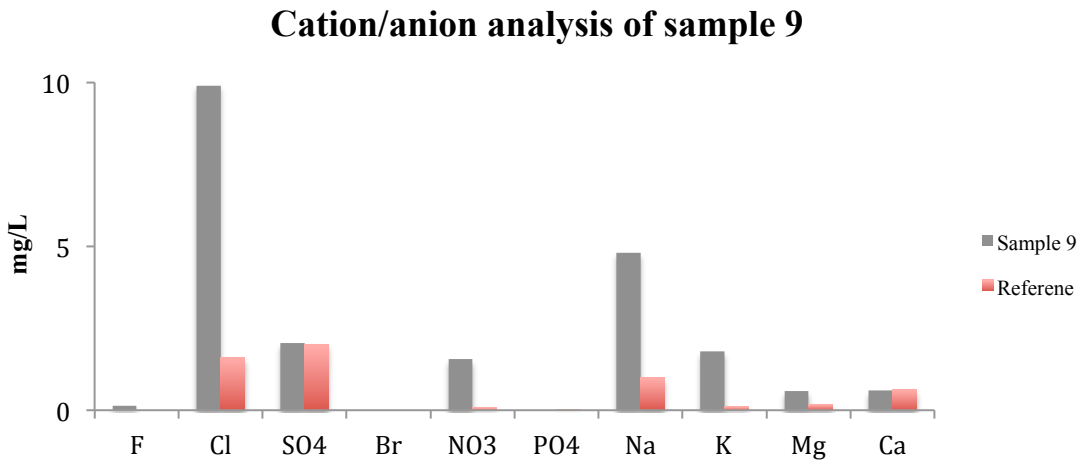

Figure 5.32: Note the scale. The cation/anion analysis of sample 8 showed Cl and Na as the dominant ions. All values elevated above the reference values of lake element composition in the south of Norway, except ca. PO_4 and Br were *n.a.*

The trace metal analysis showed that most of the elements had low concentrations, with except of Zn that once again had higher concentration in the first measurement than the second, figure 5.33. However, Zn was still below the drinking water standard.

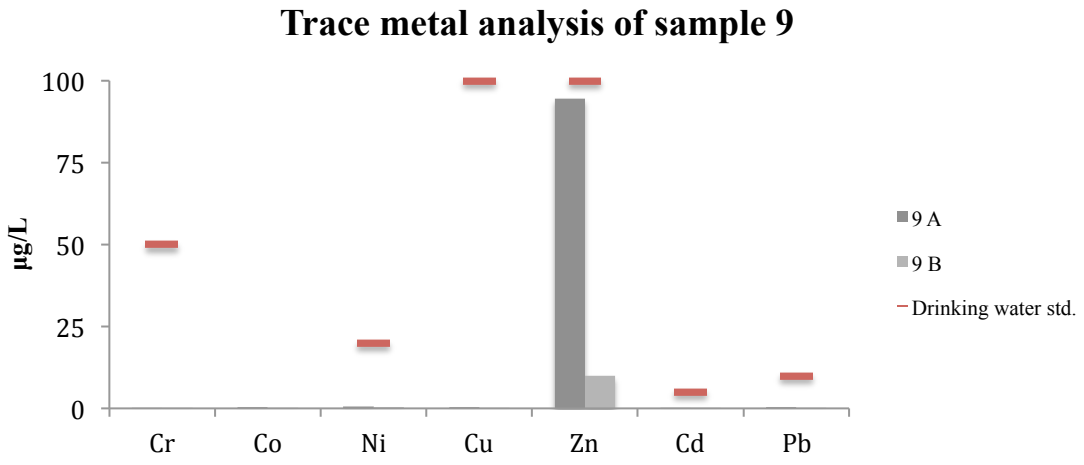

Figure 5.33: Trace metal analysis of sample 9 showed Zn as the dominant metal, but it was below the drinking water standard. Note the difference in the two measurements 9A and 9B.

Brief summary of the water samples results

Samples taken at, or in near proximity to, the mine and the tailings dam showed high concentrations of SO_4, Ca and some heavy metals. Sample 1 contained the most SO_4.
Ni and Zn were most abundant in the samples with direct link to the tailings dam and drying plant, that being sample 1, 2, 3 and 7. Besides Ni and Zn, the other trace metals were generally of low concentration.
The pH was highest closest to the tailings dam in sample 1, 2 and 7. The pH decreases with the distance from the mine area, and reaches normal lake pH values of ~ 5.6.
Sample 7, the one taken at the outlet in the bottom of the tailings dam, showed the highest trace metal concentrations, and also the highest values of cations and anions.

5.2.4 Environmental Quality Standards for Ni and Cu

Nickel and Copper is a EU (European Union) priority substance; it can subsequently be used to classify the chemical conditions in water bodies. The Environmental Quality Standards (EQS) limit values are:

- Annual Average (AA) EQS <4 µg/L for Ni and <7.8 for Cu in inland surface waters
- Maximum Allowable Concentration (MAC) < 34 µg/L for Ni and <7.8 for Cu inland surface waters

Ni and Cu are classified accordingly to the M-241 report from the Norwegian Environment Agency (Arp et al., 2014). The following tables 5.3 states the classes for environmental conditions for the priority substances Ni and Cu, and table 5.4 classifies the water samples from section 5.2.3 accordingly.

Table 5.3:Environmental Quality standard limits for Ni and Cu

(inland surface waters)	I	II	III	IV	V
Ni µg/L		AA	MAC		
	< 0.5	0.5 - 4	4 - 34	34 - 67	> 67
Cu µg/L	0.3	7.8	7.8	15.6	>15.6

Table 5.4: Water samples from section 5.2.3 classified after EQS

Ni (µg/L) classification for environmental conditions of the water samples

Sample	1	2	3	4	5	6	7	8	9
Ni µg/L	48.8	30.9	41.4	2.2	1.3	23.9	346.7	23.6	0.5
Cu µg/L	0.52	1.9	1.94	0.50	0.52	0.49	41.56	0.40	0.27

5.3 Marine: box core experiments

The results comprise of pH, Eh and sulphides electrodes measurements, metal fluxes to the water column and DGT uptake from pore water concentrations.

5.3.1 Water chemistry

Electrode measurements of pH, the redox potential (Eh) and the sulphide content (Es) were performed in order to better understand the environment in the liners with fjord bottom sediments overlain by a 2cm thick cover of mine tailings. Three control liners were used as a reference. These had no tailings, just "clean" fjord bottom sediments, but were stationed in the same mesocosm tank, see section 4.4.1. The Es measurements were so low they were evaluated in agreement with NIVA to be of no significance, however the measurements can be seen in appendix A.

The pH values measured from the sediment surface to a 75 mm depth can be seen in the figures 5.34 and 5.35. The transition tailings-fjord sediments are marked with a black line in all figures. The range of both Titania and control liners stay within the pH values of 7,5-8. The top layer displays almost the same pH value of 7,6-7,8, being tailings in Titania liners and in control liners fjord bottom sediments. The pH gradient in the Titania liners displays an increase in pH with depth, reaching a stable value at approximately 30 mm depth. The pH gradient in the control liners decreases towards a depth of 30 mm, then slowly and continuously increases up to a pH of 7,8.

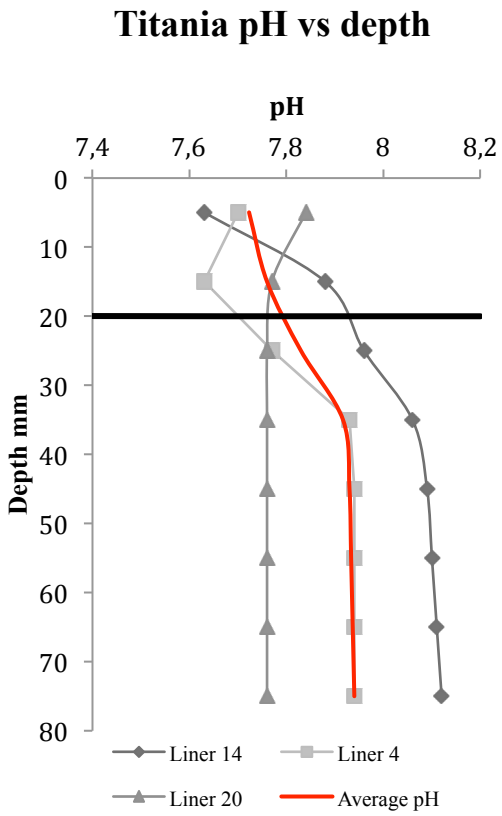

Figure 5.34: pH measurements from the sediment surface down to a depth of 75mm. The boundary between tailings and fjord bottom sediments is marked (black line) at 20 mm depth. The average pH (red line) gradually increases from 7,7 to 7,9 from sediment surface to 35 mm depth, before stabilizing downwards.

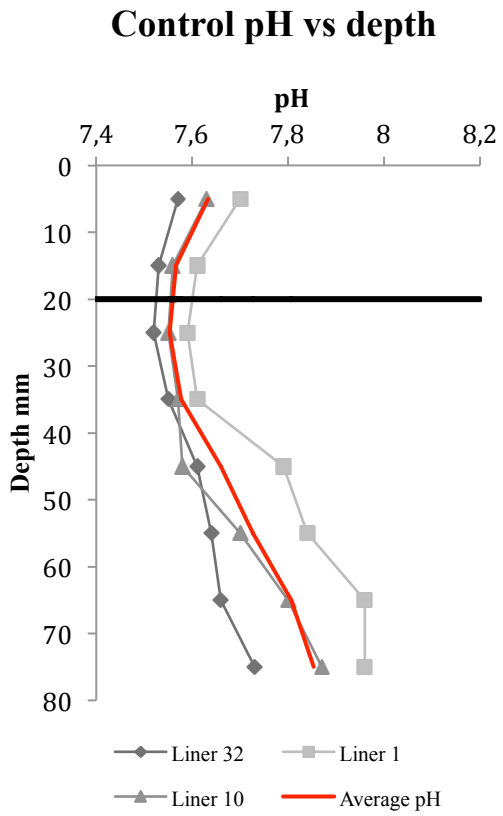

Figure 5.35: pH measurements from the sediment surface down to a depth of 75 mm The boundary between tailings and fjord bottom sediments is marked (black line) at 20 mm depth The average pH (red line) decreases slightly from sediment surface to a depth of 35 mm, for then to gradually increase up to a pH of 7,8.

The redox potential was measured at the same depth intervals, figures 5.36 and 5.37. Eh provides an insight on whether the conditions are oxidizing or reducing, or the change between the two. The redox conditions are important for the release or sorption of heavy metals (Appelo and Postma, 2005). The Titania liners showed a slow gradual decrease in Eh, indicating that the conditions slowly turn more reducing. Within the depth range measured the Eh levels never turned very reducing (anoxic). The control liners show a quite different pattern. The gradient stays almost straight before reaching a depth of 7cm where a sharp change occurs, and the redox potential drops significantly.

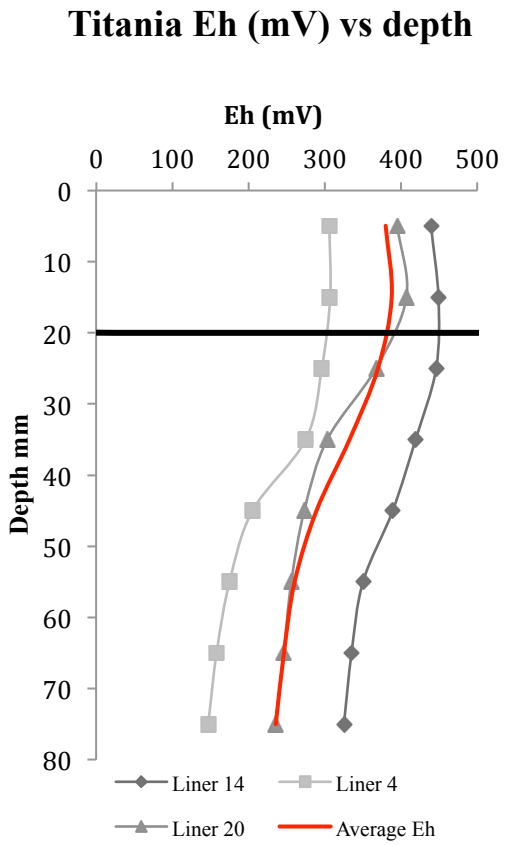

Figure 5.36: Eh measurements from the sediment surface down to a depth of 75 mm. The boundary between tailings and fjord bottom sediments is marked (black line) at 20 mm depth. The average Eh (red line) shows a gradual decrease in redox potential with depth.

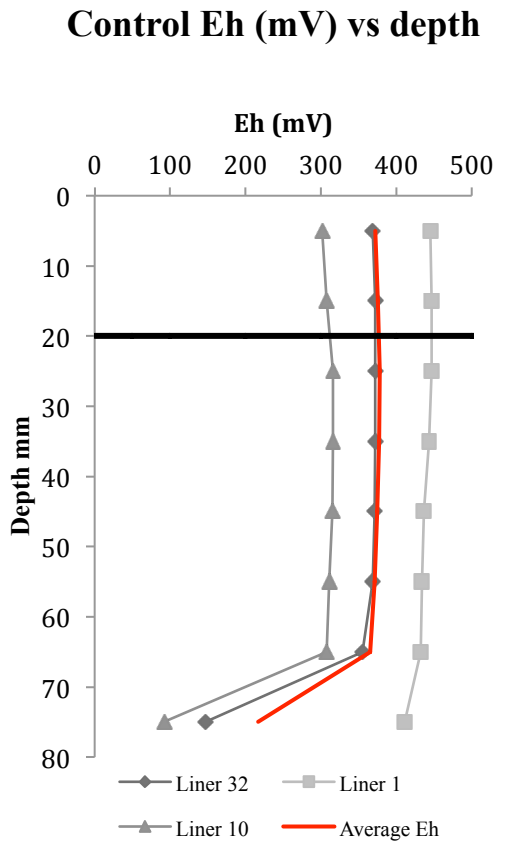

Figure 5.37: Eh measurements from the sediment surface down to a depth of 75 mm. The boundary between tailings and fjord bottom sediments is marked (black line) at 20 mm depth. The average Eh (red line) shows stable redox potential from sediment surface to a depth of 65 mm, where it rapidly decreases.

From the electrode measurements, the conditions in the Titania liners are not that different in comparison the control liners. The pH values stay within the same relatively neutral range, with no sharp gradients. The redox potential differ a bit more, with the control liners showing a consistent value until reaching a rapid decrease in Eh, while Titania has a gradual decrease with depth. To further support the redox-potential done by Eh measurements, the DGT-profiles of Fe and Mn vs. depth will be shown, as they are known to be good proxies for redox, figure 5.38.

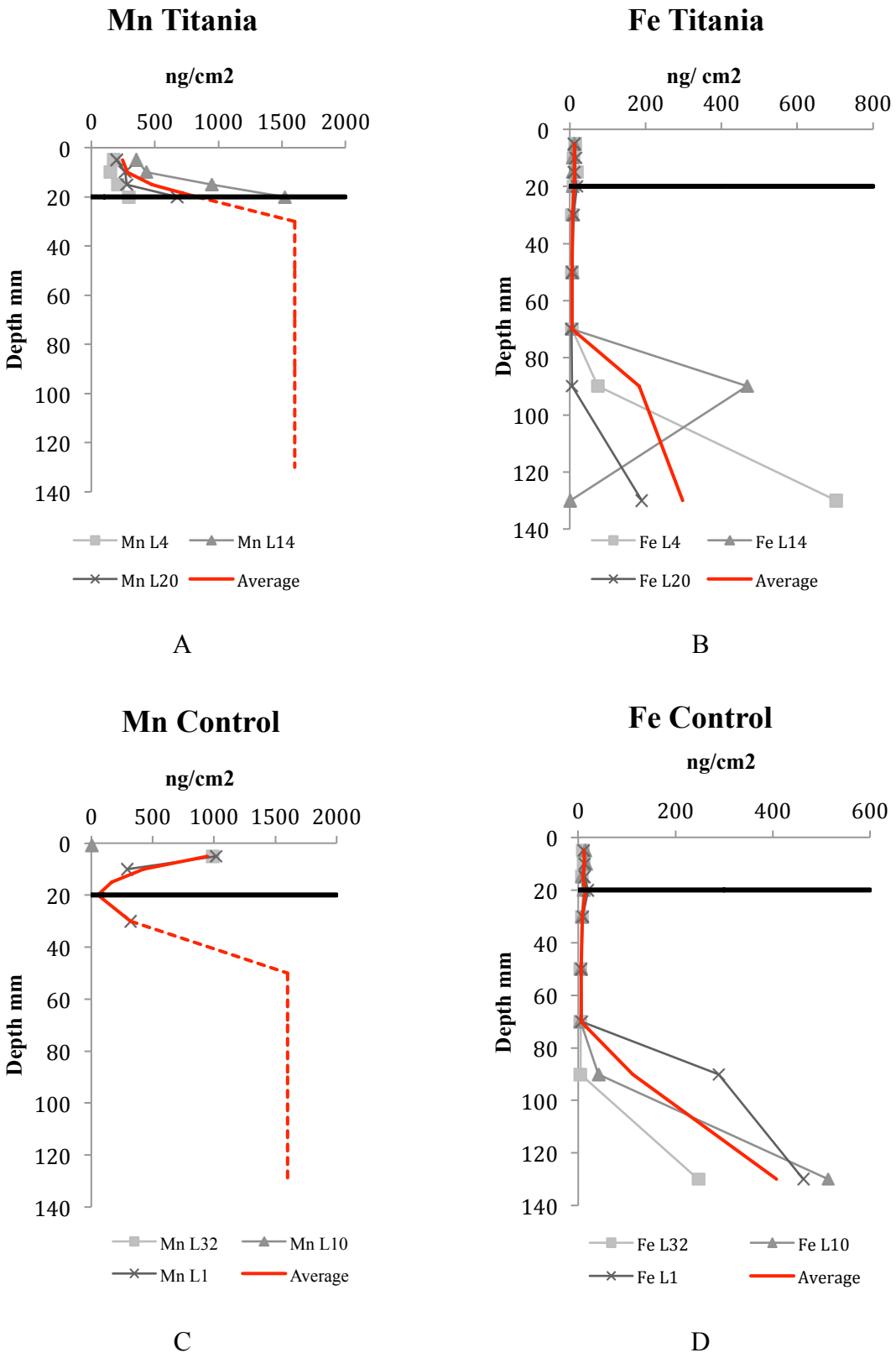

Figure 5.38: A and B represents Mn and Fe in Titania liners, respectively. C and D are the control liners.

Figure 5.38 displays the DGT-profiles for Mn and Fe in both Titania and control liners. Mn values quickly reached beyond the detection limit of the QICPMS, hence the dashed lines indicate this, plot A and C. All values, for both Titania and control liners, beneath the tailings-fjord sediments border at 20 mm depth are present to illustrate the rapid increase, and the overall high uptake.

However, both Mn and Fe plots supply information to the Eh (redox potential) plots. Firstly, in the Titania liners Mn increased rapidly with depth, indicating that more Mn was present in the pore water downwards in the liner. Yet, there was Mn present from sediment surface, hence the redox boundary is not that abrupt. Fe showed a profile where little/no Fe was present in the pore water until a depth of 70 mm, where uptake increased.

5.3.2 Trace metal concentrations

The trace metal concentrations were measured by two methods, flux measurements and DGT-probes, respectively described in sections 4.4.5 and 4.4.6. The flux was estimated by measuring the metal concentration in the water column above the sediment surface within the liner, and comparing with the concentration in the water entering each liner. The DGT- probes measures the metals adsorbed in the Chelex gel during 24h exposure to the pore water. This uptake is assumed to be proportional to the concentration in the pore water. The measurements were done in depth intervals down to 130 mm. Two metals will be presented, and the other seven's profiles can be seen in appendix. This is due to Titania's most pressing concerns, the leaching of nickel and copper. Consequently, these were the two metals that were most abundant and of special interest. The other seven; Cr, Mn, Fe, Co, Zn, Cd and Pb were all present, but are not of specific interest to this thesis. Mn showed, for the record, at many measure point so high values that the ICPMS peaked the detection limit for that element >300 ppb giving >1600 ng/cm2. The DGT uptake profiles for the seven metals can be found in appendix B.

Flux measurements

The fluxes were measured at three times in each box per element, table 5.5. Ni is the element that differ most from the control liners, with 2201 to only 1,1 µg m-2 d-1. Also, Cu, Co and Zn are elements that distinctly diverge from the "natural" values found in the control liners. Cd and Pb show similar values with or without mine tailings from Titania. Moreover, Pb has negative flux values, indicating that Pb in the system is taken up in the sediments/tailings rather than being released into the water column.

Table 5.5: Flux measurements for metals Pb, Cd, Cu, Co, Ni and Zn in each liner as well as the average flux. Treatment T and C represents being added Titania tailings or control with "clean fjord sediments," respectively.

Treatment	Liner	Pb	Cd	Cu	Co	Ni	Zn
				(µg m-2 d-1)			
T	4	-0,48	0,71	15,94	2,36	1959,02	50,11
T	14	-0,18	0,42	24,86	27.93	1382,1	16,7
T	20	-0,77	0,87	24,58	99,93	3264, 62	27,70
Average		**-0,5**	**0,7**	**21,8**	**43,4**	**2201**	**31,5**
C	1	-0,23	0,09	2,35	0,44	1,58	0,09
C	10	-0,84	0,01	0,91	0,82	0,72	5,62
C	32	-0,80	0,08	3,65	0,37	1,1	-0,34
Average		**-0,6**	**0,06**	**2,3**	**0,5**	**1,1**	**1,8**

Fluxes of Ni, Co, Cu, Zn and to a lesser extent Cd, are significantly higher from tailings than for the control sediments. For Ni the flux is increased by a factor of >1000x compared to control sediments, while for the other above-mentioned metals 10x.

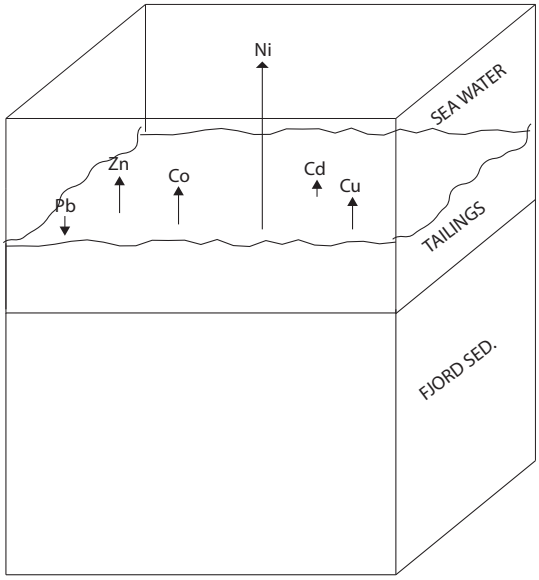

Figure 5.39: A graphic illustration of metal fluxes found the Titania liners by the average values. Note that the figure is not in scale. Ni is the metal that had the highest flux rates, followed by Co, Zn and Cu. Cd had a low flux, while Pb showed negative flux (uptake).

Figure 5.39 is a graphic presentation of the fluxes in the liners containing mine tailings from Titania. The arrows length indicates the flux of each trace metal from the tailings to the water column above, however not in accurate scale. Note that Pb has an arrow pointing downwards indicating a negative flux. Pb is sorbed to the tailings from the water column, the opposite of what is happening to the other trace metals.

Table 5.6 and 5.7 show the calculated flux values for the two marine storage sites at Titania, Jøssingfjord and Dyngadypet in kg/ year. It is evident that the tailings influence is present, and Ni is the metal that stands out as the primary pollutant. However, there are metal fluxes from natural fjord bottom sediments as well, as presented in table 5.7, although in a smaller scale. This the flux measured in the water column above the tailings/ fjord bottom sediments as illustrated in figure 5.39 above.

Table 5.6: The calculated metal fluxes from the marine storage sites Jøssingfjord and Dyngadypet under influence of Titania tailings. Calculations can be seen in appendix D.

Storage sites		Flux measurements Titania (kg/year)					
		Pb	**Cd**	**Cu**	**Co**	**Ni**	**Zn**
Jøssingfjord	0,27 km^2	0,0	0,1	2,1	4,3	217,0	3,1
Dyngadypet	0,82 km^2	-0,1	0,2	6,5	13,0	658,9	9,4

Table 5.7: The calculated metal fluxes from the marine storage sites Jøssingfjord and Dyngadypet under influence of Titania tailings.

Storage sites		Flux measurements Control (kg/year)					
		Pb	**Cd**	**Cu**	**Co**	**Ni**	**Zn**
Jøssingfjord	0,27 km^2	-0,1	0,0	0,2	0,1	0,1	0,2
Dyngadypet	0,82 km^2	-0,2	0,0	0,7	0,2	0,3	0,5

DGT- uptake

The depth vs. uptake rate (24h) profiles, Figure 5.40 and 5.41, clearly depicts the difference in Ni uptake in the liners with mine tailings and those without. The profiles show distinct differences. The scale itself indicates dissimilarity, where the Titania liners have values close to 800 ng/cm^2 while the control liners reaches a maximum of barely 8 ng/cm^2.

The Ni uptake at the Titania liners peaks sharply at 10-40 mm depth, for then to decrease to low levels at 60 mm depth. The control liners did not have measureable Ni uptake until 40 mm depth, and even then the uptake are very low ranging from 2 to 8 ng/cm^2.

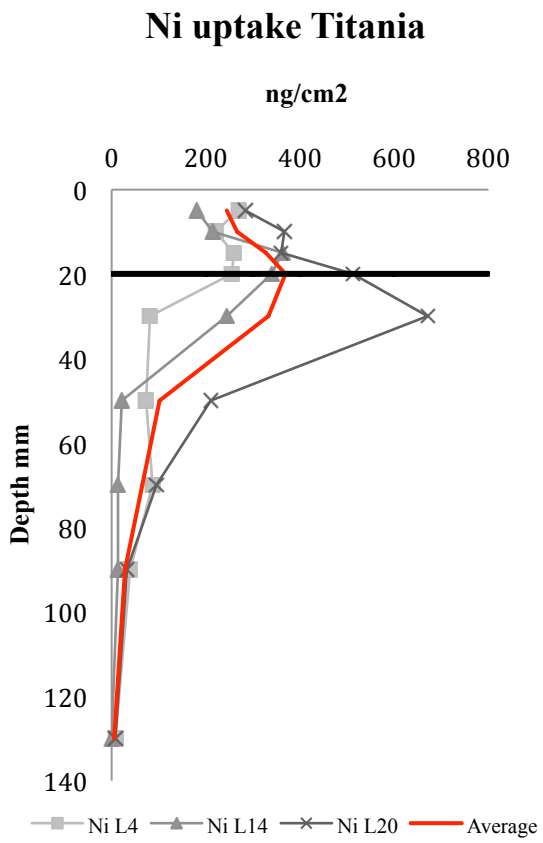

Figure 5.40: Ni uptake rate (24h) vs. depth in the Titania liners. The boundary between tailings and fjord bottom sediments is marked (black line) at 20 mm depth. The average Ni uptake (red line) increases in the upper 20 mm, for then to decrease with depth.

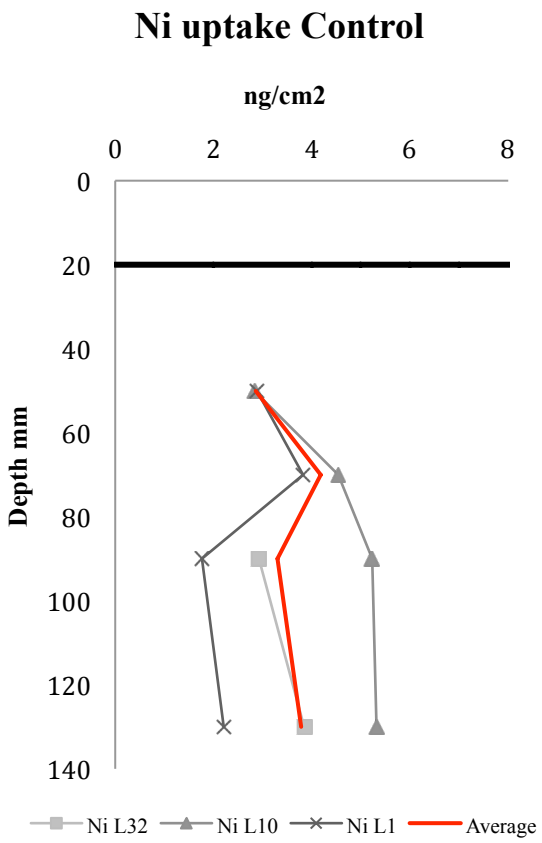

Figure 5.41: Note the difference in scale compared to Titania. Ni uptake vs. depth in the control liners. The boundary between tailings and fjord bottom sediments is marked (black line) at 20 mm depth. The Ni uptake was below detection limit until 50 mm depth. The average Ni concentration (red line) first increase to 70 mm depth, for then to decrease with depth.

Copper is the other trace metal pollutant of interest. The uptake rate (24h) vs. depth profiles can be seen in figures 5.42 and 5.43. The profile from Titania shows a rapid increase of Cu from 10-40 mm depth, for then to gradually decrease with depth. The control profile does not show much variation from the sediment surface and down. The uptake ranges between 0-1 ng/cm^2.

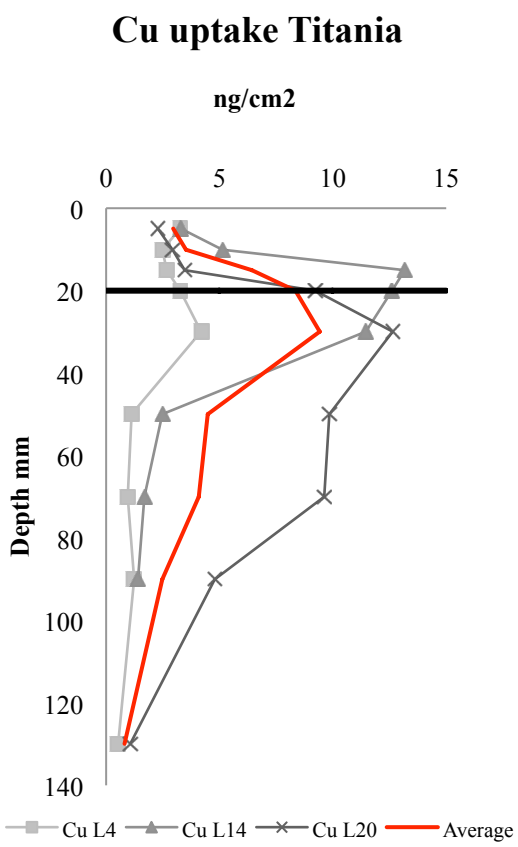

Figure 5.42: Cu uptake vs. depth in the Titania liners. The boundary between tailings and fjord bottom sediments is marked (black line) at 20 mm depth. The average Cu uptake (red line) increases beneath the tailings- sediment boundary until a depth of 35 mm, where the uptake slowly decreases with depth.

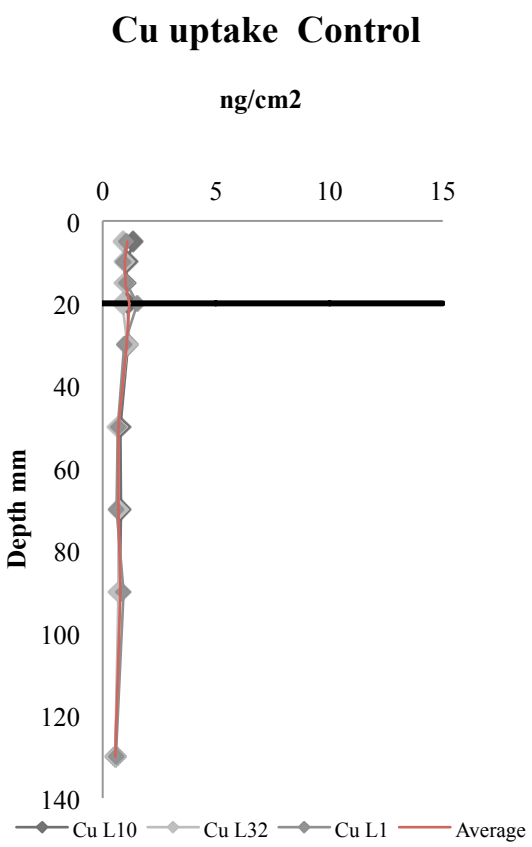

Figure 5.43: Cu uptake vs. depth in the control liners. The boundary between tailings and fjord bottom sediments is marked (black line) at 20 mm depth. The average Cu upake (red line) was quite uniform, showing little change with depth and continuous low values throughout the profile.

Flux of metals to the water column vs. DGT uptake proportional to the pore water concentration

Both flux and DGT measurements give information on the metal concentrations released from Titania mine tailings. The flux measures the release of trace metals to the water column above the tailings, while DGT measures concentration values proportional to the pore water concentration. Since they both are measuring the tailings under the same set of conditions, one could expect the results to correspond. The results were plotted in a log-log plot with a regression line to better see the fit of the methods, figure 5.44. The R^2 is the correlation coefficient, and since it is both positive and relatively high (0,65) one could argue a good fit between the methods. This plot has included the results from the Nussir mine tailings, an additional part of NIVA's project. Nussir is a Norwegian mine company that mines a copper deposit. This data was included to have a more valid regression with more data points. The liners containing Nussir tailings were placed in the same mesocosm tank as the Titania tailings and the control liner's, see figure 4.9.

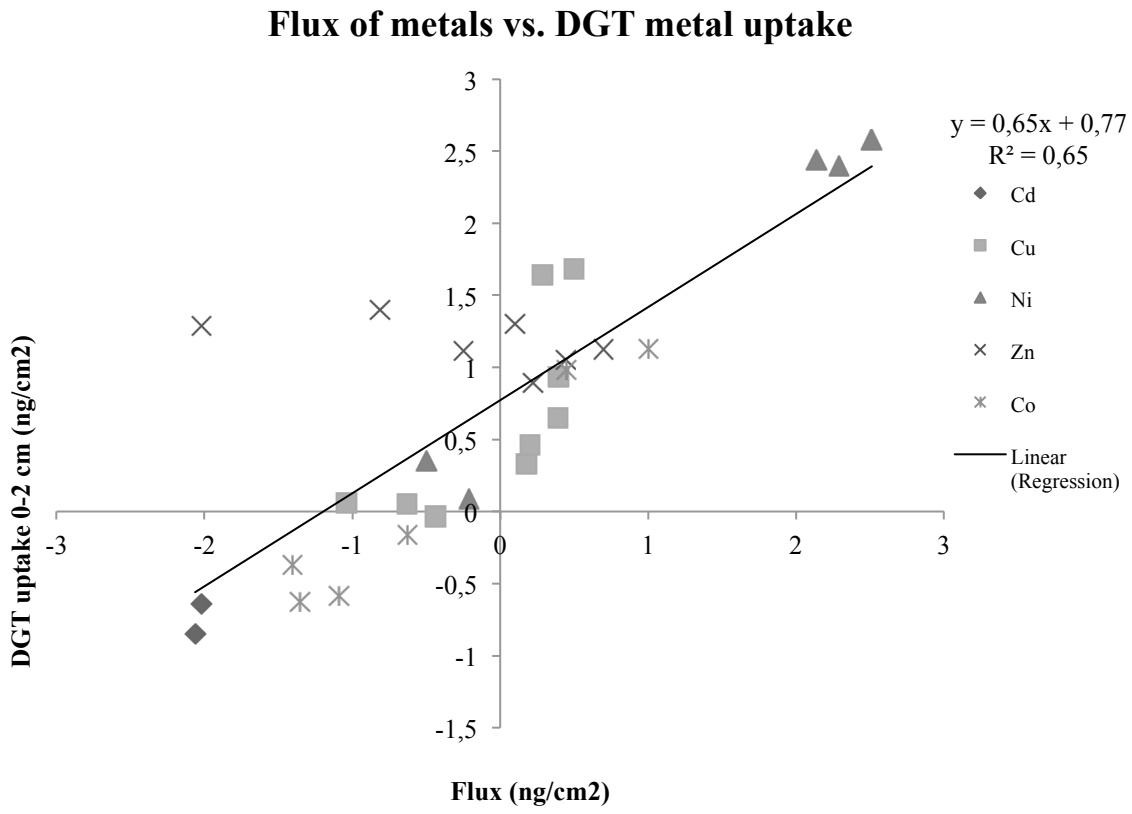

Figure 5.44: DGT metal uptake (ng/cm2) vs flux of metals to the water column (ng/cm2).

This scatter shows a positive correlation between the flux and the DGT measurements, implying that when the flux is high, the uptake on DGT is high as well.
It is evident that the concentrations of Ni from the Titania liners stretch the line upwards, as most of the other elements tend to be more gathered. This will influence the line, and hence the fit of the models. The purpose of this plot is to evaluate the correlation between the methods, so that possibly one could use the method most practical in a given setting, and then use the regression line to find the corresponding value. Thus, one could only measure concentrations by DGT-probes, and then find the corresponding value for flux by using the regression line equation.

6 Discussion

6.1 Introduction

In the discussion chapter, results presented in chapter 5 was interpreted and contextualized to better understand their meaning and significance. The structure of this chapter was based upon the previous way of separating the two disposal settings, continuing to divide the on-land setting from the marine, to finally compare and contrast the two.

6.2 On-land deposition

6.2.1 Metal constituents in the tailings

The solid sample (S-1-S) described in section 5.2 has been compared to analyses done by Titania. The main compounds are found to be plagioclase, pyroxene and ilmenite; this was also true for the suspended solid material in the water above the tailings (sample S-1-W). The result were obtained by using the well-known method described by Hillier (2000), but the *SiroQuant* programme works best if the user has knowledge of the content of the sample. This was not the case, as the previous samples run by Nilsen (2015) analysed the total gangue masses before deposition on the on-land site. However, the comparison can be seen in figure 6.1. Results obtain by this thesis is shown in light grey, and finds more ilmenite and pyroxene than Titania's measurements. Additionally, millerite and magnetite was found by this thesis' measurements. However, plagioclase and apatite were more profound in Titania's measurements. As this thesis' measurement was done directly on site and Titania's was not, this has natural implications to why the results differ. At the on-land storage site, the grains from the thesis' sample have had time to sort and settle after grain size and density.

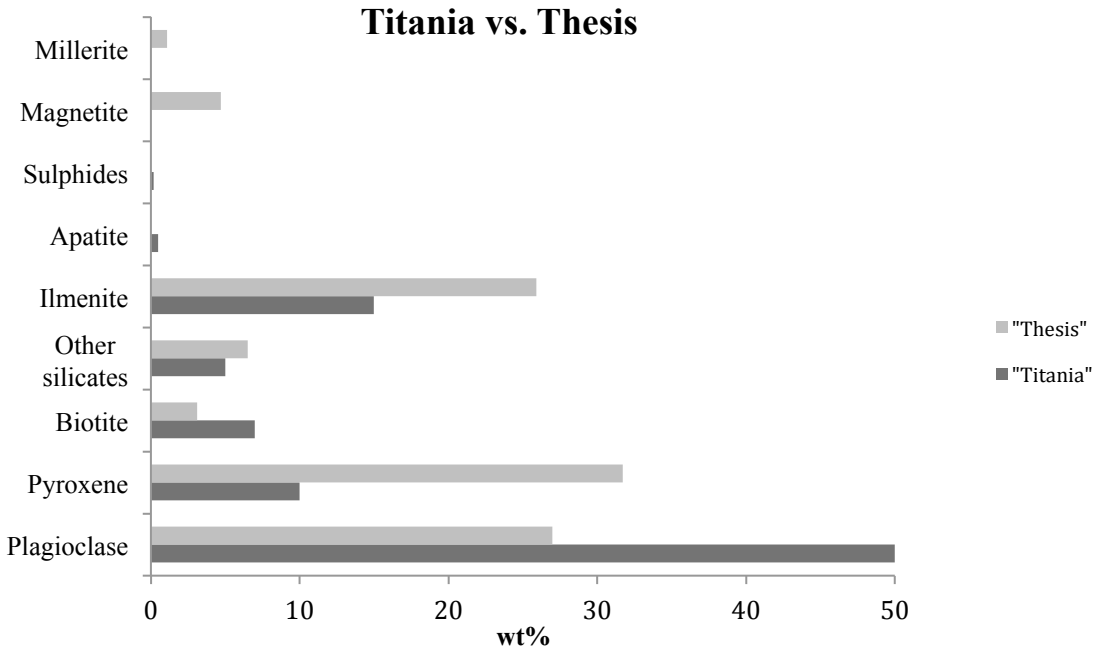

Figure 6.1: Sample S-1-S (solid tailing) vs. the measurements done by Titania.

When it comes to the suspended solid material in the water above the tailings, there is not much literature to turn to. However, the results show that pyroxene, plagioclase and ilmenite are still the dominant species, together with silicates.

6.2.2 Transport of metals by dust deposition

For the material in the tailings dam to be transported by wind to its surroundings, including Åna-Sira, the grains must be of a size in which the wind is able to transport. Hence, large grains are predicted to stay behind in the tailings dam, while the smaller fraction may be taken by the wind. This will depend on the local climate, such as the available grain size intervals, wind strength and direction, and lastly precipitation.

Aeolian transport

The transport of particles by wind is similar to those for water, but due to the wind's low viscosity and density it is after all quite different. Transport also varies with the size of the grains,

as sand-sized particles are transported by saltation and traction, while dust-sized particles by suspension (Boggs, 2014).

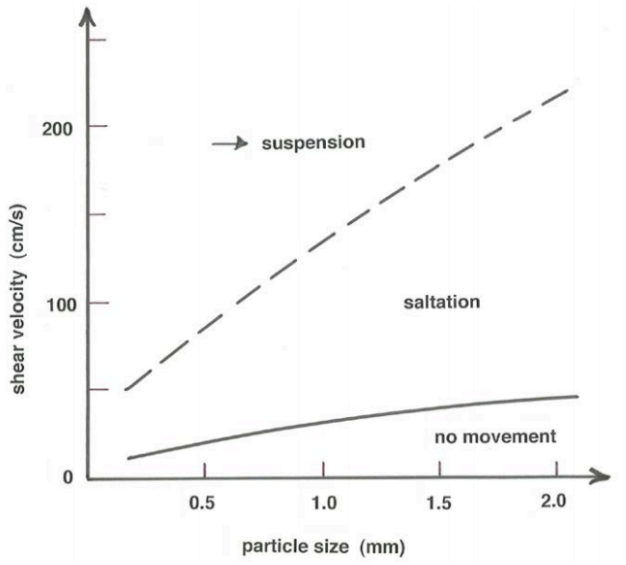

Figure 6.2: The modes of aeolian particle movements as a function of particle size and wind speed. Note that the velocity given in cm/s. (Southard, 2006).

Figure 6.2 displays the modes of aeolian particle movements as a function of particle size and wind speed, from Southard (2006). From this, small particles below 0,5mm (500 μm) will with weak wind strength barely move, and when the movement is initiated the grain will first experience transport by saltation and then by suspension. As the wind in the southwest of Norway quite frequently reaches above 2 m/s (200cm/s), suspension would be thought to be the main process.

The grain distribution analysis on the tailings sample displayed a skewed curve, with a mean value at 225 μm. The curves tail is towards the smaller grain fractions, indicating the higher presence of smaller grains to large. This can be seen in figure 5.2, section 5.2.1. The grains classify from clay fractions to fine sand. Furthermore, the analysis done by counting and placing grains found in the filters into size intervals can be seen in figure 5.3, section 5.2.2. From this, one can see that there are few grains >100 μm, and moreover the trend states an increase in abundance with a decrease in grain size. Hence, most grains blown from the tailings dam to Åna-

Sira are of the smallest fraction, <10 μm. This can perhaps be explained and understood by looking at the local climate at the time the filers were exposed to the environment, 4. -31 of August 2016.

The local climate

Titania provided monthly precipitation data from the on-land storage site; figure 6.3. 2016 showed an overall lower precipitation rate than the average measurements from 2012 until present. In August 2016, the month the filters were set out, the precipitation was measured to be 158,9 mm. Early autumn is clearly a time when it rains heavily, and this might contribute to the filter results. Heavy rain would potentially counteract the aeolian transport by providing water to saturate the tailings, making the tailings less able to leave the site.

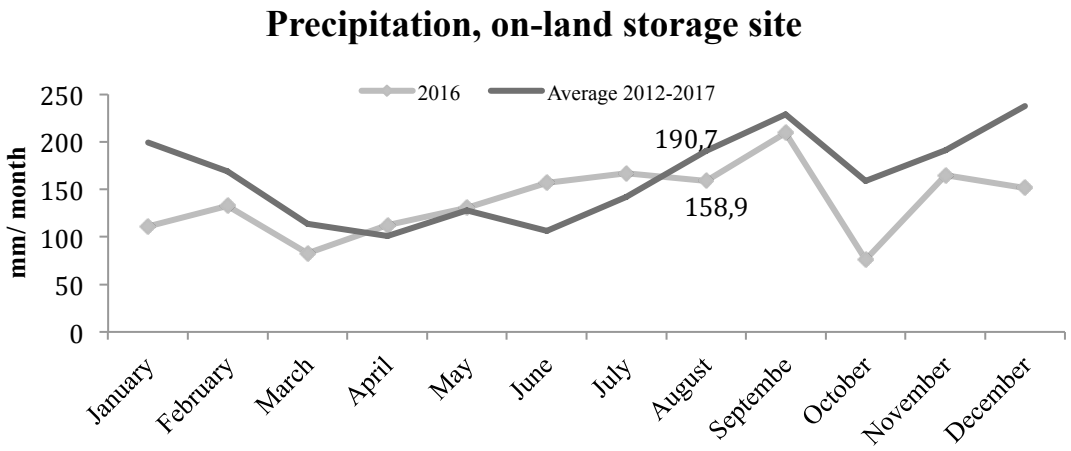

Figure 6.3: Precipitation data provided from Titania measured on the on-land storage site. Both average measurements from 2012-2017 (dark grey line) and monthly measurement from 2016 (light grey line). The filters were placed out in August 2016. Data points can be seen with specific values for average August measurements (190,7 mm) and August 2016 (158,9 mm).

Eik weather station measures the wind frequency and strength, and is situated 24,2 km from Åna-Sira. Figure 6.4 shows frequency distribution of wind, and the colour division depicts the wind speed. The figure is a wind rose, and is a common graphic tool to display how wind speed and direction are distributed in a given area. Figure 6.4 shows the wind rose for Eik in Lund municipality, Rogaland County. The columns in the wind rose diagram indicate that the wind is generally weak (0,3- 5,2 m/s), with some periods reaching the next category (5,3- 10,3 m/s). The

wind rose furthermore illustrates the most common direction that the wind blows *from*, which in this case would be north to northwest. However, the strongest winds occur when the wind blows from the south.

To provide with the context of wind strengths, the Beaufort's scale is used (MetOffice, 2010). These are generally termed light winds, with more detailed classifications such as gentle breeze and fresh breeze. Fresh breeze is 8,0- 10,7 m/s and reflects the strongest winds in this area, and occurs most frequent when the wind originates from the south.

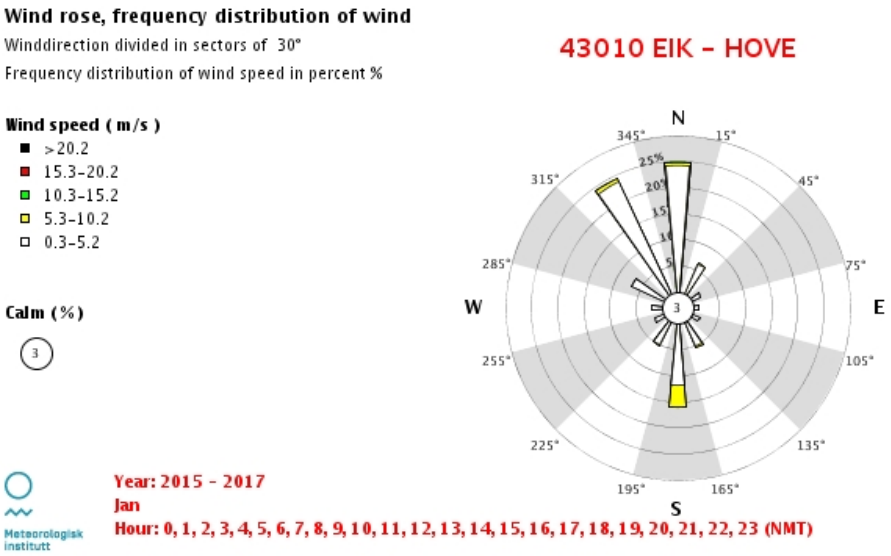

Figure 6.4: Wind rose attained from eklima.no from Eik station 43010, a service provided from the Norwegian Meteorological Institute. The wind speed is measured 10m above ground in m/s, and the wind direction is measured in degrees. The wind blows, in this case, most often from north/northwest, although in some cases also from the south with the highest speed (yellow colour in the columns). Licence: http://creativecommons.org/licenses/by/3.0/no/

The direction of the wind is unfortunate for Åna-Sira, although the wind speed is not that strong. The tailings dam (Tellenes) at Titania is situated in a northwest- direction to the small village. Consequently, as the wind blows mostly from N-NW this will affect Åna-Sira as it lies directly in the winds flow path. This is the reason for Åna-Sira to be particularly exposed to windblown material from the mine site at Titania. Additionally, the areas topography might also play a role.

Åna-Sira is located downhill from the tailing dam, and the wind could almost seem to be channelled through the landscape, as seen in figure 4.3, section 4.3.1.

Composition of the aeolian transported particles

The presence of heavy metals and where they bind is of specific interest due to this thesis' objectives. As figure 5.7, E, F and G, displays are there some heavy metals in the windblown material as well as the tailings. It would seem like the heavy metals have a preference towards the ilmenite and pyroxene, rather than the plagioclase.

The results obtained in this thesis was compared to the report written by the Norwegian University of Science and Technology (Myran, 2007). This report classifies and categorizes according to the EU's Directive 2008/50/EC of the European Parliament and of the Council on ambient air quality and cleaner air for Europe (Government, 2013). There was no law in 2004 regarding dust deposition, but that has been implemented in the Pollution Directive in September 2013. §30-5 states that the release of dust/ particulate dust from the given industry shall not exceed 5 g/m^2 during a time interval of 30 days. This applies for mineralogical component-measurements from the nearest neighbour or the most exposed neighbour (Government, 2013).

The report delivered from the Norwegian University of Science and Technology uses these two above-mentioned government acts to define the dust deposition originating from Titania's tailings dam. The filters content are classified as either of mineralogical or organic source. For the period of measurements (02.06.06- 31.12.06), with monthly filter shifts, the average dust deposition can be seen in table 6.1. These filter placements (9353 and 9354) are the same as the ones for this thesis.

Table 6.1: Average dust deposition for the entire period, from Titania AS.

	Total dust deposition (g/m^2 per month)	**Mineralogical**	**Organic**
Filter 9353 (3)	0,76	0,24 (32%)	0,52 (68%)
Filter 9354 (4)	1,22	0,35 (29%)	0,87 (71%)

As filter 4 (9354) is nearer in placement to the mine area, the total dust deposition is higher than for filter 3 (9353). These measurements were done in 2006, and unfortunately not measured in August 2006, so a direct comparison is difficult. However, this indicates that the dust deposition is generally at a low level for both categories (mineralogical and organic), and is within the acceptable limits presented in §30-5. The data from Myran (2007) also states that there is a visible difference for the measurement done in June compared with the one done in December, table 6.2.

Table 6.2: Comparison of total dust deposition measured in June and December 2006.

	Month	**Total dust deposition (g/m^2 per month)**
Filter 3	June	0,57
Filter 4	June	1,28
Filter 3	Dec.	0,11
Filter 4	Dec.	0,35

The sample provided for this thesis is from August 2016. Rainfall in August is normally higher than in June but lower than in December, which draws parallels to table 6.2 above. This can be seen in figure 6.3 where the average precipitation trend from 2012-2017 is plotted. From Myran (2007), it is evident that December differs from June in regards of dust deposition. If one could presume a direct link between precipitation rate and dust deposition, than dry months result in more dust deposition. Surely, other circumstances could play a vital role as well, such as the manual saturation of the on-land storage site.
A consequence of this fact is that there will be monthly variations in dust deposition for the residents in Åna-Sira.

To quantify the dust deposition from the on-land storage site at Titania, the grains counted as described in section 4.3.1 from the dust filters, were further used to calculate the volume of dust leaving the on-land storage site. This is an estimate scaled up to represent an area that is 3600 m (width) and 100 m up from the ground (height), figure 6.5. This estimate was done to present

dust deposition in kg/year. The sum of each size interval is firstly presented in kg/year, and finally the total sum of all the counted size intervals (kg/year).

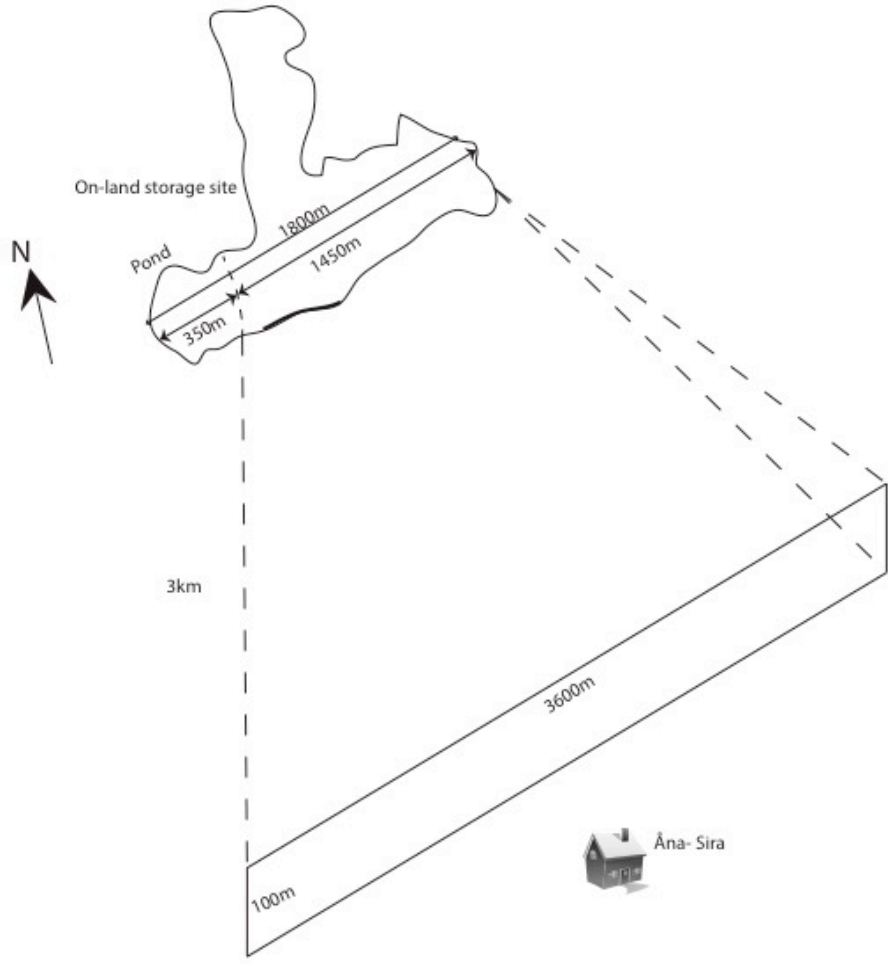

Figure 6.5: Dust deposition from the on-land storage site at Titania. Estimated area of 3600m*100m

Table 6.3 is the estimated total dust deposition, but Ni is only a minor part of the tailings stored on-land. The estimated Ni content in the tailings being deposited in the on-land storage site is 0,03% of the total solid content (Mellgren, 2002). Table 6.4 shows the estimated part of total dust deposition being Ni. Calculations can be seen in appendix C.

Table 6.3: The table provides an overview of each grain size interval's contribution to the total dust deposition from the on-land storage site at Titania. The total dust deposition over an area of 3600m width 100m height gave an estimated value of 58 576 kg/year.

	<10 µm	**10-50 µm**	**50-100 µm**	**<100 µm**
kg/day	37,4	22,5	95,6	7,3
kg/year	13445,7	8097,3	34409,1	2624,7
Total kg/year			**58 576,8**	

Table 6.4: The amount of the dust deposition being Ni. From the total kg/year dust deposition 0,03% is Ni

	Amount of Ni
kg/day	0,5
kg/year	**17,6**

From this, one can indicate that the problem with windblown dust from the on-land storage site at Titania is the amount of dust itself, not the Ni containing grains. This is an estimate based on basic calculations to get a quantitative understanding of the dust deposition from Titania's on-land storage site.

6.2.3 Transport of metals in streams and lakes in the proximity of the on-land storage site

All water samples (sample 1-9) were, as mentioned, obtained in the near proximities of the tailings dam at Titania. However, the water chemistry varied between the samples for both cation/anion and trace metal concentrations.

One must point out that the values for Zn are so dramatically different in the first measurement (November 2016) than in the second (April 2017), that one could unfortunately argue that the

first measurement was contaminated. Zn is known for being an element of high-contaminant risk due to its widespread presence. Hence, Zn values from the first measurement (November 2016) were regarded as unsuitable for this thesis.

Metal concentrations in the samples were evaluated primarily by its content of Ni. Figure 6.6 displays the Ni classification based on the Environmental Quality Standards given by the Norwegian Environmental Agency given in Miljødirektoratet (2016), from section 5.2.4.

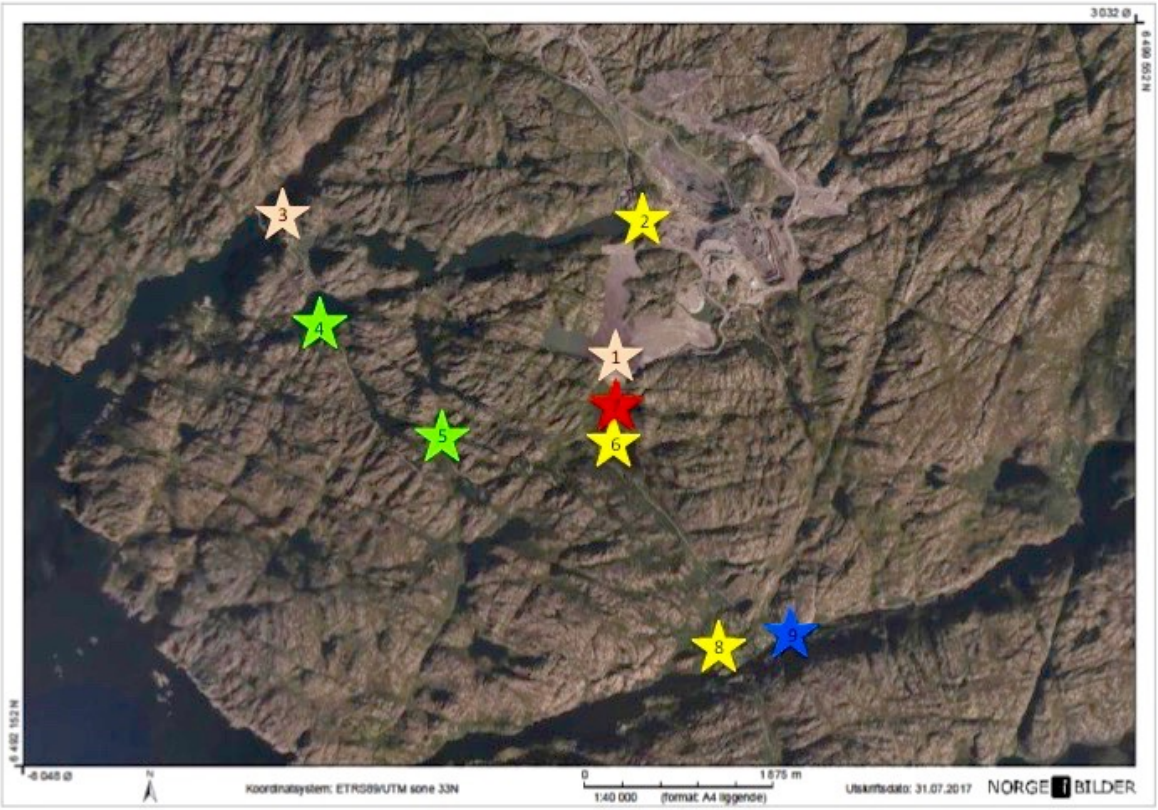

Figure 6.6: Overview of the classified water samples based on table 5.2 for Ni. The figure shows that sample 7 was the most contaminated in terms of Ni, followed by sample 1 and 3. Thereafter sample 2, 6 and 8, and lastly sample 9.

Sample 1 was taken in the tailings dam itself. Ni values were class (IV), meaning relatively high values (34-67 μg/L). By looking at Ni concentrations and the abundance of sulphate, one could easily assume that sulphide oxidation is profound and that the pH consequently is very low. However, this might not describe the whole picture. pH is above neutral (7.5), this is though by

be because of the alkaline constituents in the ore (norite) with Ca –rich plagioclase, Ca- rich clinopyroxene and apatite. This might help buffer the potential pH-lowering processes such as oxidation of sulphides. Furthermore, due to the overall low sulphide content in the tailings, the extent of sulphide oxidation will thereby be correspondingly low. However, as both sulphides and oxygen is present, and much of the tailings are not placed under water, oxidation will occur. Oxidation of millerite will presumably result in the easily soluble nickel sulphate (Konhauser, 2006):

$$NiS + 2O_2 \rightarrow NiSO_4 \qquad (6.1)$$

If Ni is present as nickel sulphate instead of nickel sulphide, then Ni can more easily be released into the surroundings, as sulphate is soluble in water. This could be the reason for sample 7's high Ni concentrations compared to sample 1, although they are very close geographically. As the on-land storage site is permeable, the system is open to exterior influence. As Ni is drained through the system, reaching the bottom of the dam wall at the location of sample 7, the nickel sulphate may have dissolved. Hence, resulting in the high Ni and SO_4 values.

Sample 6 was classified as environmental quality standard (III) for Ni with values 4 -34 μg/L, taken in Logsvatn. This lake is an outlet point in which Titania has permission to release 1.5 kg Ni/ 24h. However, sample 6 being less than 500m downstream sample 7, the Ni concentrations has decreased considerably. Along this path line from sample 7 to 6, reactions must have occurred to decrease Ni content in the aqueous phase. Perhaps presence of organic substances or iron hydroxides has sorbed Ni from solution. TOC (Total Organic Carbon) analyses have not been conducted, but as Logsvatn is a closed lake, organic substances could be present.

Sample 3 was taken in a creek that came from the hillside where Titania's drying plant is situated. Here, the concentrates of ilmenite, magnetite and sulphide undergo processes before being ready to enter their final stage: temporary storage in silos before export. Sample 3 was classified to be of class (IV) with relatively high values of Ni (34-67 μg/L). The discharge water from the drying plant is released into the Jøssingfjord, and the solid waste is deposited in the on-land storage facility at Titania. One could image that the discharge water going to Jøssingfjord may have influenced the nearby creek.

Sample 2 is from the process water that is used for mining operations at Titania. Furthermore, some of the discharge from the ore dressing plant and the drying plant are released into Tellenesvannet to finally reach the Jøssingfjord through tunnel (Sørby and Storbråten, 2016). Hence, sample 2 is categorized into class (III) with values of 4-34 μg/L.

Sample 4 and 5 both display Ni values of class (II) of 0. 5-4 μg/L. Cation/anion analyses showed low concentrations for everything but Na and Cl, which could have a costal origin. They indicate no influence by the mining operations at Titania, which is supported by the topography as well, since water cannot flow uphill.

Sample 8 and 9 display clear differences despite being taken in close proximities from each other. Sample 8 being clearly influenced by the mining operations, with category (III) values of Ni (4- 34 μg/L) and SO_4 57.8 μg/L. This implies that the sample location is downstream the mining site. From figure 4.3, topography could allow the river/creek to directly arrive Åna Sira where the sample was taken. On the contrary, sample 9 is more alike sample 4 and 5, with overall concentrations similar to the reference values presented.

The first measurement almost consequently shows higher concentrations for both analyses, indicating that there is a difference in contaminant transport in the winter (mid November) and late spring (end of April). Looking back to section 6.2.2 and figure 6.3, April is generally a month with little precipitation in contrast to November. April has only half the precipitation measured in November, with 100,6 mm in contrast to 191,1 mm.

6.3 Marine deposition

6.3.1 Transport of metals from the sea deposits

The marine environment is important, as the processes here could to some extent explain the leaching of heavy metals to the water column. The results obtained in section 5.3.1 was investigated, and compared to a conference presentation (article in prep.) from Schaanning et al. (2017) at NIVA. This presentation presents results obtained by the same methods as in this thesis, but the liners' were taken in the Jøssingfjord and Dyngadypet directly, hence having both fjord bottom sediments and tailings form the storage site.

Eh and pH measurements were done in intervals of 1 cm, so changes that occur in a smaller scale can not be been in the depth-profiles. As redox measurements with Eh- electrodes are quite difficult, Mn and Fe are used as proxies for the redox environment, according to section 3.2.3. Eh showed a gradual decrease in redox potential with depth, from approximately 400 mV to 200 mV. This indicates that environment changes from being oxic near the sediment surface, and decreasing towards anoxic at 75 mm. Mn and Fe concentration vs. depth profiles can help distinguish the processes in between. Mn had generally very high values, but the gradient show that the Mn concentration rapidly increases at a 20 mm depth, indicating that oxygen content is /low minimal at a few cm depths, and microbial processes are reducing Mn^{5+} to Mn^{2+} which are here stable in solution. A typical indicator that the environment is less affected by oxygen is that the pore water concentration of Fe and Mn increases, as Fe^{2+} and Mn^{2+} become stabile in the lack of oxygen (Ruus et al., 2012). The Fe profile shows that there is minimal Fe in the upper cm of the sediments, but increase at a 65 mm depth and downwards. This may indicate that Fe^{3+} is reduced to Fe^{2+}, which is stable in solution. These findings correspond to the redox zones in sediments from Konhauser (2006), section 3.2.3.
Mn^{2+} and Fe^{2+} ions accumulate in their redox zones, and some of these ions may migrate upwards in the sediment column. When Mn^{2} and Fe^{2+} are exposed to oxygen, oxidation can occur together with precipitation of respectively MnO_2 and $Fe(OH)_3$, equation 3.10 and 3.11. These precipitation processes are acid producing, with 2 H^{+} being produced per mole MnO_2 and $Fe(OH)_3$ each. Furthermore, this acid production may lead to pH drop in the upper sediment column where oxygen in present. This can somewhat be seen in the pH profile, however the

depth intervals were not small enough to capture small-scale changes. Titania liners' showed that near the surface, the pH levels were at it's lowest, with values at 7,7. pH gradually increase up to 7,9, but do not stabilize until a depth of 35 mm, thus below the tailings placement. This may indicate that there are processes in the top 30 mm that produce acidity, which may just be the oxidation of Mn^{2+} and Fe^{2+}ions. However, the buffer capacity of seawater will limit the extent of the pH drop.

The control profiles show some similarities in the pH profile, where pH decreases down to the tailings-sediment boundary at 20 mm depth, where is gradually increases with depth to a value of 7,8. This can be explained by the above-mentioned oxidation of Mn^{2+} and Fe^{2+} ions in the redox zones, which is applicable also here. The redox potential measured by the Eh electrode tells a more uniform story, with stable values of 380 mV down to a rapid decrease at 65 mm depth, which corresponds to when Fe^{2+} concentrations increase substantially.

To compare the results obtained, data from the gathered liners' from the Jøssingfjord were used (Schaanning et al., 2017). The results from this study showed similarities to this thesis experiments. Depth profiles of Fe and Mn reveal low uptake in the top cm, near the surface with increasing uptake with depth, figure 6.7. Fe was in this case mobilized at a shallower depth, and Mn showed an over all lower uptake gradient. However, this material is the deposited mine tailings which has been on the fjord bottom for many years, in contrast to the experiments done in this thesis which the fjord bottom sediments only has been exposed to the tailings for approximately 1 month.

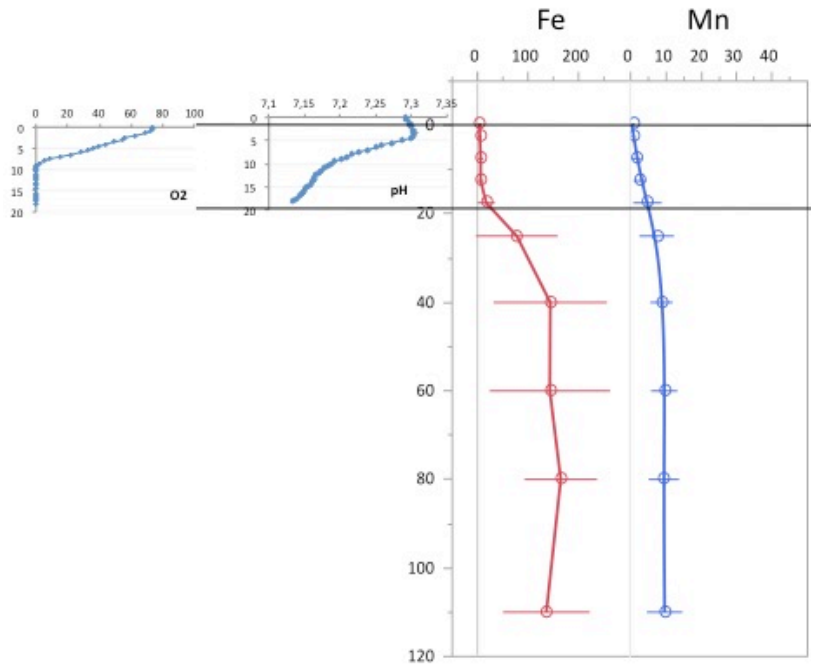

Figure 6.7: Results from Schaanning et al. (2017), describing the environment in liners' from Jøssingfjord with tailings on top of the fjord bottom sediments. The boundary is also here at 20 mm depth. Fe uptake increase from a 20 mm depth, with almost no Fe near the surface. Mn has a more gradual increase, but uptake is higher beneath 20 mm depth. From microelectrodes (to the left) O_2 and pH is measured with smaller intervals, revealing a similar pattern: a decrease in pH and O_2 at equal depths.

The heavy metal profiles of Ni and Cu from Titania liners show that the highest uptake was at a shallow depth, from the surface and down to 30 mm. This could indicate that heavy metals in the tailings are mobilized by the oxygen access, and that also here oxidation of sulphides is occurring at some extent. This will probably not be so profound as in the on-land setting due to the decreased dissolution and diffusion of oxygen in water by a factor 10^4 compared to air (Matthies et al., 2011). Additionally, as the metal profiles show a considerable decrease in uptake with depth, there is no sign of metal mobilization from deeper layers.

The control liners show very low values for Ni and Cu, as expected. For Ni, there were not even measurements above detection limit (0,52 µg/L) for the ICPMS until a depth of 60 mm. Here, the uptake was barely 2 ng/cm^2, in contrast to Titania liner's with up 800 ng/cm^2.

This coincides with the results that Schaanning et al. (2017) found in their study with fjord bottom sediments from Jøssingfjord where the actual coverage of tailings done when the site was operative (1960-1984), figure 6.8.

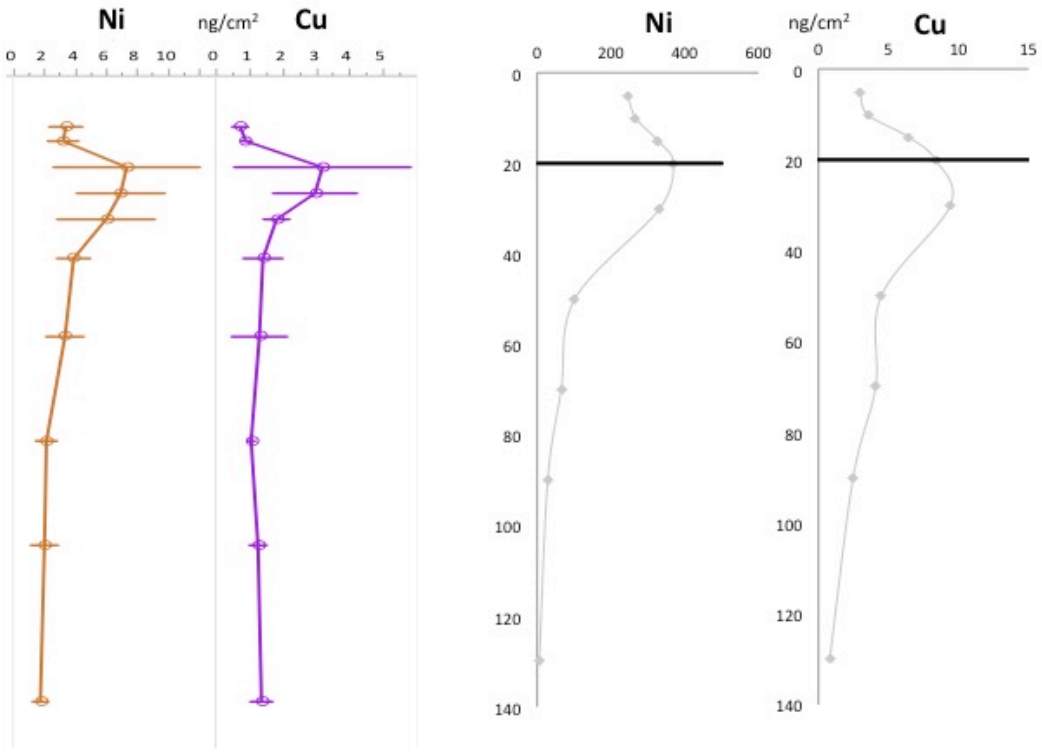

Figure 6.8: Uptake profiles from Schaanning et al. (2017) taken in Jøssingfjord sediments with tailings (left pair), and concentration profiles obtained by this thesis by experimental setup with fjord bottom sediments from the Drøbak straight covered with Titania tailings (right).

6.3.2 The role of benthic fauna and bioturbation

The benthic fauna on and near the area where tailings are being deposited will be affected not only when the deposition is active, but also for some time after. Due to the rapid sedimentation (tailings deposition) the fauna will be severely impacted and while deposition is ongoing, not

much benthic life can withstand. However, the fjord bottom will recolonize rapidly and this occurs during the very first year after tailings disposal. Yet, decades can pass before the fauna is identical to what it was before deposition, due to the new sediment arrangement with a different grain size, permeability and porosity than before (Ramirez-Llodra et al., 2015, Trannum, 2016). When the benthic fauna is restored, the effect of this must be evaluated as these organisms live on top of and in the deposition environment.

As discussed in the previous section 6.3.1, the access to oxygen is a key factor in mobilizing heavy metals. Therefore, characterizations as stable and undisturbed, anoxic at shallow depths, and buffer capacity are desirable when storing tailings (Matthies et al., 2011). Keys constituent in these environments are the polychaetes, or marine bristle worms. These tend to dig holes, burrows or build tubes in the sediments (Trannum, 2011). Thus, disturbing the upper centimetres of the sediment column, and providing oxygen and migration pathways for heavy metals, figure 6.9. Furthermore, this could be increasing the metal fluxes form the marine storage site. One could potentially argue that this can be the reason for the not perfect fit between the DGT- uptake and the metal fluxes in figure 5.44, section 5.3.2. This is as the obtained fluxes are higher than the measured DGT- uptake that represents the pore water concentration, and would not take into account the effect of bioturbation. Especially is this evident for the elements with the overall lowest concentration, for example Cd. Hence, when diffusion is relatively fast (for example Cu) the link between DGT and flux is better than when the diffusion is slow (Cd).

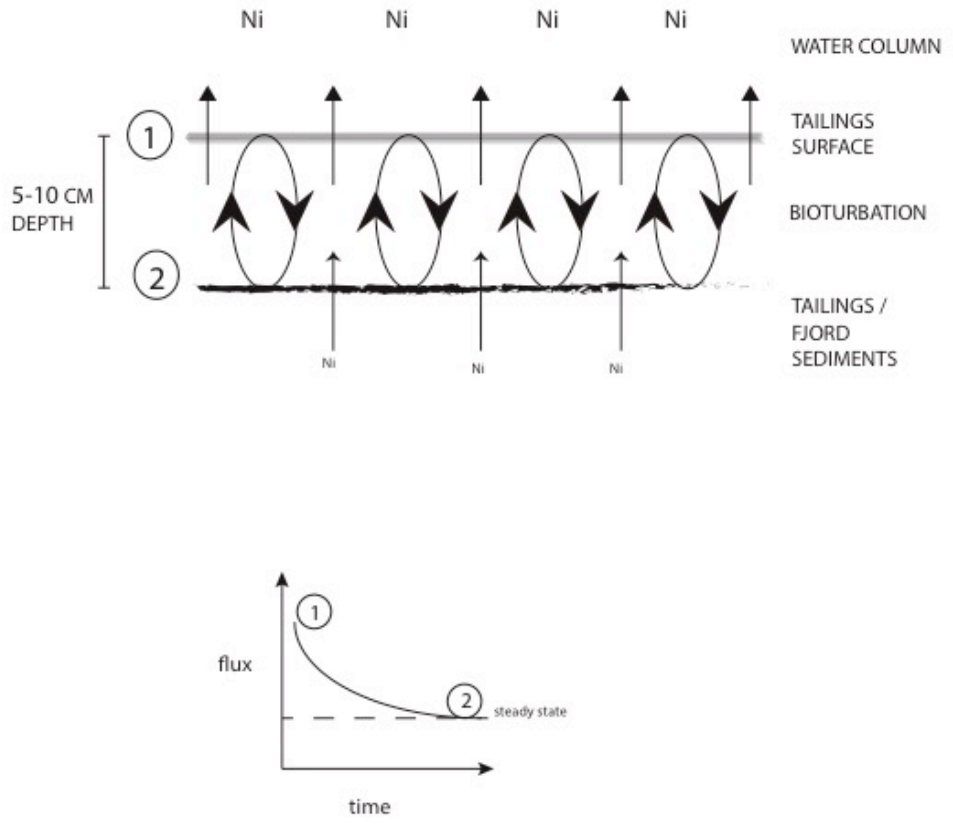

Figure 6.9: The effect on bioturbation on release of contaminants from the tailings and into the water column. Benthic fauna has the ability to relocate and disturb the sediment/tailings surface, by burrowing holes etc. adding oxygen to a deeper sediment depth. This may then cause mobilization of contaminants that otherwise was relatively unreactive. 1. The fluxes are higher by the influence of bioturbation 2. The system reaches a steady state.

Tailings disposal in the marine environment is known to cause disturbance on the sediment surface, and impacting benthic life both on the surface and below. As the placement is ongoing, benthic life on the sea bottom will be buried by the high sedimentation rates (Ramirez-Llodra et al., 2015). The effect is most profound in close proximities to the tailings placement, and will decline with distance, figure 6.10.

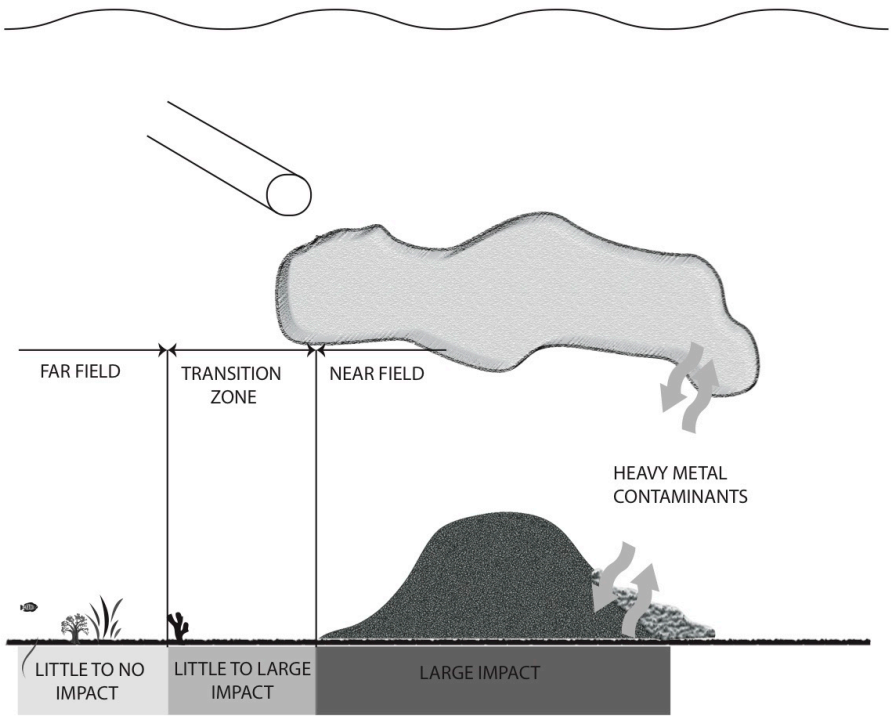

Figure 6.10: On-going subsea tailings placement with impact levels. The heap represents the settled tailings on the sediment surface, while the "cloud" represents the temporary suspended fine-grained tailings. Contaminants can be released from both suspended and settled tailings. Impact zones characterize the zones that are affected by the tailings placement (in depth). Benthic life increase with increased distance. Modified from Schaanning et al. (2017).

It is known that there is a risk of the tailings being widely dispersed for example due to currents and disposal outlet points being too close to the water surface. Hence, to make the tailings settle and remain, one must evaluate the disposal site carefully. The Jøssingfjord and Dyngadypet sites are categorized in table 2.4, which states weak currents and moderate water residence time indicating suitable deposition sites. This could contribute to the tailings placement being limited to the planned area, preventing the benthic life being impacted more than necessary.

6.4 Compare and contrast ways of transport from land and sea deposits

To be able to compare and contrast the two storage options at Titania, the data and calculations previously presented was directly compared. First, the on-land storage site's discharge ways was presented together in context of Ni, table 6.5. Secondly the same was done for the marine sites, table 6.6.

Table 6.5: An approximate total Ni discharge from the on-land storage site at Titania. Ni discharge from the calculated dust deposition, and the permits granted by the Norwegian Environmental Agency, as reported in section 2.2.1.

	Ni kg/day	**Ni kg/year**
Dust deposition	0.5	17.6
Jøssingfjord	6	2190
Logsvann	1.5	547.5
Total	8	2755.1

Table 6.6: An approximate total Ni discharge from the marine storage sites at Titania, Jøssingfjord and Dyngadypet. Ni calculations are from the flux measurements as reported in section 5.3.2.

	Ni kg/day	**Ni kg/year**
Jøssingfjord	0.6	217.0
Dyngadypet	1.8	658.9
Total	2.4	875.9

From table 6.5 and 6.6 above, the daily and yearly discharges of Ni are presented. It is evident that the Ni contribution from dust deposition is quite small. Flux of nickel from sea deposits corresponded to 30.8 % of the leakage from the land deposit. However, this is true when a 2cm thick layer of fresh tailings is overlain fjord sediment. This is not the case in the Jøssingfjord

today, or any disposal site that is not active, where the flux from the tailings will probably decrease with time as found by Schaanning et al. (2017), where flux of Ni from sea deposits corresponded to 5,2% of the leakage from the land deposit. The calculated flux from Schaanning et al. (2017) gives a total flux (Jøssingfjord + Dyngadypet) of 0.4 kg Ni/ day or 146 kg Ni/ year, with the total here being determined to 7,5 kg Ni/day as set by discharge permits.
This could indicate that the results obtained from this thesis represent the maximum values for leakage from the sea deposit, where fresh tailings is exposed to the fjord bottom environment. Natural sedimentation will slowly reduce leakage after deposition is ended (Schaanning et al., 2017).

Put somewhat extremely; figure 6.11 illustrates the Jøssingfjord in two contrasting scenarios, with the effect in which the storage solution at Titania is on-land or marine. At the present, Titania has a permit to release a total of 6 kg Ni/day to the Jøssingfjord, an absolute from four different outlet points. However, if the storage option is marine, the Ni flux to the environment is 0,6 kg Ni/day, this reflects a flux change by a factor of 10x.

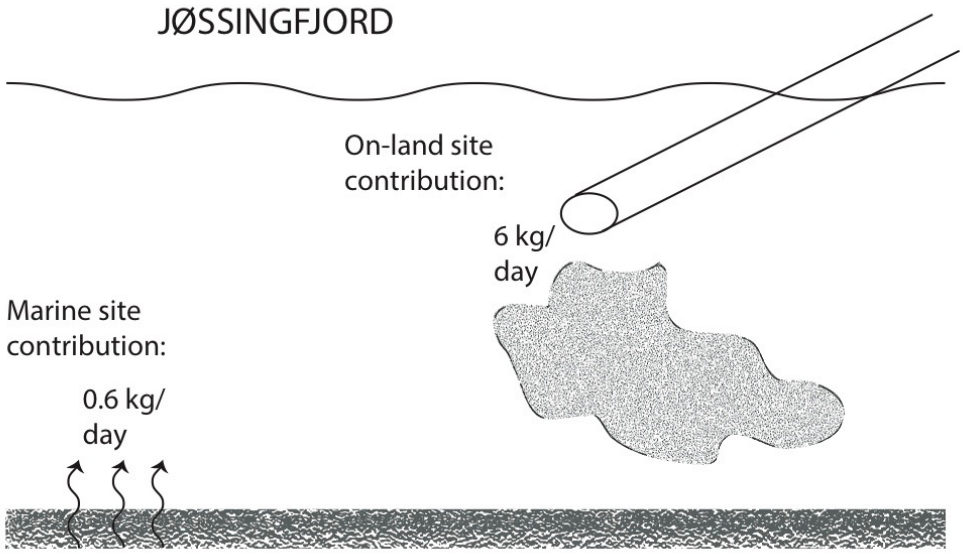

Figure 6.11: Comparison of Ni discharge on-land storage vs. the marine storage at Titania.

The calculations are estimated by the available information provided by Titania and obtained by the analyses; hence the total picture might not be fully represented. Assumptions were consequently made to be able to quantify the discharge of Ni. The dust deposition calculations were based upon manually counting grains in dust filters, which undoubtedly has uncertainties connected. Furthermore, the area of spread (100m height * 3600m width) could be an either too large or too small area. However, the calculations supply and indicate whether the Ni from dust deposition is large or small scale. Tailings were assumed alike in the Jøssingfjord and Dyngadypet, so data obtained from the liner's could be used to determine fluxes in both areas. This was done on the basis of Schaanning et al. (2017) which stated that the leakage from the sediments are only marginally dependent on the thickness of the tailings, but rather proportional to the surface area of the deposit.

7 Summary and conclusion

As stated by Vogt (2013): *"Mining is essential to living as we know it."*. Meaning that society today is dependent on the metals mined all over the world, including the resources found in Norway such as Titania's ilmenite. The Norwegian legislation and government acts ensure a regulated and, to the best extent possible, environmental friendly mineral processing industry. However, as further stated by Vogt (2013) *"The biggest environmental challenge in mining is the management of mine tailings"*. This gives the basis for this thesis, which aim was the transport of metals from mine waste at Titania AS.

The thesis has investigated the two storage options at Titania AS in Rogaland County, Norway as the present solutions is estimated to reach its capacity within 2025. From 1994 until present Titania utilize an on-land storage site, but has prior to that used the marine storage option. Thus, this thesis has investigated metal transport from each storage option, and the thesis format has been relied on this division of land and sea throughout the chapters.

The on-land site has been investigated by means of quantitative mineral analyses of tailings and dust deposition from filters and water analyses of cation/anion content and heavy metals from creeks and lakes in near proximities of the storage site, all with an overall aim to understand by which means the transport occurs and the amount.
The marine site has been investigated in cooperation with NIVA, by use of gathered box-cores of fjord sediments overlain by a 2cm thick layer of tailings. These were placed in a mesocosm, a setup that simulates the natural fjord bottom environment. Here, electrode measurements of pH, Eh and Es were conducted, and concentrations of the heavy metal fluxes and DGT measurements (proportional to pore water concentrations), was obtained.

From the above-mentioned analyses, the results were examined in light of the metal of biggest concern; nickel.
As the on-land site is a permeable dam construction, the whole surface of the impoundment cannot be saturated as this would only drain through the system. This has implications on the mineral reactions occurring, due to the access to oxygen. It could be reasonable to think that if Ni

were bound to sulphate rather than sulphide, the release of Ni would increase substantially as sulphate is a water-soluble compound. This could be the reason for the increased Ni concentration in the sample just below the tailings dam. Furthermore, the water samples show that only 2-3 km away from the storage site, waters show little to no impact from mining activity, indicating that samples further away is rapidly diluted. Locations with the highest content of Ni were also the locations where the permit was authorized, denoting a regulated and controlled industrial site by Titania. The on-land site has a permit to release 7,5 kg Ni/ day, and this thesis has additionally estimated the dust deposition contribution of 0,5 kg Ni/ day. This gives that the dust deposition is less than 10% of the discharge from on-land deposit. Furthermore, a total of 8 kg Ni/ day, thus 2755 kg Ni/ year, is discharged from the on-land site.

The marine storage sites, the Jøssingfjord and Dyngadypet, are water bodies with moderate water residence time and generally weak currents, these are evaluated as good storage sites where the tailings will remain where disposed. This is an important factor, as benthic life must be protected to the greatest extent possible, as well as the surrounding water bodies such as the coastal areas in the proximities of the Jøssingfjord and Dyngadypet sites. The metal fluxes measured were quite high in the Titania liners compared to the control, a difference by a factor of 1000x, not unexpected, as Ni is the primary metal of concern. When calculated and scaled up to represent the Jøssingfjord and Dyngadypet, the fluxes were 0,6 and 1,8 kg Ni/ day respectively, corresponding to 217 and 658,9 kg Ni/ year. This gave a total of 875,9 kg Ni7 year from the two sites combined.
Comparing the on-land and marine discharge of Ni by the transport paths explored, the sea deposit discharged 30% of what the on-land site released.

To summarize the demands on the industry, Lottermoser (2007) states three aims that mining companies should pursue:

- To reduce and to recycle waste;
- To ensure that there are no or minimal impacts from wastes on the environment and humans; and
- To understand the composition, properties, behaviour and impacts of wastes

Mining is a key constituent in the modern life, not only as a workplace or for economic growth, but also as the production of resources that contribute to a provident and environmental shift. Society must work together to provide a sustainable and up to date industry, and Norway with Titania AS and others must play its part. When deciding the placement of tailings placement at Titania, and also other sites, one must always base the decision on science and studies performed, to best ability, predict the fate of potential leaks, spread and transport of metals and contaminants that may be hazardous to human and biota. Hence, to quantify and understand the means of transport are crucial information.

The hope and purpose for this thesis was to contribute to the objective scientific approach of evaluating mine tailings placement at Titania AS, as the present site will reach its capacity within 2025.

8 Future work

As with most masters' thesis, there is neither room nor time to look at every aspect and do every analysis, despite the desire to. Additionally, through the process ideas and different perspectives appear, as one gets deeper into the subject of study. This study tries to reach its aim, but many aspects remains unsolved and unexplored. Hence, a short list of suggested future work is presented:

- *Identify the specific mineral reactions regarding Ni at the on-land storage site*

Ideally, one could use chemistry and the geochemical environment in such a manner that one could prevent/accelerate precipitation or solution of the mineral phases of interest. For example, keeping a pH in a specific range so that the metals are precipitated as relatively unsoluble metal sulphides.

- *Understand better the role of bioturbation on the observed and measured fluxes of heavy metals from sea deposits*

Look at the role of bioturbation in terms of flux vs DGT, and generally the role of bioturbation in the marine storage context

- *Geochemical modelling with PHREEQC*

Simulate the diffusion coefficient to fit with data obtained from DGT- measurements, and see the effect over time. By this means, one could explore the metal diffusion in a long-time perspective

- *Experiment with non-uniform appliance of tailings in liners placed in the mesocosm-tank*

Experiment with how the system reacts to having a mesocosm- setup using liners that have been treated with different thickness- layers of tailings. Will the thickness have a strong influence in the fluxes to the water column above, or will the thickness have a stronger influence on the sediment environment.

Bibliography

(NSA), N. S. A. 2007. Environmental monitoring of marine fish farms. *NS 9410.* Norwegian Standards Association.

ALLEN, J. & VOILAND, A. 2015. *Dam breach at Mount Polley mine in British Columbia* [Online]. NASA (Visible Earth). [Accessed 11.07.17].

ANDERSEN, T. 2015a. ICP-MS. *GEO4830 Analytical Methods in Geochemistry.* University of Oslo.

ANDERSEN, T. 2015b. Scanning Electron Microscopy. *GEO4830 Analytical Methods in Geochemistry.* University of Oslo.

ANDERSEN, T. 2015c. X-Ray Diffraction. *GEO4830 Analytical Methods in Geochemistry.* University of Oslo.

APPELO, C. A. J. & POSTMA, D. 2005. *Geochemistry, groundwater and pollution,* Leiden, Balkema.

ARP, H. P., RUUS, A., MACKEN, A. & LILLICRAP, A. 2014. Quality assurance of environmnetal quality standards.

BECKMANCOULTER 2009. Particle Size Analyzer Brochure - Beckman Coulter LS 13 320.

BOGGS, S. J. 2014. *Principles of Sedimentology and Stratigraphy,* Essex, England, Pearson Education Limited.

CHARLIER, B., NAMUR, O., BOLLE, O., LATYPOV, R. & DUCHESNE, J. C. 2015. Fe–Ti–V–P ore deposits associated with Proterozoic massif-type anorthosites and related rocks.

CHARLIER, B., SKÅR, Ø., KORNELIUSSEN, A., DUCHESNE, J.-C. & VANDER AUWERA, J. 2007. Ilmenite composition in the Tellnes Fe–Ti deposit, SW Norway: fractional crystallization, postcumulus evolution and ilmenite–zircon relation. *Contributions to Mineralogy and Petrology,* 154**,** 119-134.

CYR, M. & TAGNIT-HAMOU, A. 2001. Particle size distribution of fine powders by LASER diffraction spectrometry. Case of cementitious materials. *Materials and Structures,* 34**,** 342-350.

DAVLSON, W. & ZHANG, H. 1994. In situspeciation measurements of trace components in natural waters using thin-film gels. *Nature,* 367**,** 546-548.

DIOT, H., BOLLE, O., LAMBERT, J., LAUNEAU, P. & DUCHESNE, J. C. 2003. The Tellnes ilmenite deposit (Rogaland, South Norway): magnetic and petrofabric evidence for emplacement of a Ti-enriched noritic crystal mush in a fracture zone. *Journal of Structural Geology,* 25**,** 481-501.

DONEY, S. C., FABRY, V. J., FEELY, R. A. & KLEYPAS, J. A. 2009. Ocean Acidification: The Other CO2 Problem. *Annual Review of Marine Science,* 1**,** 169-192.

DUTROW, B. L. & CLARK, C. M. 2016. *X-ray Powder Diffraction (XRD)* [Online]. Science Education Resource Center: Carleton College. Available: http://serc.carleton.edu/research_education/geochemsheets/techniques/XRD.html [Accessed 19.03.17 2017].

ELLIS, D. V. 2001. A Review of Some Enviromental Issues Affecting Marine Mining. *Marine Georesources & Geotechnology,* 19.

ETTNER, D. C. & SANNE, E. H. 2016. Tiltaksorientert overvåkning, resultater 2015. Titania AS. Geode Consulting AS.

EUROPEAN PARLIAMENT, C. A. T. C. 2006. Management of waste from extractive industries. *In:* (EU), T. E. U. (ed.) *206/21/EC.*
EUROPEANCOMMISSION 2011. Recommendation from the Scientific Comittee on Occuoational Exposure Limits for nickel and inorganic nickel compounds.
FRANKS, D. M., BOGER, D. V., COTE, C. M. & MULLIGAN, D. R. 2011. Sustainable development principles for the disposal of mining and mineral processing wastes. *Resources Policy,* 36**,** 114-122.
GARMO, Ø. A., RØYSET, O., STEINNES, E. & FLATEN, T. P. 2003. Performance Study of Diffusive Gradients in Thin Films for 55 Elements. *Analytical Chemistry,* 75**,** 3573-3580.
GOVERNMENT, T. 2013. *Luftkvalitetsdirektivet* [Online]. The Government. Available: https://www.regjeringen.no/no/sub/eos-notatbasen/notatene/2005/okt/luftkvalitetsdirektivet/id2432778/ [Accessed 2017 05.08].
GRAVDAL, J. K. S. 2013. *Stability of heavy metals in submarine mine tailigs: a geochemical study.* MSc, University of Bergen.
GRØNNEBERG, T., HANNISDAL, M., PEDERSEN, B. & RINGNES, V. 2013. *Kjemien stemmer Kjemi 2*, Cappelen Damm.
HILLIER, S. 2000. Accurate quantitative analysis of clay and other minerals in sandstones by XRD: comparison of a Rietveld and a reference intensity ratio (RIR) method and the importance of sample preparation. *Clay minerals,* 35.
HUISMAN, J. L., SCHOUTEN, G. & SCHULTZ, C. 2006. Biologically produced sulphide for purification of process streams, effluent treatment and recovery of metals in the metal and mining industry. *Hydrometallurgy,* 83**,** 106-113.
IBREKK, H. O., BERGE, J. A., GREEN, N., GULBRANDSEN, R., IVERSEN, E., PEDERSEN, A., SKEI, J. & THAULOW, H. 1989. Miljøkonsekvensutredning
Landdeponi og sjødeponi, Titania A/S. *In:* IBREKK, H. O. (ed.). Norsk institutt for vannforskning (NIVA): NIVA.
IMR. 2013. *Fjords- water exchange and currents* [Online]. Institute of Marine Research. Available: http://www.imr.no/temasider/kyst_og_fjord/fjorder_vannutskiftning_og_strom/en [Accessed 18.03.2017].
IVERSEN, E. & AANES, K. J. 2011. Konsekvensutredning Nussir ASA: Delutredning landdeponi. NIVA: NIVA.
JRC DIR.B, J. R. C. 2015. *SUSPROC*
Waste and recycling [Online]. European Commission, Joint Research Centre: European Union. Available: http://susproc.jrc.ec.europa.eu/activities/waste/index.html [Accessed 30.10 2016].
KING, E. J. 1959. *Quantitative Analysis and Electrolytic Solutions,* New York, Harcourt, Brace and Co.
KONHAUSER, K. O. 2006. *Introduction to Geomicrobiology*, Wiley-Blackwell.
KORNELIUSSEN, A. & ROBINS, B. 1985. *Titaniferous magnetite, ilmenite and rutile deposits in Norway : a collectioin of papers on Norwegian titanium and iron-titanium deposits,* Trondheim.

KOSSOFF, D., DUBBIN, W. E., ALFREDSSON, M., EDWARDS, S. J., MACKLIN, M. G. & HUDSON-EDWARDS, K. A. 2014. Mine tailings dams: Characteristics, failure, environmental impacts, and remediation. *Applied Geochemistry,* 51**,** 229-245.
KRAUSE, H., GIERTH, E. & SCHOTT, W. 1985. Ti-Fe deposits in the South Rogaland igneous complex, with special reference to the Åna-Sira Anorhosite Massif. *Norsk Geologisk Undersøkelse,* Bulletin 402**,** 25-37.
LOTTERMOSER, B. G. 2007. *Mine Wastes: Characterization, Treatment, Environmental Impacts*, Springer Berlin Heidelberg.
LOTTERMOSER, B. G. 2017. *Environmental Indicators in Metal Mining,* Switzerland, Springer International.
MARION, G. M., MILLERO, F. J., CAMÕES, M. F., SPITZER, P., FEISTEL, R. & CHEN, C. T. A. 2011. pH of seawater. *Marine Chemistry,* 126**,** 89-96.
MATTHIES, R., BOWELL, R. J. & WILLIAMS, K. P. 2011. Geochemical assessment of gold mine tailings proposed for marine tailings disposal. *Geochemistry: Exploration, Environment, Analysis,* 11**,** 41-50.
MELLGREN, A. 2002. *Dissolved nickel in the Lundetjern land deposit- Identification of main causes and methods for treatment.* Master of Sciene, Norwegian University of Science and Technology.
METOFFICE 2010. Fact sheet 6 - The Beaufort Scale. Devon, United Kingdom: National Meteorological Library and Archive.
MILJØDEPARTEMENTET, K.-O. 1981. Lov om vern mot forurensning og om avfall (forurensningsloven). *In:* MILJØDEPARTEMENTET, K.-O. (ed.) *LOV-1981-03-13-6.* Lovdata.
MILJØDIREKTORATET 2016. Quality standards for water, sediment and biota.
MILJØDIREKTORATET 2017. Revisjonsrapport: Revisjon ved Titania AS. *In:* JØRGENSEN, A. (ed.) Final ed. Miljødirektoratet.
MOORE, D., MCCABE, G. & CRAIG, B. 2014. *Introduction to the practice of statistics*, W.H.Freeman and Company.
MYRAN, T. 2007. Rapport støvnedfall Titania, Åna Sira. Trondheim, Norway: Norwegian University of Science and Technology.
NEEB, P.-R., SANDVIK, G., TANGSTAD, R., LØSETH, L., STRAND, G.,, ERICHSEN, E., BOYD, R.,, BRUGMANS, P. J., WENNEBERG, H. & KAASBØLL, B. 2012. Mineralressurser i Norge 2011 - Mineralstatistikk og bergindustriberetning. *In:* NEEB, P.-R. (ed.) *Mineralstatistikk og bergindustriberetning.* 1 ed.: Norges geologiske undersøkelser (NGU),
Direktoratet for mineralforvaltning.
NILSEN, A. H. 2014. Erfaringer med landdeponi. *Norsk Bergforenings Vårmøte 2014.* Mo i Rana.
NILSEN, A. H. 2015. 100 år med deponering. *Miljøringens temamøte: Gruver og Miljø.* Miljødirektoratet, Oslo.
PARBHAKAR-FOX, A. & LOTTERMOSER, B. G. 2015. A critical review of acid rock drainage prediction methods and practices. *Minerals Engeneering,* 82**,** 107-124.
PAULL & NESTERENKO, B. P. N. 2013. Ion Chromatography.
PESAVENTO, M., ALBERTI, G. & BIESUZ, R. 2009. Analytical methods for determination of free metal ion concentration, labile
species fraction and metal complexation capacity of environmental waters:

A review. *Analytica Chimica Acta,* 631**,** 129-141.
RAMIREZ-LLODRA, E., TRANNUM, H. C., EVENSET, A., LEVIN, L. A., ANDERSSON, M., FINNE, T. E., HILARIO, A., FLEM, B., CHRISTENSEN, G., SCHAANNING, M. & VANREUSEL, A. 2015. Submarine and deep-sea mine tailing placements: A review of current practices, environmental issues, natural analogs and knowledge gaps in Norway and internationally. *Marine Pollution Bulletin,* 97**,** 13-35.
REICHL, C., SCHATZ, M. & ZSAK, G. 2014. World Mining Data. Vienna: International Organizing Committee for the World Mining Congress.
RINCÓN-TOMÁS, B., KHONSARI, B., MÜHLEN, D., WICKBOLD, C., SCHÄFER, N., HAUSE-REITNER, D., HOPPERT, M. & REITNER, J. 2016. Manganese carbonates as possible biogenic relics in Archean settings. *International Journal of Astrobiology,* 15**,** 219-229.
RITCEY, G. M. 2005. Tailings management in gold plants. *Hydrometallurgy,* 78**,** 3-20.
RUUS, A., SCHAANNING, M., IVERSEN, E., ØXNEVAD, S. & RØYSET, O. 2012. Quantifying fluxes of heavy metals to the inner Sørfjord, Hardanger. Norweigan Institute for Water Research.
SAMPAIO, R. M. M., TIMMERS, R. A., XU, Y., KEESMAN, K. J. & LENS, P. N. L. 2009. Selective precipitation of Cu from Zn in pS controlled continuously stirred tank reactor. *Journal of Hazardous Materials,* 165**,** 256-265.
SANDSTAD, J. S., BJERKGARD, T., BOYD, R., IHLEN, P., KORNELIUSSEN, A., OFTEN, M., EILU, P. & HALLBERG, A. 2012. Metallogenic areas in Norway. *Special Paper of the Geological Survey of Finland,* 2012**,** 35-41.
SCHAANNING, M., NDUNGU, K., ØXNEVAD, S. & TRANNUM, H. C. 2017. Metal fluxes from a sea deposit site for mine tailings. *SedNet.* Genoa, Italy: NIVA.
SCHAANNING, M. T., BJERKENG, B. & KÄLLQVIST, T. 1992. Konsekvenser av utslipp fra tørkeanlegget ved Titania A/S. NIVA: NIVA.
SHIMMIELD, T. M., BLACK, K. D., HOWE, J. A., HUGHES, D. J. & SHERWIN, T. 2010. Final report: Independent Evaluation of Deep-Sea Mine Tailings Placement (DSTP) in PNG. SAMS.
SKJELKVÅLE, B. L. 2008. Nasjonal Innsjøundersøkelse 2004-2006, Del 1: Vannkjemi. *Statlig program for forurensingsovervåkning.* Statens Forurensingstilsyn: Norwegian Institute of Water Reseach.
SOUTHARD, J. 2006. *Introduction to Fluid Motions, Sediment Transport, and Current-Generated Sedimentary Structures* [Online]. Massachusetts Institute of Technology: MIT OpenCourseWare. Available: https://ocw.mit.edu [Accessed 04.08 2017].
STUMM, W. & SULZBERGER, B. 1992. The cycling of iron in natural environments: Considerations based on laboratory studies of heterogeneous redox processes. *Geochimia et Comsochimisa Acta,* 56**,** 3233-3257.
SÆLAND, F. 2007. A Recording Experience. *International Conference BigStuff.* Bochum 2007.
SØRBY, H. 2016. Myndighetenes syn på BAT for deponering av mineralavfall. *Norsk bergindustris miljøkonferanse.* Clarion Hotel Oslo Airport: Miljødirektoratet.
SØRBY, H. & STORBRÅTEN, G. 2016. Tillatelse til virksomhet etter forurensingsloven for Titania AS. *In:* AGENCY, N. E. (ed.). Norwegian Environment Agency.
SØRBY, H., STORBRÅTEN, G., BRAASTAD, G., LØKELAND, M., DALEN, M., THORNHILL, M., BØE, R., RYE, H., FOSSÅ, J. H., DEKKO, T., JENSEN, T. & SKEI, J. 2010. Bergverk og

avgangsdeponering: Status, miljøutfordringer og kunnskapsbehov. *In:* SKEI, J. (ed.). Klima- og forurensingsdirektoratet (Klif)
Norsk institutt for vannforskning (NIVA).
THOMAS, R. 2001. A Beginner's Guide to ICP-MS. *Spectroscopy,* 16**,** 56.
TRANNUM, H. C. 2011. *Environmental effects of water-based drill cuttings on benthic communities*
- biological and biogeochemical responses in mesocosm- and field-experiments. Ph.D, University of Oslo.
TRANNUM, H. C. 2016. Overvåking av marin bløtbunnsfauna for Titania A/S i 2015. Norwegian Institute for Water Research.
U.S GEOLOGICAL SURVEY 2016. Mineral commodity summaries 2016. U.S.G.S.
VOGT, C. 2013. International Assessment of Marine and Riverine Disposal of Mine Tailings. International Maritime Organization, London Convention/Protocol, IMO.

Appendix A – E_s values

The electrode measurements for Es, corrected after equation 4.3.

Depth (mm)	Titania liners (mV)			Control liners (mV)		
	14	**4**	**20**	**32**	**1**	**10**
5	294	176	269	185	297	198
15	292	176	279	186	296	200
25	294	176	280	187	296	198
35	296	176	283	185	295	198
45	296	176	283	181,8	296	196
55	297	176	286	181,4	297	194
65	298	177	287	183,5	297	194
75	299	177	289	185,5	297	194
5	294	176	269	185	297	198

Appendix B – DGT profiles

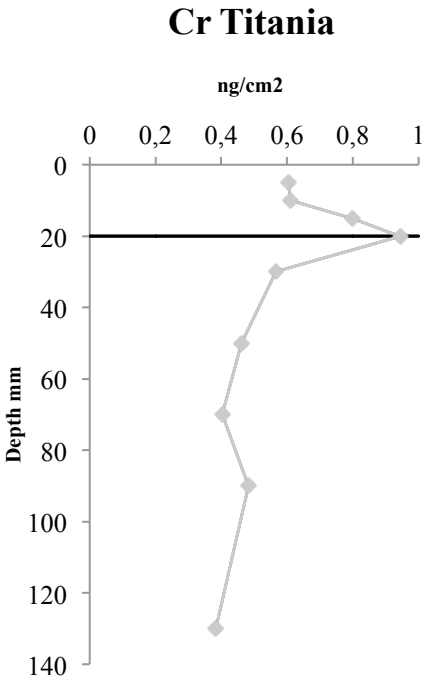

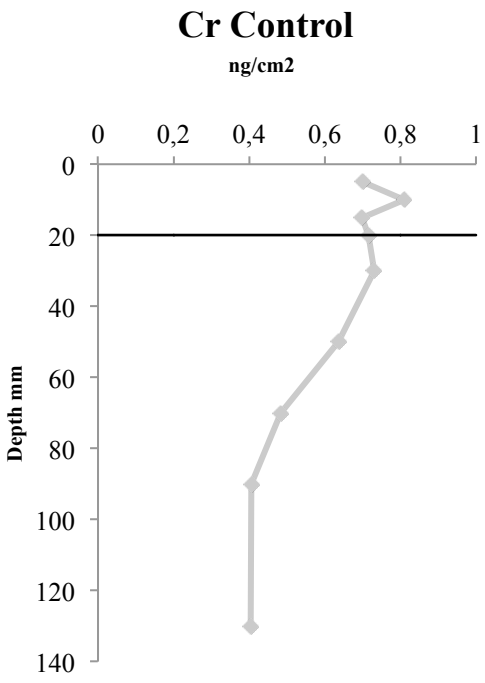

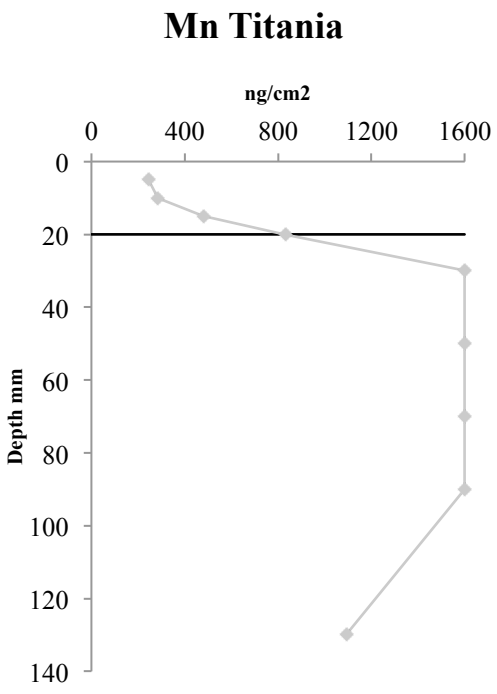

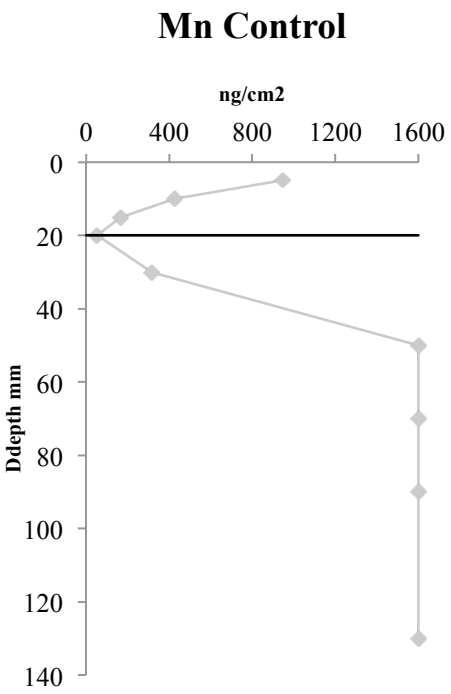

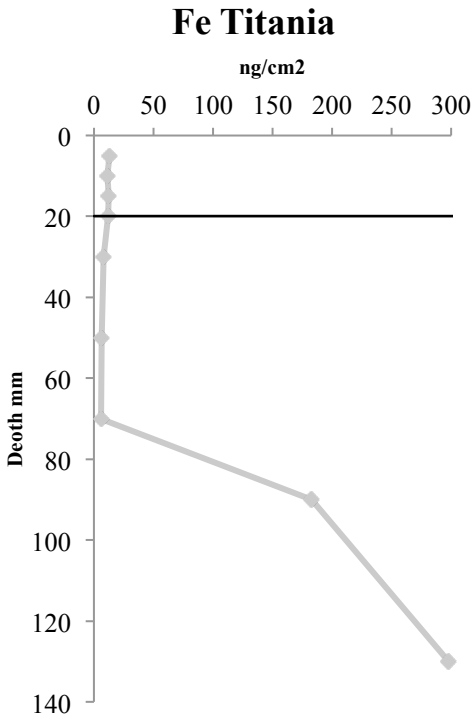
Fe Titania
ng/cm2
0 50 100 150 200 250 300
0 20 40 60 80 100 120 140
Deoth mm

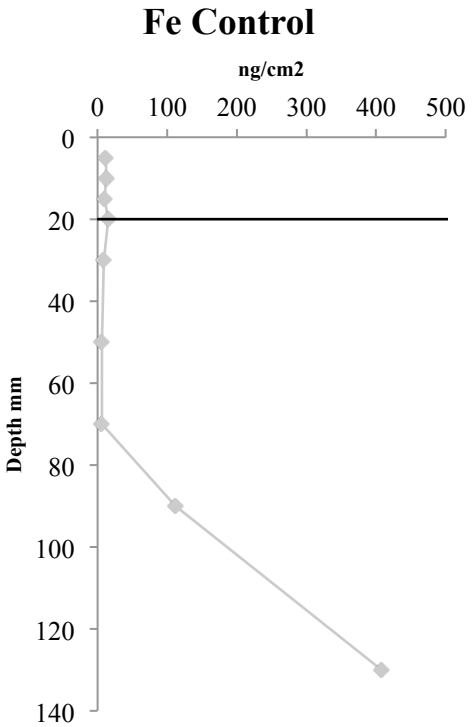
Fe Control
ng/cm2
0 100 200 300 400 500
0 20 40 60 80 100 120 140
Depth mm

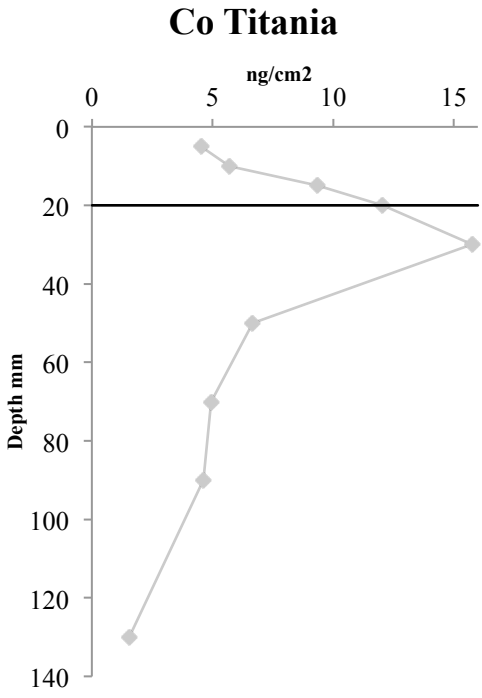
Co Titania
ng/cm2
0 5 10 15
0 20 40 60 80 100 120 140
Depth mm

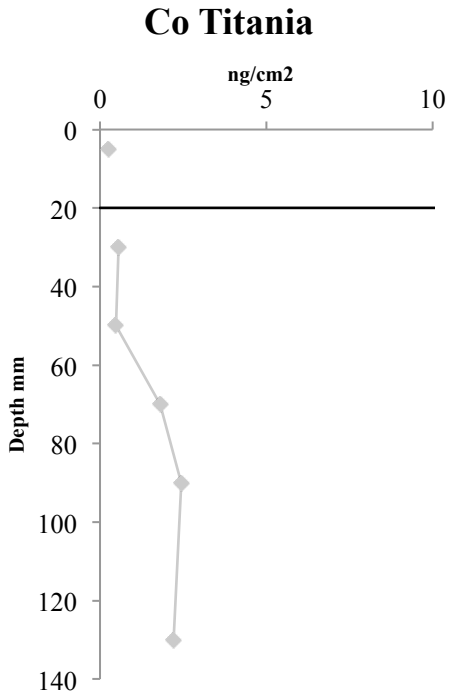
Co Titania
ng/cm2
0 5 10
0 20 40 60 80 100 120 140
Depth mm

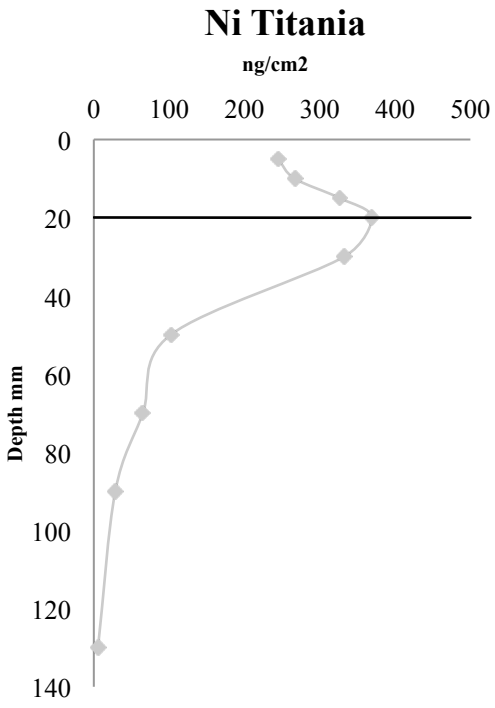
Ni Titania
ng/cm2
0
100
200
300
400
500
Depth mm
0
20
40
60
80
100
120
140

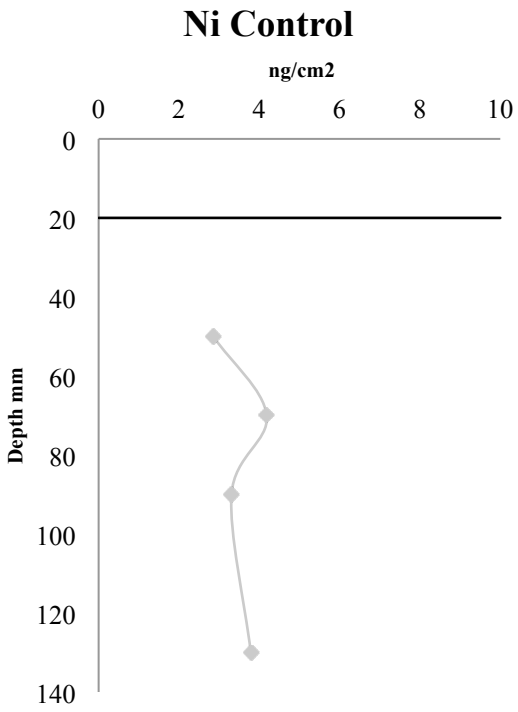
Ni Control
ng/cm2
0
2
4
6
8
10
Depth mm
0
20
40
60
80
100
120
140

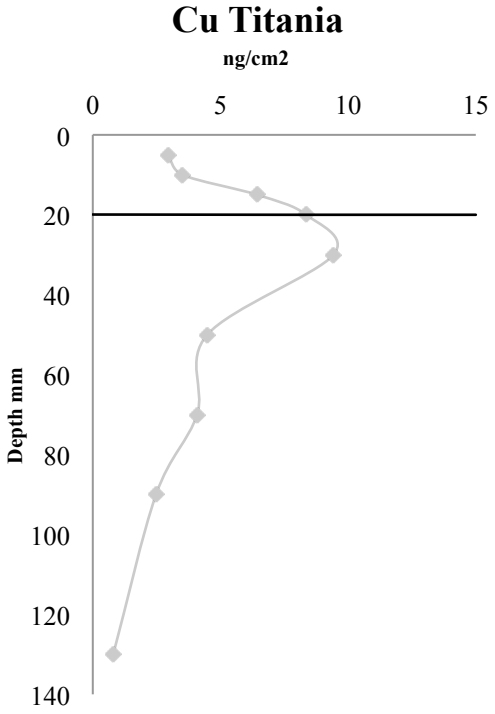
Cu Titania
ng/cm2
0
5
10
15
Depth mm
0
20
40
60
80
100
120
140

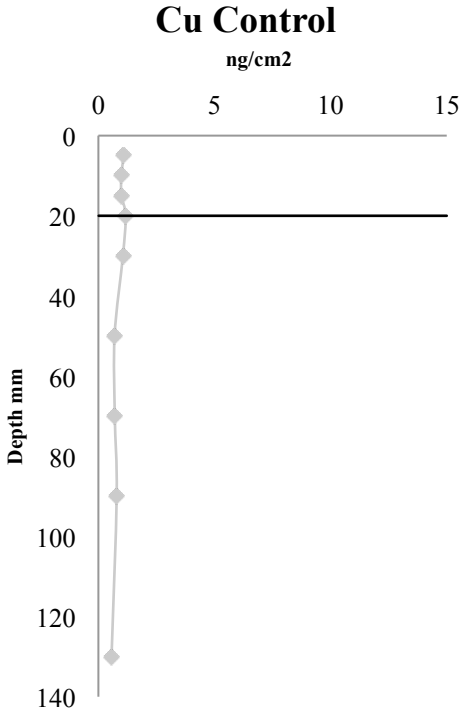
Cu Control
ng/cm2
0
5
10
15
Depth mm
0
20
40
60
80
100
120
140

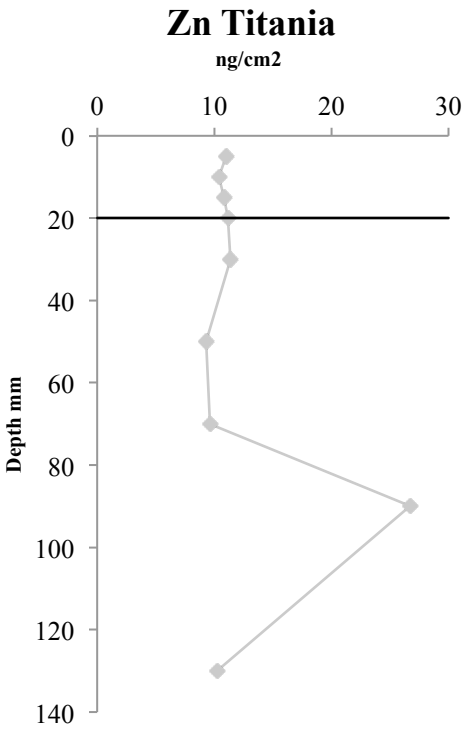
Zn Titania
ng/cm2
0
10
20
30
Depth mm
0
20
40
60
80
100
120
140

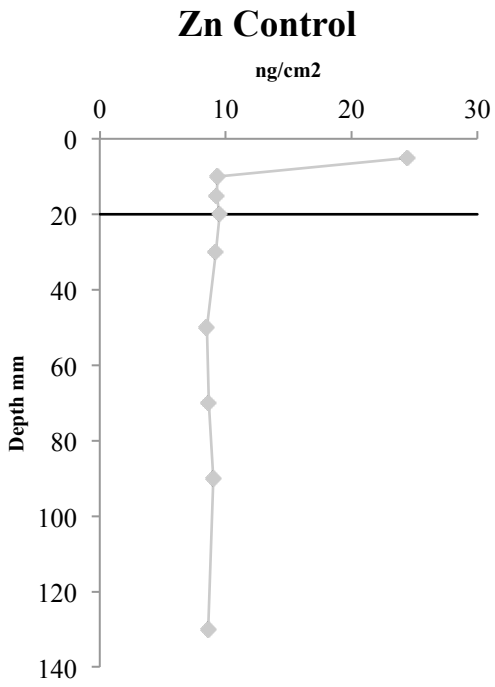
Zn Control
ng/cm2
0
10
20
30
Depth mm
0
20
40
60
80
100
120
140

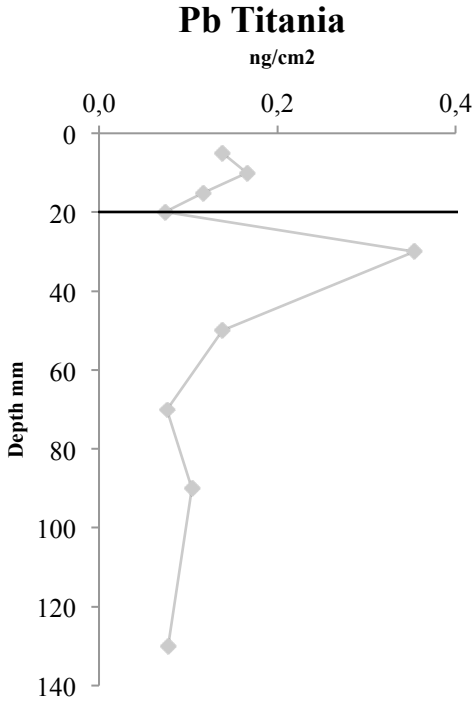
Pb Titania
ng/cm2
0,0
0,2
0,4
Depth mm
0
20
40
60
80
100
120
140

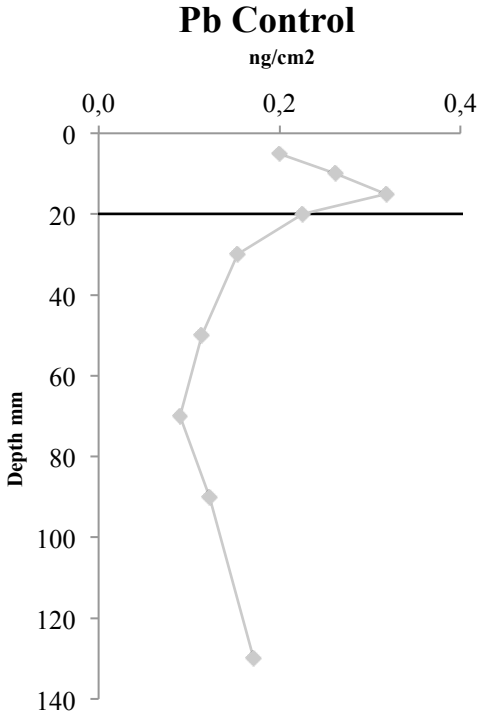
Pb Control
ng/cm2
0,0
0,2
0,4
Depth mm
0
20
40
60
80
100
120
140

Appendix C- dust deposition calculations

Example of the grain size 10μm

Radius= 5μm

Density used = 2800 kg/m^3 due to plagioclase and ilmenite being the dominant grains

Area: height*width = 100m*3600m = 360000 m^2

Number of grains/m^2: grains counted from filters, and up scaled from grains/μm. See figure 5.3.

Step 1: Number of grains (10μm) to volume

Number of grains/ m^2:	2122963477,5	
Volume $(\mu m)^3$ / grain:	$\frac{4}{3}\pi r^3$ =	523 $(\mu m)^3$
Volume m^3		5,23E-16

Step 2: Volume to mass

Mass/ grain (kg):	density=2800kg/m^3	1,46E-12 kg/grain

Step 3: Total mass of 10μm/m^2

Kg/grain * grains/ m^2	1,46E-12 kg/grain*2122963477,5 grains/ m^2
	= 0,0031 kg/m^2

Step 4: Scaling up to area

Area 360000m^2 * 0,0031 kg/m^2 =	1120,5 kg/month
	13445,7 kg/year

Step 1 to 4 conducted for the four grain-size intervals and summarized. Ni is 0,03% of total.

Appendix D – flux calculations

Calculations of Ni flux

Area Jøssingfjord 0,27km^2= 270 000m^2

Area Dyngadypet 0,82km^2= 820 000m^2

Average flux of Ni from Titania: 2201,6 µg m-2 d-1

= 2,20 E-06 kg m-2 d-1

Average flux of Ni from Control 1,12 µg m-2 d-1

=1,12 E-09 kg m-2 d-1

Flux from the marine storage sites

	kg/month		**kg/year**	
	Titania	Control	Titania	Control
Jøssingfjord	17,83	0,01	216,97	0,11
Dyngadypet	54,16	0,03	658,94	0,34